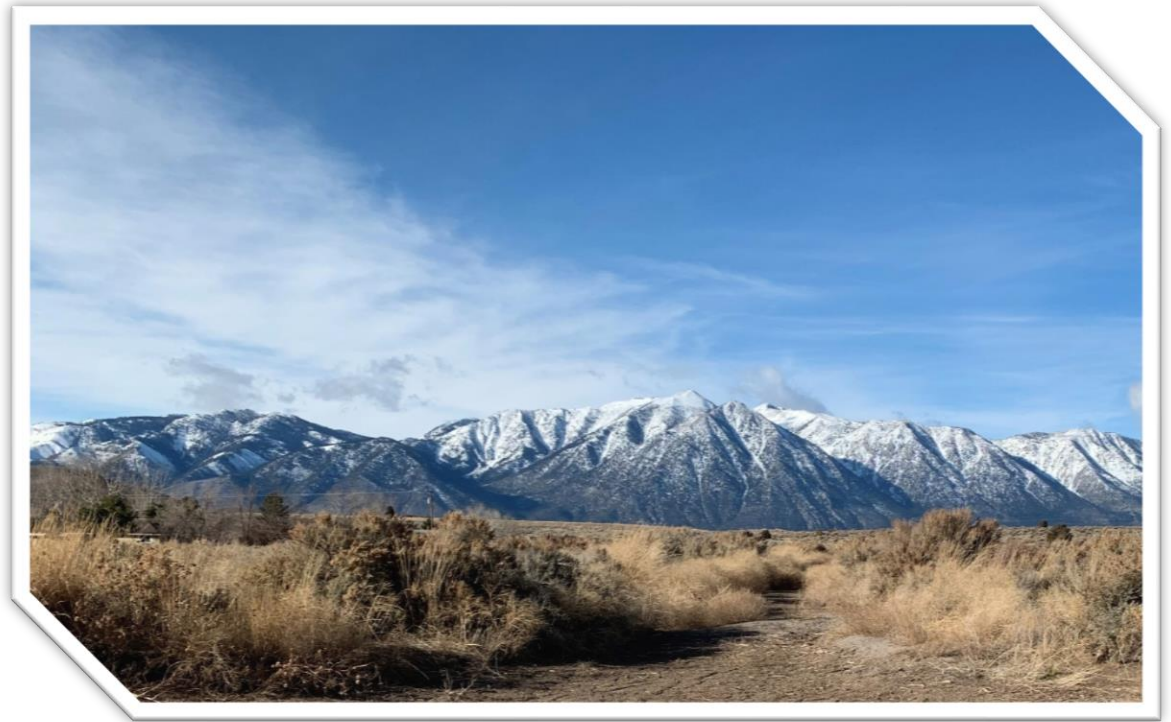


DRAFT

Ruhenstroth Area Drainage Master Plan

Phase 1

Technical Support Data Notebook



September
2020

prepared for
Douglas County | Carson Water Subconservancy District



8400 S Kyrene Rd, STE 201
Tempe, AZ 85284
www.jefuller.com

Table of Contents

1 Introduction 1

 1.1 Project Purpose..... 1

 1.2 Project Location 1

 1.3 Previous Studies..... 3

 1.3.1 Subdivision Drainage Reports 3

 1.3.2 Flood Insurance Studies 4

 1.3.3 U.S. Army Corps of Engineers Alluvial Fan Mapping..... 7

 1.3.4 Smelter Creek Regional Flood Control Project..... 9

 1.4 Historical Flowpath Assessment 11

 1.4.1 Aerial Photography 12

 1.4.2 Summary 12

2 Hydrologic and Hydraulic Modeling..... 16

 2.1 Method Description 16

 2.2 Model Development 16

 2.2.1 Spatial Reference System..... 16

 2.2.2 Model Domain and Grid Size 16

 2.2.3 Grid Element Elevations..... 18

 2.2.4 Precipitation Development..... 19

 2.2.5 Grid Element Roughness (Manning’s n Values) 20

 2.2.6 Infiltration Development 23

 2.2.7 Hydraulic Structures..... 32

 2.2.8 Buildings (as Flow Obstructions)..... 35

 2.2.9 Model Control Parameters 35

 2.3 Model Results 36

 2.3.1 Floodplain Cross-Sections 36

 2.3.2 Depth and Discharge Results 38

 2.3.3 Animations 39

 2.4 Verification of Results 46

 2.4.1 Comparison with USGS Regression Equations 46

 2.4.2 Additional USGS Data..... 49

 2.4.3 Historical Flooding Documentation 51

2.5 Summary 56

3 Sedimentation Analyses..... 57

3.1 Sediment Sampling and Transport Analysis..... 57

3.1.1 Sediment Sampling 57

3.1.2 Sediment Transport Analyses 60

3.2 Results 61

3.2.2 Sediment Profiles 63

4 Flood Hazard Classification 65

4.1 Purpose 65

4.2 Flooding Hazards to Pedestrians..... 65

4.3 Flooding Hazards to Passenger Vehicles..... 68

4.4 Flooding Hazards to Structures..... 74

4.5 Building Inundation Assessment..... 77

4.5.1 Methodology..... 77

4.5.2 Existing Conditions 77

4.6 Summary 79

5 All-Weather Access 80

5.1 Introduction 80

5.2 Methodology and Results 82

5.2.1 Smelter Creek Conveyance Improvements..... 82

5.2.2 New Culverts 84

5.2.3 Cost Estimates..... 87

6 References 88

List of Figures

| | |
|---|----|
| Figure 1-1. Study area vicinity map..... | 2 |
| Figure 1-2. Effective FEMA Floodplains | 6 |
| Figure 1-3. Distribution of relative risk rankings by watershed, from Floyd (2017) | 7 |
| Figure 1-4. USACE alluvial fan risk ranking..... | 8 |
| Figure 1-5. 1948 aerial photography | 13 |
| Figure 1-6. 2017 aerial photography | 14 |
| Figure 1-7. Historical flowpath comparison..... | 15 |
| Figure 2-1. Modeling domain used in the Ruhenstroth ADMP..... | 17 |
| Figure 2-2. Comparison of 6- and 24-hour hyetographs used in the RADMP | 20 |
| Figure 2-3. Surface classification used to assign grid element roughness in the FLO-2D model | 22 |
| Figure 2-4. Spatial variability of the saturated hydraulic conductivity | 24 |
| Figure 2-5. XKSAT values used in the FLO-2D modeling | 25 |
| Figure 2-6. Values of DTHETA as a function of XKSAT, reproduced from Mohave County (2018). | 26 |
| Figure 2-7. Values of PSIF as a function of XKSAT, reproduced from Mohave County (2018). | 27 |
| Figure 2-8. DTHETA values used in the FLO-2D modeling | 28 |
| Figure 2-9. PSIF values used in the FLO-2D modeling..... | 29 |
| Figure 2-10. Spatial variability of the depth to a restrictive layer, from NRCS (2019) | 30 |
| Figure 2-11. Locations of all modeled hydraulic culverts | 33 |
| Figure 2-12. Typical driveway culverts..... | 34 |
| Figure 2-13. Rating table comparison..... | 35 |
| Figure 2-14. Floodplain cross-section locations..... | 37 |
| Figure 2-15. Existing conditions 25-year, 24-hour flow depth results..... | 40 |
| Figure 2-16. Existing conditions 100-year, 6-hour flow depth results..... | 41 |
| Figure 2-17. Existing conditions 100-year, 24-hour flow depth results..... | 42 |
| Figure 2-18. Existing conditions 25-year, 24-hour discharge results..... | 43 |
| Figure 2-19. Existing conditions 100-year, 6-hour discharge results..... | 44 |
| Figure 2-20. Existing conditions 100-year, 24-hour discharge results..... | 45 |
| Figure 2-21. Comparison of FLO-2D results with the relations between 100-year peak discharge and drainage area and plot of maximum peak discharge of record and drainage area for gaged sites in the Eastern Sierras Region 5, adapted from USGS (1997) | 47 |
| Figure 2-22. Drainage basins used for comparison of FLO-2D results to the USGS 100-year regression equations | 48 |
| Figure 2-23. Drainage area statistics for USGS crest stage sites..... | 49 |
| Figure 2-24. Location and drainage areas of USGS crest stage sites | 50 |
| Figure 2-25. Comparison of FLO-2D results, 1997 100-year regression equation, and peak flow estimates from crest stage sites..... | 51 |
| Figure 2-26. Verification for the Buckskin Court crossing area..... | 52 |
| Figure 2-27. Verification for the Horseman Court crossing area | 53 |
| Figure 2-28. Verification for the Lacey Court/Mustang Lane area | 54 |
| Figure 2-29. Verification for the Bennett Court/Pinto Circle area (resident-provided comment) | 55 |
| Figure 3-1. Example of sediment deposition at culvert..... | 57 |
| Figure 3-2. Sediment sample locations and sample ID..... | 58 |

Figure 3-3. Gradation curves for the collected sediment samples 59

Figure 3-4. Total accumulated sediment transport capacity by the Yang methodology for the 100-year, 24-hour event 62

Figure 3-5. Cumulative sediment transport profile for the primary overland flow path throughout the 100-year 24-hour event 64

Figure 4-1. Depth-Velocity flood danger level relationship for children, from USBR (1988) 66

Figure 4-2. USBR criteria flooding hazards to pedestrians based on the 100-year, 6-hour results..... 67

Figure 4-3. Depth-Velocity flood danger level relationship for passenger vehicles, from USBR (1988) ... 68

Figure 4-4. USBR criteria flooding hazards to vehicles based on the 100-year, 6-hour results..... 69

Figure 4-5. Hazardous road crossings during a 25-year, 24-hour storm (USBR criteria) 71

Figure 4-6. Hazardous road crossings during a 100-year, 6-hour storm (USBR criteria) 72

Figure 4-7. Hazardous road crossings during a 100-year, 24-hour storm (USBR criteria) 73

Figure 4-8. Depth-Velocity flood danger level relationship for structures built on foundations, from USBR (1988) 74

Figure 4-9. USBR criteria flooding hazards to buildings based on the 100-year, 6-hour results 76

Figure 4-10. Building inundation assessment (100-Year, 6-Hour) result example 78

Figure 5-1. Location of all-weather access roadway crossings, shown with 100-year 6-hour maximum discharges 81

Figure 5-2. 25-year typical section 83

Figure 5-3. 100-year typical section..... 83

Figure 5-4. 25-year concept improvements..... 85

Figure 5-5. 100-year concept improvements 86

List of Tables

Table 1-1. Collected subdivision drainage reports..... 3
Table 1-2. Flood Insurance Studies 4
Table 1-3. FEMA flood zones within the study area 5
Table 2-1. FLO-2D model domain areas and number of grid elements..... 16
Table 2-2. LiDAR settings and specifications, reproduced from QSI (2019) 18
Table 2-3. Maximum NOAA14 point rainfall estimates (in inches) by recurrence interval 19
Table 2-4. Surface classification and corresponding Manning’s n value 21
Table 2-5. Surface classification with corresponding percent impervious and initial abstraction 31
Table 2-6. Peak flow and volume results from the FLO-2D floodplain cross-sections 38
Table 2-7. Comparison with 100-year USGS regression equation 47
Table 3-1. Major characteristics of the sediment within the lower watershed 59
Table 4-1. Building flooding hazard classification results (USBR criteria)..... 75
Table 4-2. Buildings that are impacted by various depths (base conditions) 77
Table 5-1. 25-year concept cost estimates 87
Table 5-2. 100-year concept cost estimates 87

Appendices

Appendix A – QSI LiDAR Report

Appendix B – Supporting Data (Digital)

1 INTRODUCTION

1.1 PROJECT PURPOSE

Phase I of the Ruhenstroth Area Drainage Master Plan (RADMP) was developed to meet three primary objectives:

1. Evaluate and identify flooding and sedimentation hazards within the project area by completion of a technical study that includes data collection, review of previous studies, information gathering from public agencies and residents, hydrologic and hydraulic modeling, geomorphic assessments, and field surveys.
2. Develop concepts for all-weather access crossings of Smelter Creek for existing conditions.
3. Provide stakeholder coordination and public outreach of the project through a series of public meetings to inform of the existing hazards and to present the mitigation alternatives.

Each major task of the project is presented herein with a description of the technical approach, analysis results, interpretation of results, and applicability to the overall project purpose. The results of this study can be used as a planning tool and as input to the design of potential future drainage infrastructure and flood mitigation measures that are appropriate for the physical environment for both existing and future development.

Phase II of the Ruhenstroth ADMP is a future study that will be used to develop a series of alternatives to either partially or wholly mitigate the hazards identified in Phase I of the ADMP.

1.2 PROJECT LOCATION

The Ruhenstroth ADMP watershed area is 18 square miles and is located on the western slopes of the Pine Nut Mountains, approximately 16 miles south of Carson City (Figure 1-1). The study area is located entirely within Douglas County about 6 miles southeast of the Minden-Gardnerville area. The primary focus area of the RADMP is the lower watershed area downstream of the mountains, also shown on Figure 1-1.

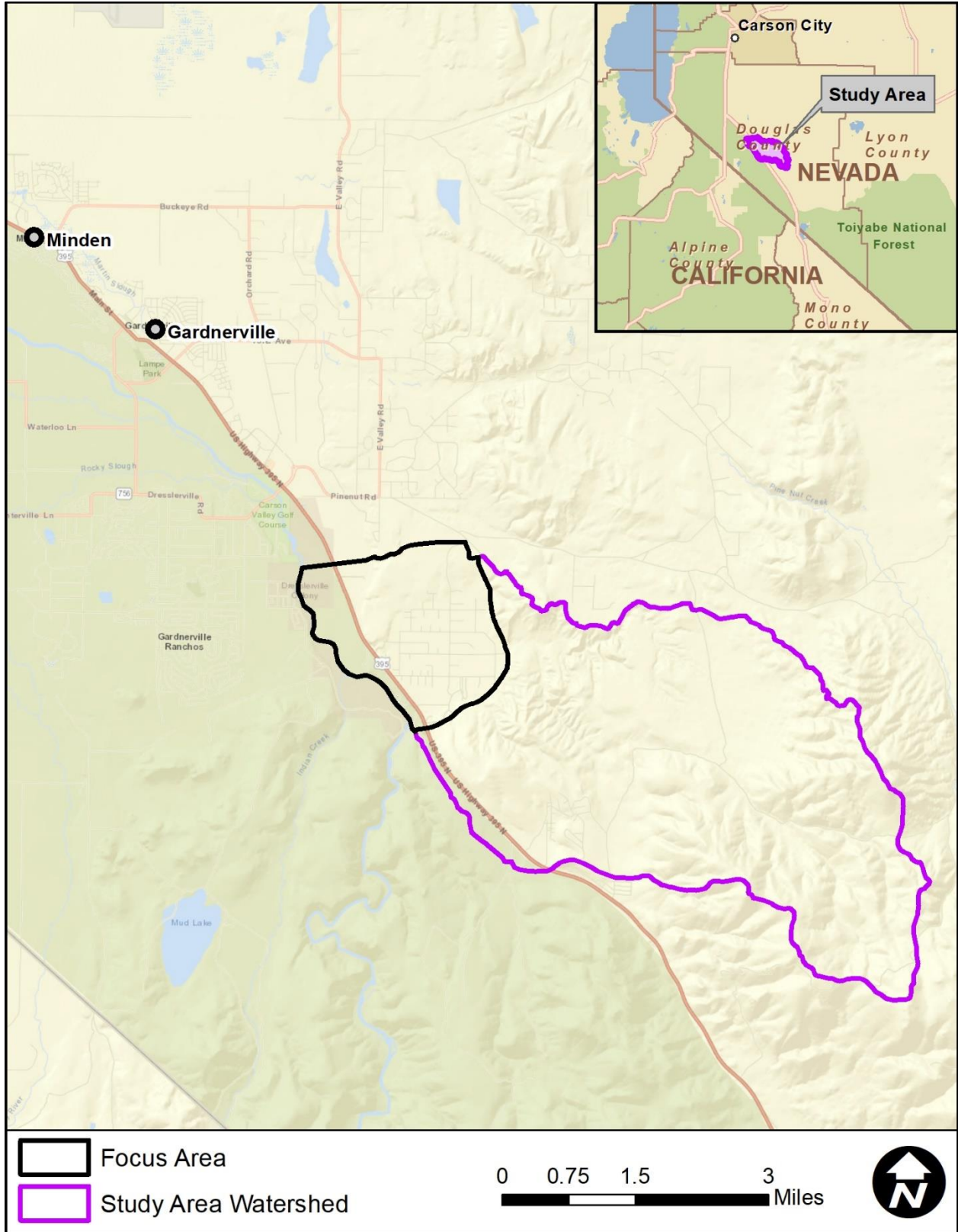


Figure 1-1. Study area vicinity map

1.3 PREVIOUS STUDIES

An early phase of the study included research and collection of previous reports and studies relevant to the ADMP area. These included drainage reports for local subdivisions, flood insurance studies (FIS), and geologic reports. A summary of the different types of reports are summarized in the following sections.

1.3.1 Subdivision Drainage Reports

Several drainage reports and drainage studies were collected from the county agencies and included information that was used directly in the development of the existing conditions hydraulic model (Section 2). The documents provided information on the location and design for drainage facilities within the individual subdivisions. All the collected drainage reports are included in the digital data appendix (Appendix B). Table 1-1 lists the collected documents.

Table 1-1. Collected subdivision drainage reports

| Title | Author | Date | Subdivision |
|--|--|-------------------|---------------------|
| Drainage Reports and Drainage Studies | | | |
| Dry Creek Estates Planned Unit Development Drainage Report | Lumos & Associates | May 1999 | Dry Creek Estates |
| Technical Drainage Study for Pinto & Palomino Parcel Maps | Western Engineering & Surveying Services | March 2, 2001 | N/A |
| Settelmeyer Ranches Conceptual Drainage Study | RO Anderson Engineering | June 19, 2004 | Settelmeyer Ranches |
| Conceptual Drainage Study Tentative Parcel Map, Cayuse Drive | Western Engineering & Surveying Services | August 16, 2004 | N/A |
| AU LLC Map Technical Drainage Study | RO Anderson Engineering | October 31, 2004 | N/A |
| Shoemaker Parcel Map Conceptual Drainage Study | RO Anderson Engineering | September 9, 2005 | N/A |
| Scott Parcel Map Technical Drainage Study 629 Appaloosa Lane | RO Anderson Engineering | December 7, 2005 | N/A |
| Technical Drainage Study for 733 Mustang Lane | Building & Site Engineering, Inc. | December 10, 2005 | N/A |
| Scott Parcel Map Addendum to Technical Drainage Study 629 Appaloosa Lane | RO Anderson Engineering | March 1, 2006 | N/A |
| Technical Drainage Report for Saddlerock Development | EXD Engineering | November 7, 2006 | Saddlerock |

| Title | Author | Date | Subdivision |
|--|-------------------------|-------------------|-------------|
| Drainage Report for Mullen Site Improvement Permit, 1894 Palomino Lane | EXD Engineering | December 14, 2006 | N/A |
| Conceptual Drainage Study for 616 Appaloosa Lane | Keith R. Schaffer, PE | July 2, 2007 | N/A |
| Technical Drainage Report for Saddlerock Development | EXD Engineering | July 23, 2007 | Saddlerock |
| Conceptual Drainage Study for Pasek Property 670 Mustang Lane | Resource Concepts, Inc. | April 20, 2010 | N/A |
| Technical Drainage Study for 1901-1905 Arabian Lane | RO Anderson | December 16, 2015 | N/A |

1.3.2 Flood Insurance Studies

Federal Emergency Management Agency (FEMA) Flood Insurance Studies (FIS) for Douglas County were collected and reviewed for historical flooding records and regulatory discharge estimates for watercourses in the study area. Table 1-2 lists the collected studies and derived information. Although the goal of this study is not to “match” the FIS discharge estimates, they do provide a base-level comparison for the hydraulic model results (see Section 2.3). The consistency of discharges between years in Table 1-2 suggests that there has been no revision to the hydrology for FEMA regulatory studies since at least 1999.

Table 1-2. Flood Insurance Studies

| Study Date | County | Ruhenstroth ADMP Watercourses | 100-year Discharge (cfs) |
|---------------|-----------------------------|-------------------------------|--------------------------|
| November 1999 | Douglas | Smelter Creek | 1,050 |
| January 2010 | Douglas | Smelter Creek | 1,050 |
| June 2016 | Douglas (current effective) | Smelter Creek | 1,050 |

1.3.2.1 Effective FEMA Floodplain Mapping

As of the date of this study, Smelter Creek is the only watercourse in the study area with FEMA regulatory floodplains (Figure 1-2). Table 1-3 lists the descriptions for each flood zone within the study area. Like the FIS discharges, FEMA floodplain mapping provides a base-level comparison of flood risk for the hydraulic modeling results from this study. The 1% chance floodplain is the only zone with a flood insurance requirement for homes with federally backed mortgages.

Table 1-3. FEMA flood zones within the study area

| Flood Zone | Definition | Flooding Type | Recurrence Interval |
|------------------|---|--------------------|---------------------|
| AO | Average depths have been determined; flood depths range from 1 to 3 feet. | Shallow sheet flow | 1% chance |
| A | No base flood elevation is provided | Riverine | 1% chance |
| AE | Base flood elevation (BFE) is provided | Riverine | 1% chance |
| AE with Floodway | BFE and Floodway is provided | Riverine | 1% chance |
| Shaded X | 0.2 Percent annual chance flood hazard | Riverine, Other | 0.2% chance |
| Unshaded X | Area of minimal flood hazard | - | - |

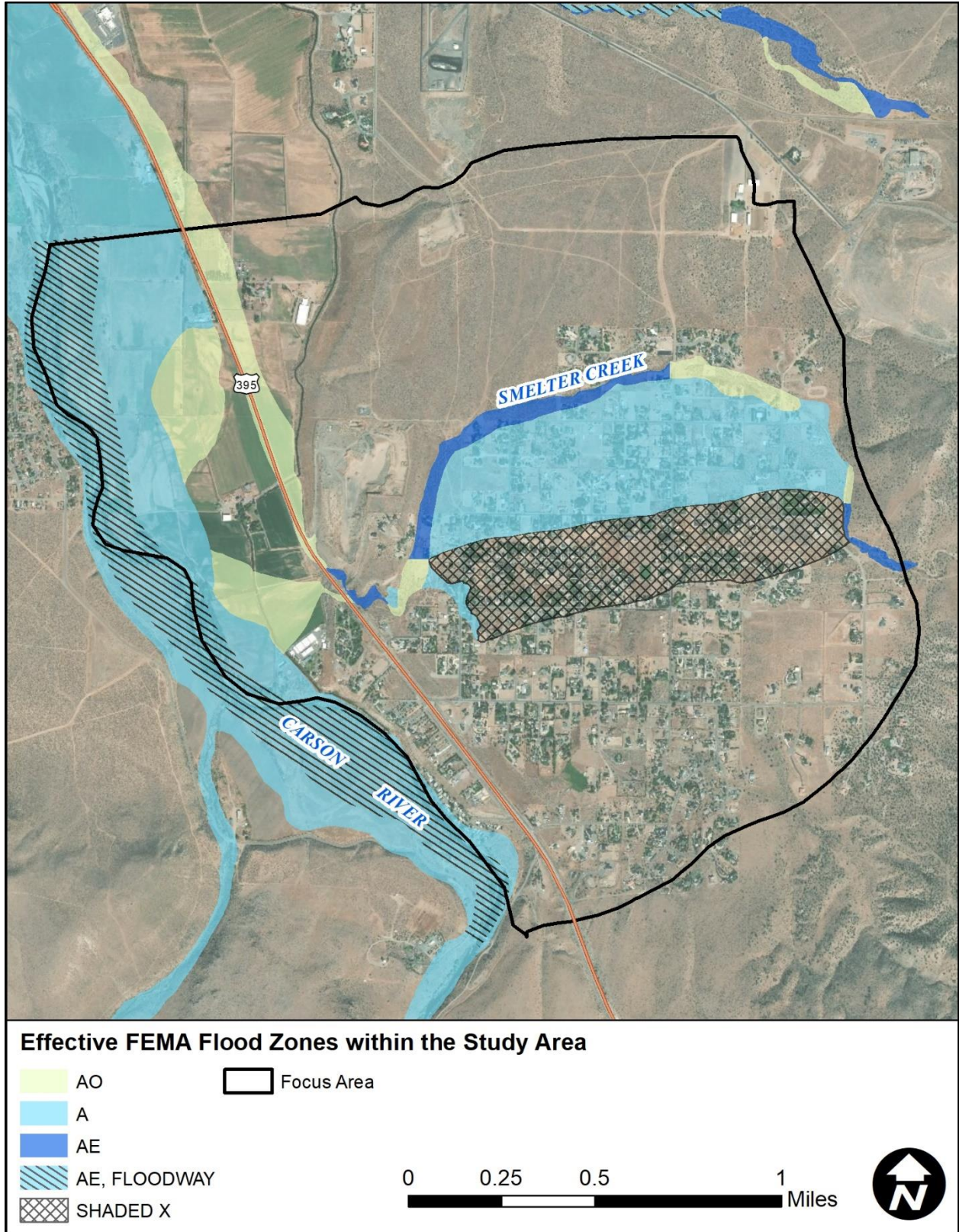


Figure 1-2. Effective FEMA Floodplains

1.3.3 U.S. Army Corps of Engineers Alluvial Fan Mapping

In December 2017, the U.S. Army Corps of Engineers (USACE), Sacramento District, published a study titled *Alluvial Fan Mapping for the Carson River Watershed Methodology* (Floyd, 2017) which included the RADMP study area. The purpose of the mapping study was to classify the relative risk of alluvial fan landforms within the Carson River Watershed. Alluvial fan landforms were identified and assigned a risk ranking based on the following categories:

- Appearance of active or inactive
- Existence of disturbances
- Presence of infrastructure

Within each category, a series of risk factors were examined. For example, the Active/Inactive category included four risk factors:

- Soil Development
- Alluvium
- Unconfined Flow
- Incised Channels

The risk factors were assigned a relative score and summed to derive an overall hazard ranking by watershed. Figure 1-3 from the report depicts the distribution of relative risk rankings by watershed. Figure 1-4 shows the identified alluvial fan landforms near the RADMP study area and their assigned risk.

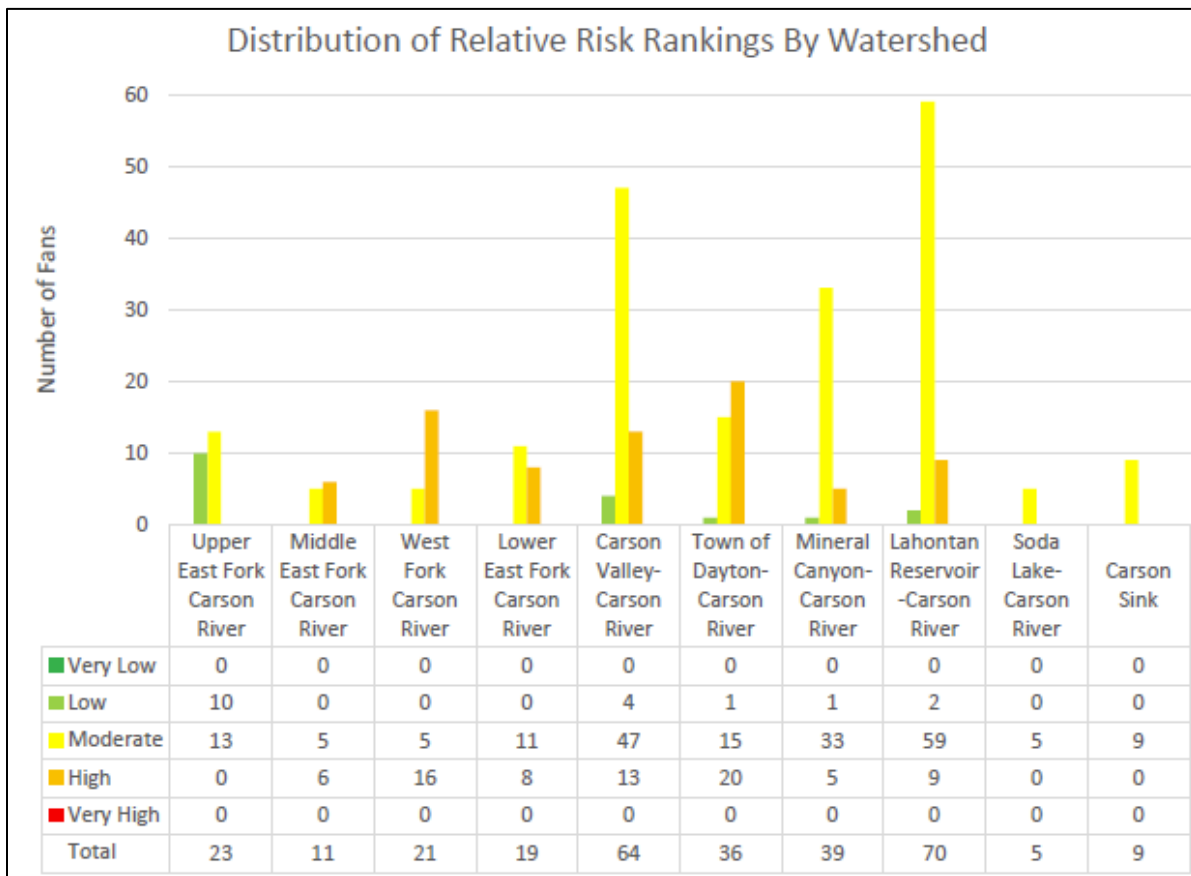


Figure 1-3. Distribution of relative risk rankings by watershed, from Floyd (2017)

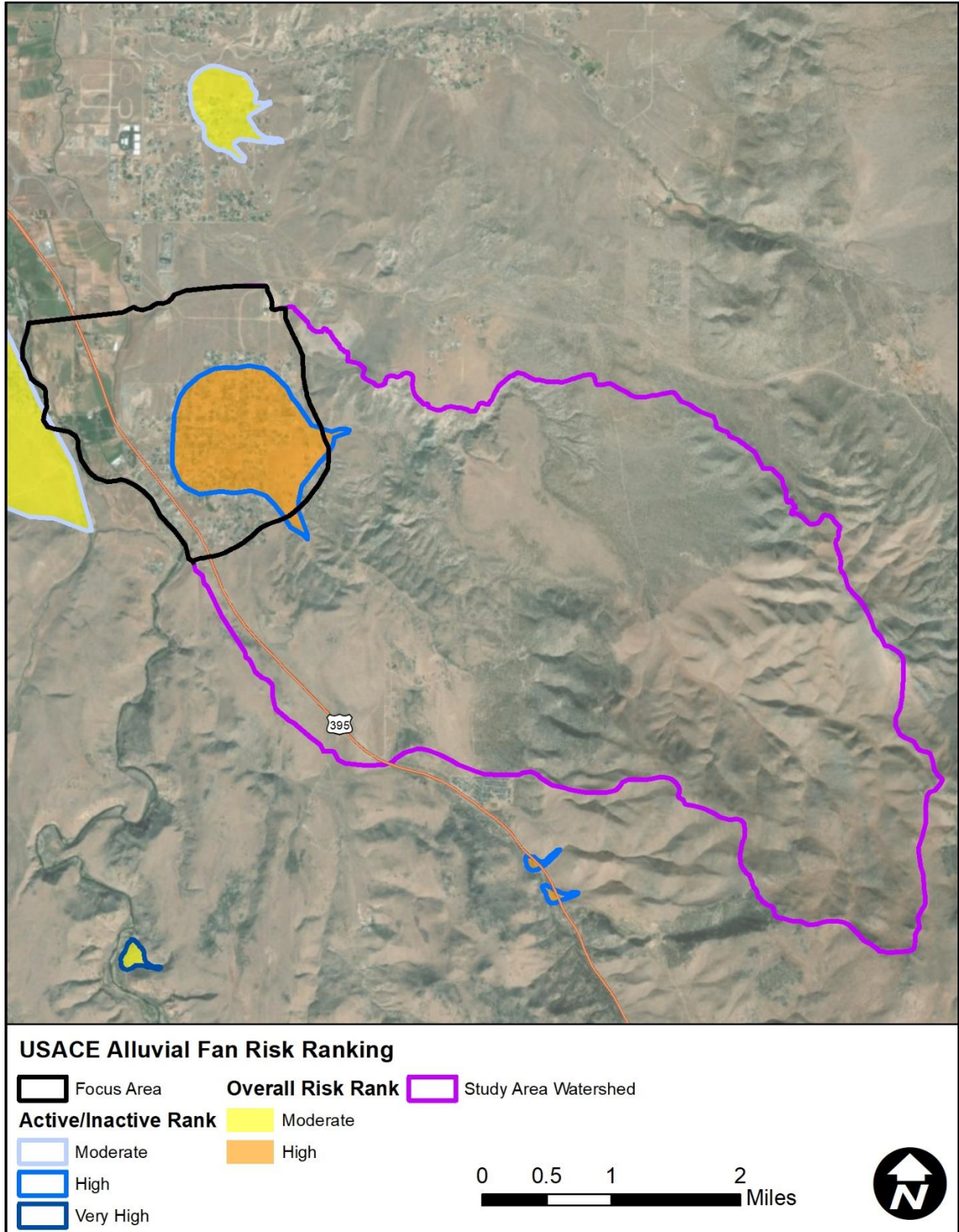


Figure 1-4. USACE alluvial fan risk ranking

1.3.4 Smelter Creek Regional Flood Control Project

In 2015 CWSD and Douglas County initiated a study on the feasibility of a regional flood control project for Smelter Creek (RO Anderson Engineering, 2015). The study included hydrologic modeling of the Smelter Creek watershed, conceptual design of a flood control reservoir, and an estimate of probable costs. The following is from the conclusions section of the study report:

The Smelter Creek watershed has experienced several large hydrologic events in recent years, including the most recent events in 2014 and 2015 that caused unquantified damage to private property, roads, and drainage structures in the Ruhestroth subdivision in Douglas County, Nevada. In order to alleviate flood risks to these downstream areas, construction of an on-stream (Smelter Creek) regional flood control reservoir, just east of the Ruhestroth subdivision on BLM managed land was first proposed in early 2011. Subsequently, CWSD retained ROA to prepare a feasibility-level study to identify alternative solutions to alleviate future flooding resulting from severe hydrologic events that occur in Smelter Creek Watershed. The following is the summary of our findings and conclusions:

The effective FIS lists only 1-percent annual chance peak flow for Smelter Creek watershed. This peak flow rate estimate was probably based on the hydrologic study that was performed in late 1980s using HEC-1, and may not accurately represent current land use characteristics or available hydrologic data generated since that former analysis was prepared. It is therefore, appropriate and prudent to evaluate the hydrology of this watershed and estimate 1-percent annual chance peak flows based on updated precipitation data developed by NOAA.

- The hydrologic study performed by ROA personnel and presented in this report used current NOAA precipitation data to build balanced design storm hyetographs for each sub-basin that takes area-reduction factors, altitude, etc. into consideration thereby producing reliable peak runoff estimates. In addition, the revised hydrologic study also includes estimated peak flows resulting from 0.2-percent-annual chance and ½ PMP events.*
- This hydrologic study estimated peak runoff resulting from 1-percent annual chance flood to be approximately 730 cfs, which is 350 cfs lower than the effective peak flow (1,080 cfs). The proposed discharge entering the flood control reservoir during the occurrence of 0.2-percent-annual-chance event is approximately 2,183 cfs.*
- General PMP rainfall depths were computed using HMR-49 guidelines, and the resulting rainfall data was used to construct a hyetograph that was applied uniformly over the entire watershed. The resulting hydrograph at the most downstream end of the watershed was taken and the ordinates of this flood hydrograph were divided in half to obtain ½-PMF. The resulting ½-PMF was routed through the proposed flood control reservoir.*
- While preparing this feasibility analysis, Nevada Division of Water Resources, Bureau of Dam Safety was contacted to confirm the design inflow event that the proposed structure will be required to be designed to safely mitigate. From those discussions, the proposed structure will likely be characterized as a High Hazard Dam. The Design Inflow criteria will therefore be the ½-PMP event. That is, the*

proposed dam and its appurtenances must be sized to pass the ½-PMF through the proposed spillway with approximately three feet of freeboard before overtopping.

- *After reviewing the estimated peak flood flows from 1-, 0.2-percent, and ½-PMF events, four alternate flood control basin locations were considered, and a feasibility analysis was performed, which culminated in the selection of two potential locations for this regional flood control basin — Alternative 3 and Alternative 4.*
- *The embankment of the proposed Alternative 3 flood control structure is 36 feet high with a normal storage capacity of 202.5 acre-feet, and a storage capacity of 392.6 acre-feet at dam crest. The proposed flood control basin incorporates a 60-inch low level primary outlet, and an emergency spillway with 20-ft bottom width.*
- *The embankment of the proposed Alternative 4 flood control structure is 32 feet high with a normal storage capacity of 176.8 acre-feet, and a storage capacity of 391.5 acre-feet at dam crest. The proposed flood control basin incorporates a 60-inch low level primary outlet, and an emergency spillway with 20-ft bottom width.*
- *The primary and emergency outlet works were designed such that during the 1-percent annual chance flood, the outflow discharge is limited to 380 cfs through the 60-inch primary outlet; and, during 0.2-percent annual-chance flood and ½-PMF events, the emergency spillway safely conveys incoming flood flows with sufficient freeboard and some attenuation.*
- *The Engineer’s Preliminary Estimate of Probable Costs for Alternative 3 is \$3,170,000, and for Alternative 4 is \$2,550,000, which amount includes allowances for construction contingencies, land acquisition, engineering design, permitting and construction phase services.*
- *A hydraulic model of downstream reach of Smelter Creek below the proposed flood control facility was developed using HEC-RAS. A set of three steady flow rates that represent discharges from the proposed reservoir during the occurrence of 1-, 0.2-percent, and ½-PMF events were used to perform steady state flow simulations. The results of these simulations were processed in ArcGIS environment and preliminary floodplain boundary maps were produced.*
- *The resulting floodplain boundary maps were compared with FEMA effective FIRMs, and number of structures / parcels that may be removed from the SFHA was estimated. It is estimated that only 3 structures will remain in the revised SFHA compared to 120 structures that are currently in the effective SFHA for this area of Douglas County.*
- *Building an instream flood control basin on Smelter Creek with an estimated cost of \$3.17 million dollars for Alternative 3 or \$2.55 million dollars for Alternative 4 results in direct and substantial benefit to the residents of Ruhenstroth subdivision, particularly those within the regulatory floodplain of Smelter Creek. The project provides additional indirect benefits to the residents of Douglas County by reducing potential damage to public infrastructure such as roads and drainage structures in this area.*
- *The Smelter Creek Regional Flood Control project is eligible for FEMA’s Hazard Mitigation Grant Program that currently provides 75% grants for qualified projects.*

- *If successful in obtaining a Hazard Mitigation Grant for this project, the required local match to complete Alternative 3 improvements is estimated to be \$792,250. Assuming this amount could be funded through a Flood Control District (NRS 543.170-543.830, or a local Assessment District at an effective interest rate of 5% and a term of 25 years, the annual payments would be about \$225/benefitted parcel. Without grant funding, using the same financing terms, the estimated annual payment is about \$900 per benefitted parcel. These per parcel amounts, \$225/year and \$900/year, are understood to be less than what many of the homeowners impacted by this floodplain currently pay for flood insurance in this area.*
- *For Alternative 4, the required local match to complete the planned improvements is estimated to be \$637,500. Assuming this amount could be funded through a Flood Control District (NRS 543.170-543.830, or a local Assessment District at an effective interest rate of 5% and a term of 25 years, the annual payments would be about \$180/benefitted parcel. Without grant funding, using the same financing terms, the estimated annual payment is about \$720 per benefitted parcel. These per parcel amounts, \$180/year and \$720/year, are understood to be less than what many of the homeowners impacted by this floodplain currently pay for flood insurance in this area.*
- *Preliminary BCA shows a BCA of 2.27 for Alternative 3, and a slightly better BCA of 2.82 for Alternative 4.*
- *The proposed locations of the regional flood control basins were compared to the locations of USGS- documented earthquake faults (Quaternary Faults). There are no identified active faults within the limits of the proposed dam and reservoir.*
- *From these investigations, we conclude that the project is eminently feasible and worthy of pursuing further.*

Following the completion of the 2015 Smelter Creek study, Douglas County applied for construction funding for the project through a FEMA Hazard Mitigation Grant Program (HMGP) application in December 2016. The initial grant request was unsuccessful. Douglas County revised the grant application Benefit-Cost Analysis (BCA) and resubmitted to FEMA in December 2017. The second grant application was also unsuccessful. Douglas County conducted a more robust BCA analysis and concluded that the benefit-cost ratio was not favorable to receive HMGP funding. As of the date of this ADMP report the Smelter Creek Flood Control Project has not been constructed.

1.4 HISTORICAL FLOWPATH ASSESSMENT

Understanding the historical evolution of a geomorphic system is critical to understanding present-day processes and predicting future trends. Natural systems can take hundreds of thousands of years to develop, and their morphology is a direct reflection of this long-development period. Anthropogenic changes to a natural system often result in abrupt changes that can be managed for a brief period, but quite often the disturbed system will trend back to its natural condition, despite efforts to change and maintain it.

A historical flowpath assessment was conducted for the ADMP study area to assess the natural flowpaths of the study watercourses with the goal that understanding the natural flowpaths will aid in understanding the current flooding patterns and potential future flooding trends.

1.4.1 Aerial Photography

Historical aerial photography from 1954 (earliest year available) were collected and semi-rectified using ArcGIS software tools. The natural flowpaths for the project watercourses were identified and delineated from the photography. Figure 1-5 shows the historical aerial photography and Figure 1-6 the modern aerial photography (2018) for the ADMP focus area. The 1954 photographs pre-date much of the development within the focus area and shows the landforms in a (mostly) natural condition. The locations of the dominant flowpaths for the major drainage channels were interpreted and delineated from the 1954 photographs to compare with the 2019 locations. The 2019 channel locations were derived from the ADMP LiDAR mapping which was flown in October 2019 (see 2.2.3).

1.4.2 Summary

The most significant changes in flowpath alignment since 1954 have occurred due to manmade channel realignments as development progressed in the watershed (Figure 1-7).

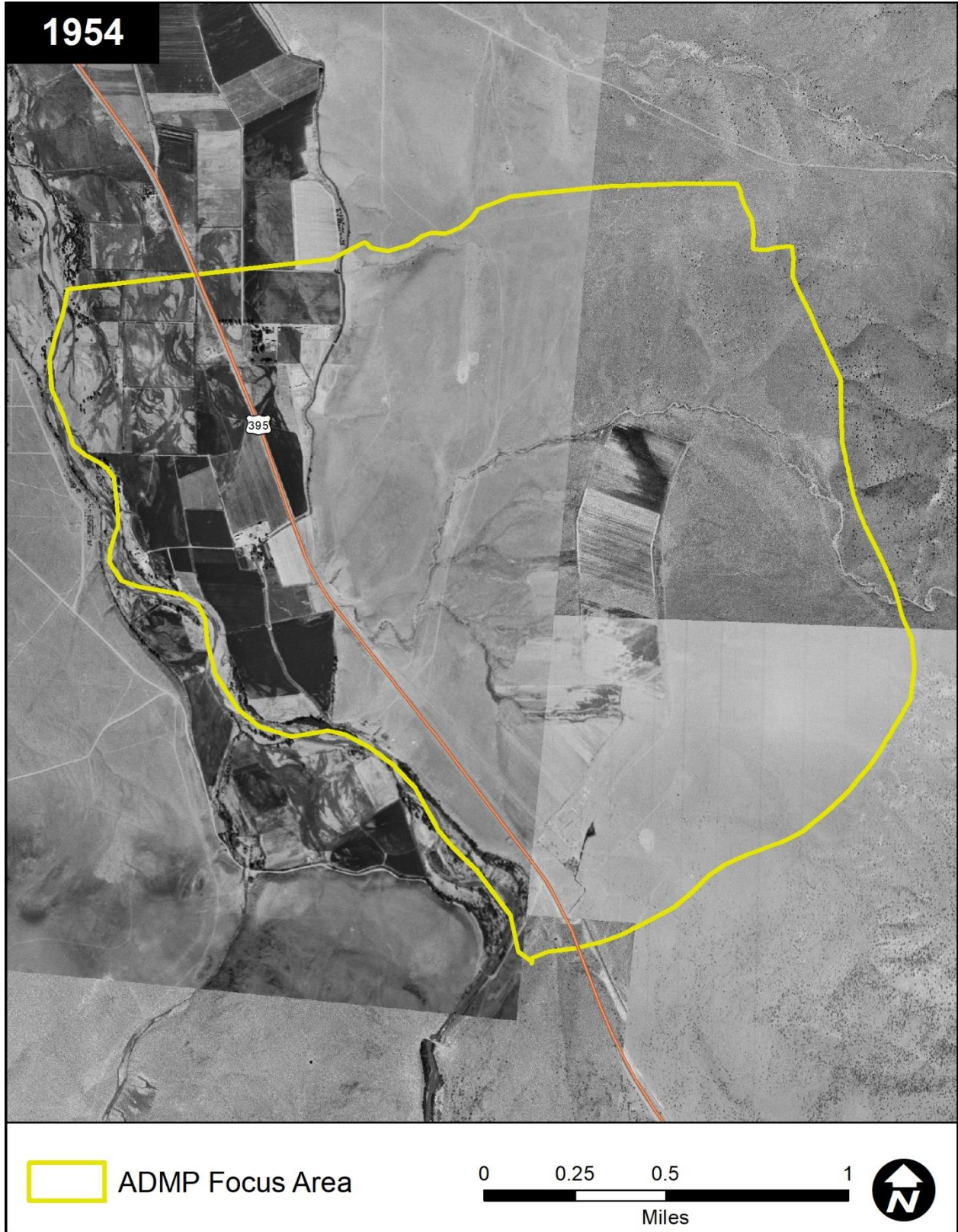


Figure 1-5. 1948 aerial photography

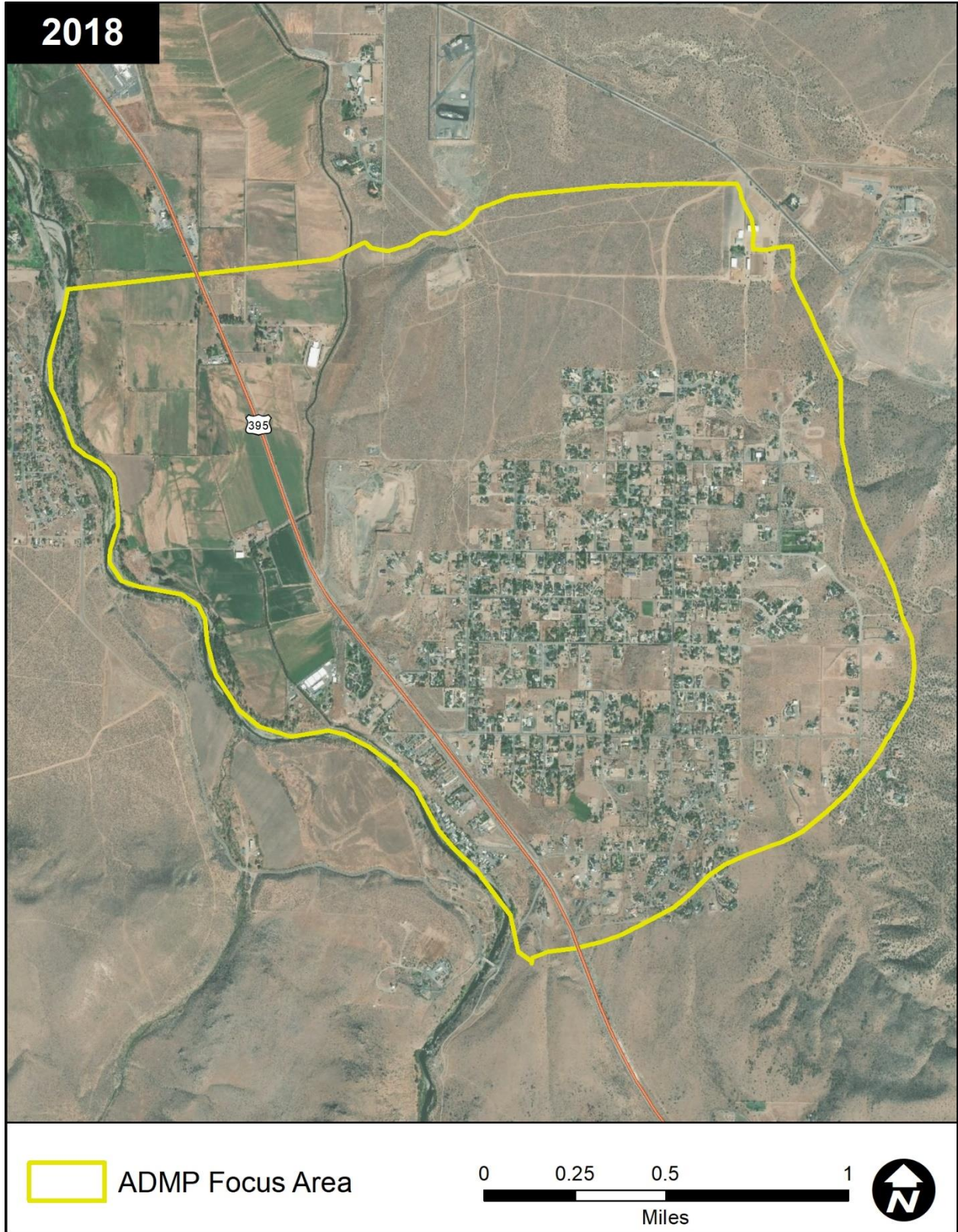


Figure 1-6. 2017 aerial photography



Figure 1-7. Historical flowpath comparison

2 HYDROLOGIC AND HYDRAULIC MODELING

2.1 METHOD DESCRIPTION

Modeling for the Ruhenstroth ADMP study area was completed using the FLO-2D Pro software package¹, Build No. 19.07.21 with an executable dated June 10, 2020. This version has extensive improvements in model runtime and accuracy. In addition, this version has been tested by the Flood Control District of Maricopa County and is approved for use in their studies.

FLO-2D is a combined rainfall-runoff model (i.e., both hydrologic and hydraulic). Therefore, both on-site and off-site modeling was completed using the FLO-2D software.

2.2 MODEL DEVELOPMENT

2.2.1 Spatial Reference System

All data that was generated for the RADMP used the horizontal control of the Nevada Coordinate System, West Zone, NAD83; while the vertical datum was the North American Vertical Datum of 1988 (NAVD 88). The units of measurement were US survey feet.

2.2.2 Model Domain and Grid Size

The Ruhenstroth watershed contains many small drainage structures that need to be adequately captured in the model to provide the most accurate results. Some of these features include small (12- to 18-inch) driveway culverts and minor roadside drainage ditches. Therefore, a high-resolution, 10-foot grid size was selected to provide the necessary detail to model these features.

With the Build No. 19.07.21 FLO-2D executable, model runtime is significantly reduced. Therefore, the entire watershed was able to be modeled in one domain with a 10-foot grid size. The grid size and the number of cells in the model are shown in Table 2-1, while the spatial location of modeling domain boundary in relation to the focus area is shown in Figure 2-1.

Table 2-1. FLO-2D model domain areas and number of grid elements

| Grid Size | Domain Area (sq. miles) | Number of Grid Elements |
|--------------|-------------------------|-------------------------|
| 10-ft | 18.2 | 5,072,033 |

¹ <https://www.flo-2d.com/>

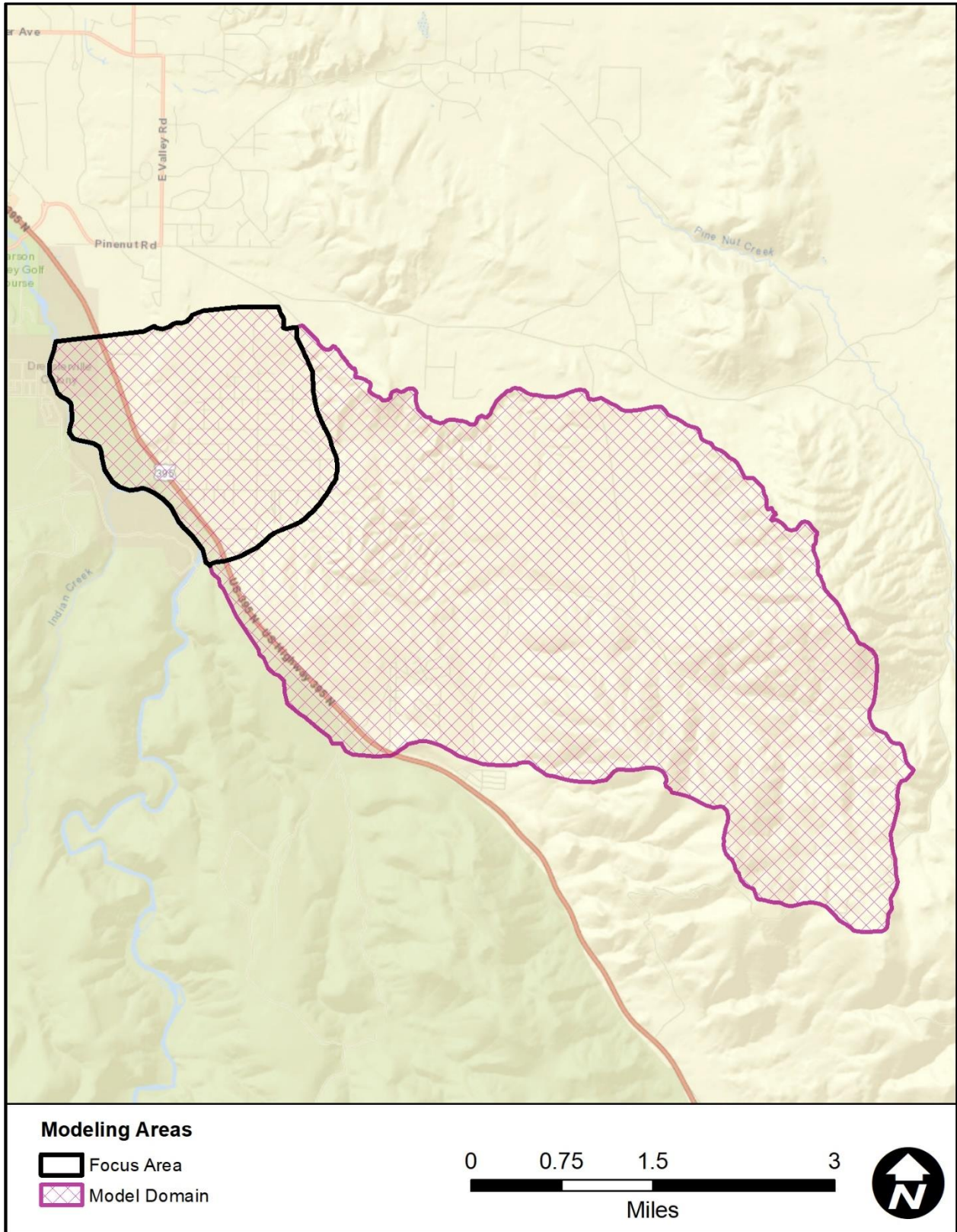


Figure 2-1. Modeling domain used in the Ruhestroth ADMP

2.2.3 Grid Element Elevations

As a part of this project, LiDAR data was collected by aircraft at an average density of 8 pulses per square meter on October 24, 2019. The detailed specifications for the LiDAR acquisition are shown in Table 2-2, while the LiDAR product survey report is included in Appendix A.

Through software processing, the mapping contractor, Quantum Spatial, Inc. (QSI) developed a bare earth ESRI grid raster with a 3-foot pixel resolution. This 3-foot bare earth raster was then resampled to a 10-foot raster that reflects the average grid elevations that are used in the actual FLO-2D model.

Table 2-2. LiDAR settings and specifications, reproduced from QSI (2019)

| LiDAR Survey Settings & Specifications | |
|--|--|
| Acquisition Dates | October 24, 2019 |
| Aircraft Used | Cessna Caravan 208B |
| Sensor | Riegl |
| Laser | VQ-1560i |
| Maximum Returns | Unlimited |
| Resolution/Density | Average 8 pulses/m ² |
| Nominal Pulse Spacing | 0.35 m |
| Survey Altitude (AGL) | 1825 m |
| Survey speed | 145 knots |
| Field of View | 58.5° |
| Mirror Scan Rate | 117 lines/sec per channel |
| Target Pulse Rate | 700 kHz per channel |
| Pulse Length | 3 ns |
| Laser Pulse Footprint Diameter | 32.85 cm |
| Central Wavelength | 1064 nm |
| Pulse Mode | Multiple Times Around (MTA) |
| Beam Divergence | 0.18 mrad |
| Swath Width | 2,045 m |
| Swath Overlap | 55% |
| Intensity | 16-bit |
| Accuracy | RMSE _z (Non-Vegetated) ≤ 9 cm |
| | NVA (95% Confidence Level) ≤ 20 cm |

2.2.4 Precipitation Development

The Douglas County *Design Criteria and Improvements Standards* (2017) specify that storm drains and other drainage facilities be designed to convey the 25-year, 24-hour recurrence interval design storm. This manual also specifies that the 100-year, 24-hour recurrence interval design storm be used under certain situations. Additionally, the 100-year, 6-hour storm event was chosen because this higher intensity duration usually results in higher peak flow estimates for smaller (i.e., < 20 square miles) drainage areas, such as those that exist within the study area.

Therefore, to meet the design standards and the objectives of the Ruhenstroth ADMP, three design storms were simulated. These were:

- 25-year, 24-hour
- 100-year, 24-hour
- 100-year, 6-hour

2.2.4.1 Precipitation Depths

NOAA Atlas 14 (NOAA14) precipitation depth estimates were downloaded from the National Weather Service (NWS) website (2018) as raster images, then used to apply the spatially varied rainfall estimate for each grid element in the model. This means that the point statistics are used at each grid cell in the FLO-2D model, which is different than the typical centroid-based precipitation estimates that are used in lumped parameter (e.g., HEC-HMS or HEC-1) modeling. Point rainfall statistics were selected because:

- 1) using point rainfall has been the general procedure for other ADMP studies in the southwest
- 2) using point statistics results in reasonable but conservative flow estimates.

The maximum rainfall point values for each submodel are shown in Table 2-3.

Table 2-3. Maximum NOAA14 point rainfall estimates (in inches) by recurrence interval

| Storm Event | | |
|-------------|--------|---------|
| 25Y24H | 100Y6H | 100Y24H |
| 4.594 | 2.619 | 5.901 |

2.2.4.2 Hyetographs

For this study, two different hyetographs were selected – one for the 24-hour storms and one for the 6-hour storm. The NDOT (2015) hyetograph for the HUC-12 region was used for the 24-hour storms since it represents the latest research on hyetograph development in Nevada and has performed well on other ADMPs, such as the Dayton Valley ADMP (JEF, 2019b).

Since the drainage areas are all less than 20 square miles in the Ruhenstroth study area, a very intense hyetograph was chosen for the 6-hour storm to simulate a short duration, high intensity summer event. This approach was taken for the Johnson Lane Area Drainage Maser Plan (JEF, 2018) and produced reasonable results. Thus, the 6-hour pattern 1 distribution from the Flood Control District of Maricopa County (FCDMC, 2018) was used to simulate the 100-year 6-hour storm event. The two different hyetographs are shown in dimensionless form in Figure 2-2.

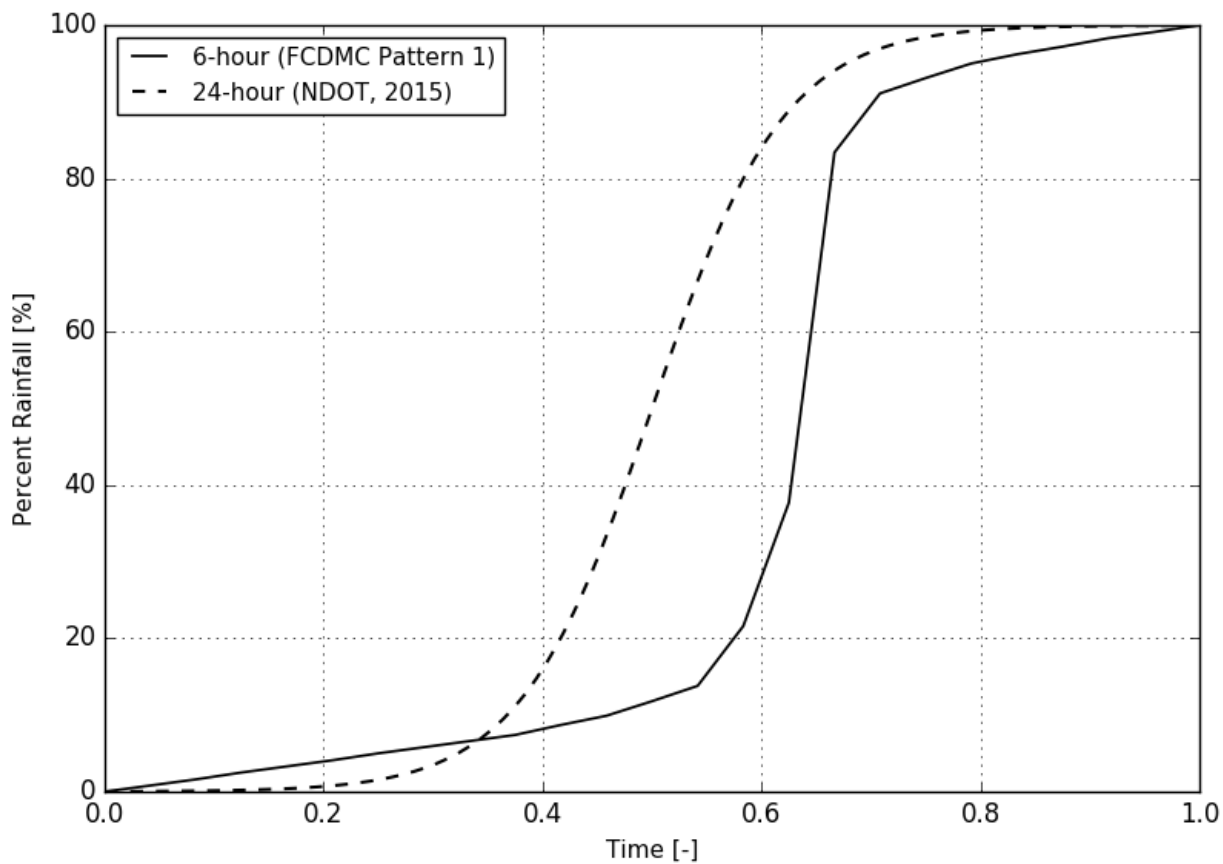


Figure 2-2. Comparison of 6- and 24-hour hyetographs used in the RADMP

2.2.5 Grid Element Roughness (Manning's n Values)

The FLO-2D model uses two Manning's n values to estimate roughness on each element. These are the shallow n value and the base n value. These two parameters allow FLO-2D to calculate a depth-varying roughness, which better approximates physical flood routing in a natural system. For depths below 0.5 feet, the shallow n or half the shallow n value is used. Between 0.5 feet and 3 feet, a function based on the base n value is used; and, at depths greater than 3 feet, the base n value is used. Please see the FLO-2D Data Input Manual (FLO-2D Software, Inc., 2019) for the details about how depth-varying roughness is applied in the software.

Each grid element is assigned an average shallow n and base n value based on the underlying surface conditions. For this study, a detailed surface feature classification was developed by refining land use data provided by Douglas County and adding more detail in areas where the initial delineations were too generalized. For example, major areas of pavement (parking lots and roads) and wash corridors were delineated in the modeling area since these features can act as major conveyances. Buildings and other structures were also added based on the latest available aerial photography (see Section 2.2.8).

The base and shallow n values for each classification were chosen based on experience on other studies, engineering judgment, and research papers, such as Yochum *et al.* (2014), Jarret (1985), and JEF (2020a). Table 2-4 lists the surface classification and its corresponding Manning's n values that were used in this analysis. The spatial distribution of the surface classification is shown in Figure 2-3.

Table 2-4. Surface classification and corresponding Manning's n value

| Surface Classification | Base n | Shallow n |
|---------------------------|--------|-----------|
| Upper Watershed Rangeland | 0.080 | 0.40 |
| Focus Areas Rangeland | 0.055 | 0.18 |
| Maintained Turf | 0.045 | 0.12 |
| Rural Residential | 0.035 | 0.15 |
| Unimproved Road | 0.026 | 0.10 |
| Agriculture | 0.060 | 0.30 |
| Building | 0.024 | 0.10 |
| Pavement | 0.020 | 0.10 |
| Wash | 0.060 | 0.18 |
| Water | 0.040 | 0.10 |

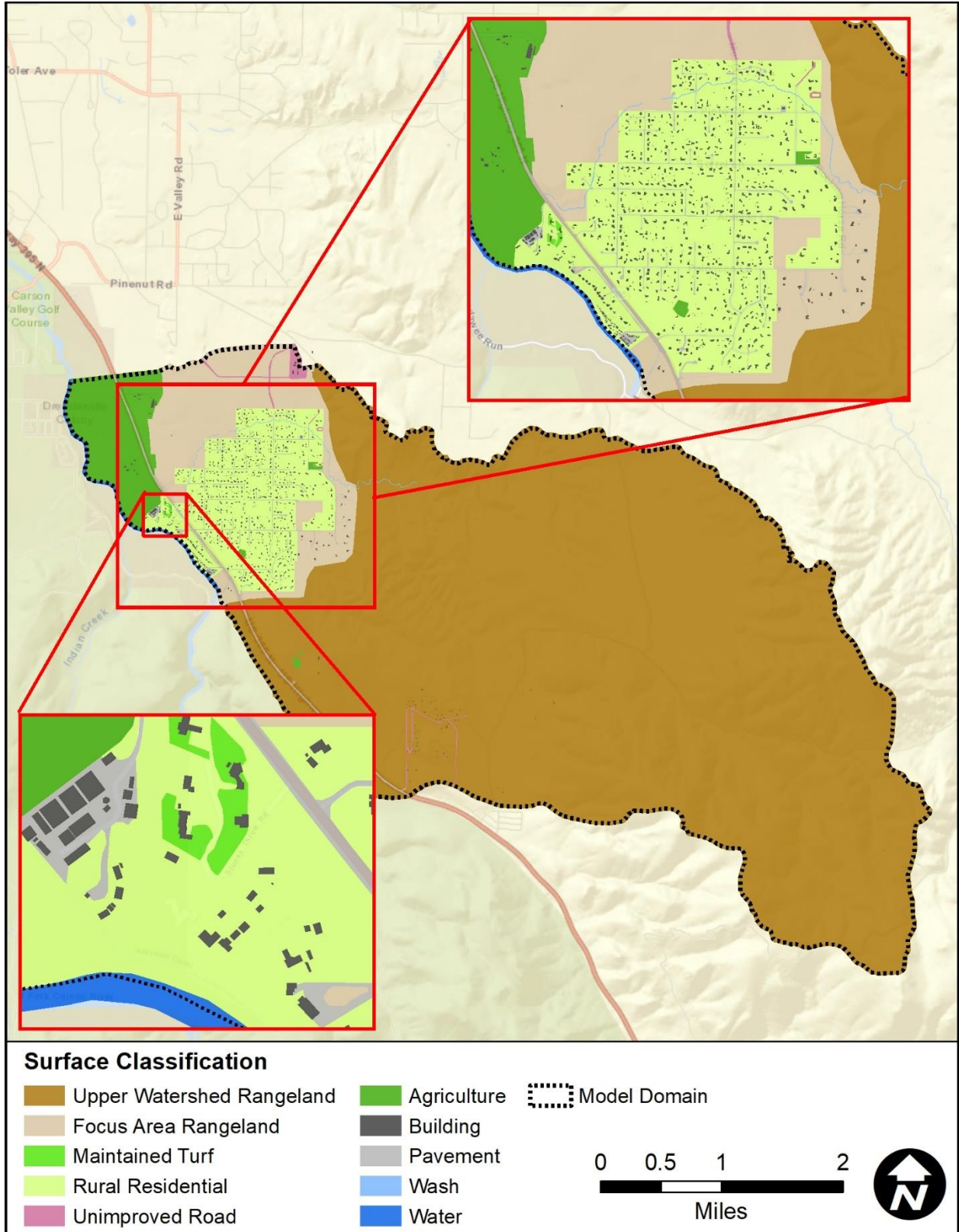


Figure 2-3. Surface classification used to assign grid element roughness in the FLO-2D model

2.2.6 Infiltration Development

Since 1) the previous flood insurance study used the Green and Ampt (GA) infiltration methodology and 2) this methodology is a more physically based infiltration model, the GA methodology was used for this study. In general, the GA infiltration parameters are a function of the subsurface soil type or the features on the ground surface (e.g., a layer of asphalt that covers the soil). As such, the NRCS (2019) soils data was used to develop the soils-based infiltration values. For the ground features, a detailed surface classification shapefile was developed for this study (see Section 2.2.5). This shapefile helped define the surface-based infiltration parameters that were used in the modeling. Additionally, the Smelter Creek Feasibility Engineering Study (RO Anderson Engineering, 2015) was also reviewed to maintain consistency with that study.

2.2.6.1 Soils-based

The infiltration parameters more dependent on the subsurface soils are:

- The hydraulic conductivity at natural saturation (XKSAT) in inches per hour,
- The soil moisture deficit (DTHETA),
- The wetting front suction in inches (PSIF),
- Rock outcrop as a percentage, and
- Limiting infiltration depth in feet, which is the depth at which infiltration stops.

The XKSAT parameter was developed from the NRCS saturated hydraulic conductivity (KSAT). The KSAT values were calculated with the NRCS Soils Data Viewer² for the dominant soils condition at a depth range from 0 to 20 inches. The spatial variability of the KSAT values within the study watershed is shown in Figure 2-4.

These KSAT values were converted to inches per hour and adjusted by equation (1), which is from the *Drainage Design Manual for Mohave County* (Mohave County, 2018). Equation (1) is:

$$XKSAT = CF * KSAT \quad (1)$$

where *CF* is a correction factor and *KSAT* is the saturated hydraulic conductivity. Based on the discussion in the Mohave County manual, the *CF* can range 0.1 to 0.9; but both the Arizona Department of Transportation (ADOT) and Mohave County recommend 0.5 as the *CF*. Therefore, a value of 0.5 was used as the *CF* in this study. Finally, calculated XKSAT values that exceeded 2 inches per hour were capped at 2 inches, per the Mohave County methodology. The final XKSAT values that were used in the FLO-2D modeling are shown in Figure 2-5

² https://www.nrcs.usda.gov/wps/portal/nrcs/detailfull/soils/survey/geo/?cid=nrcs142p2_053620

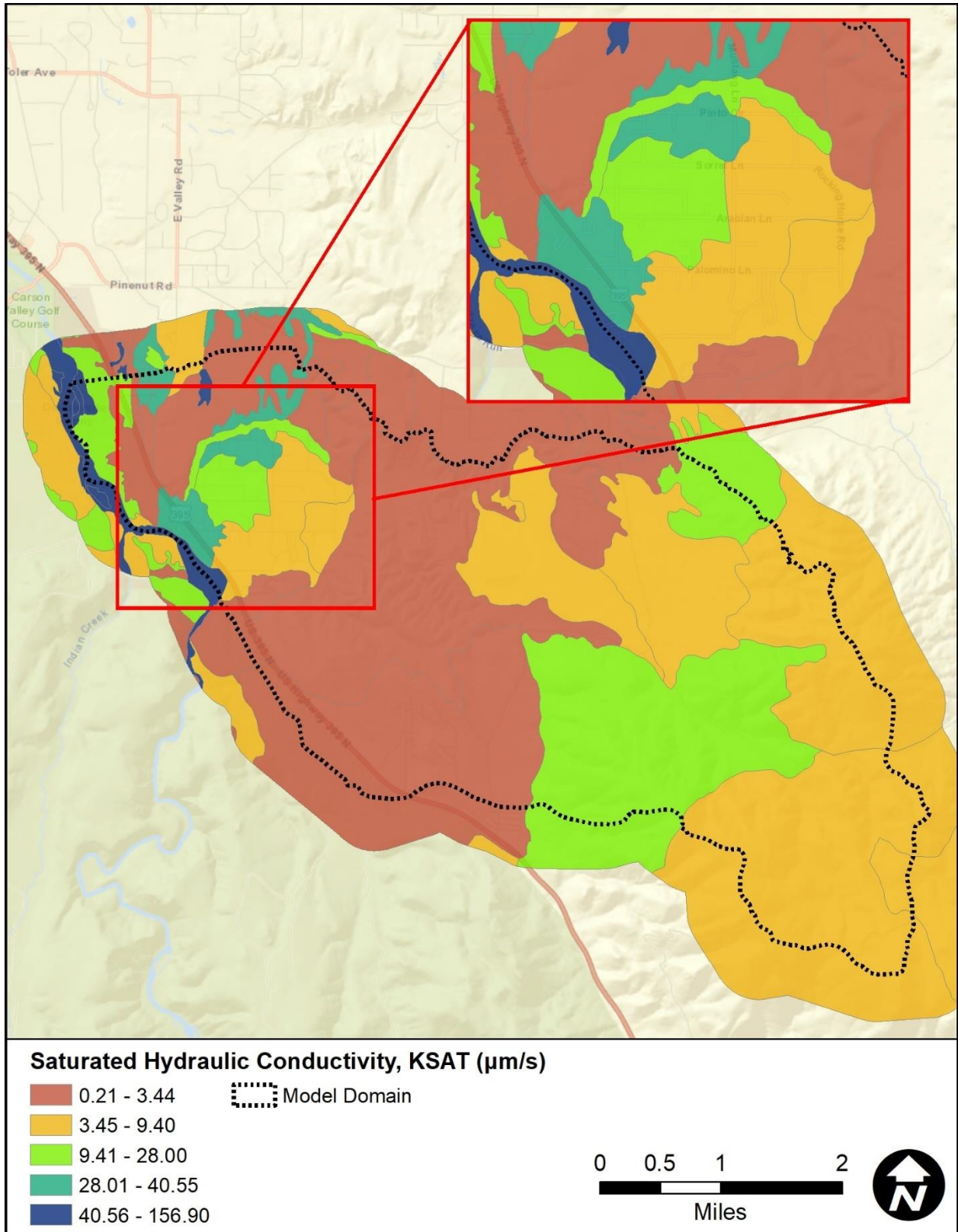


Figure 2-4. Spatial variability of the saturated hydraulic conductivity

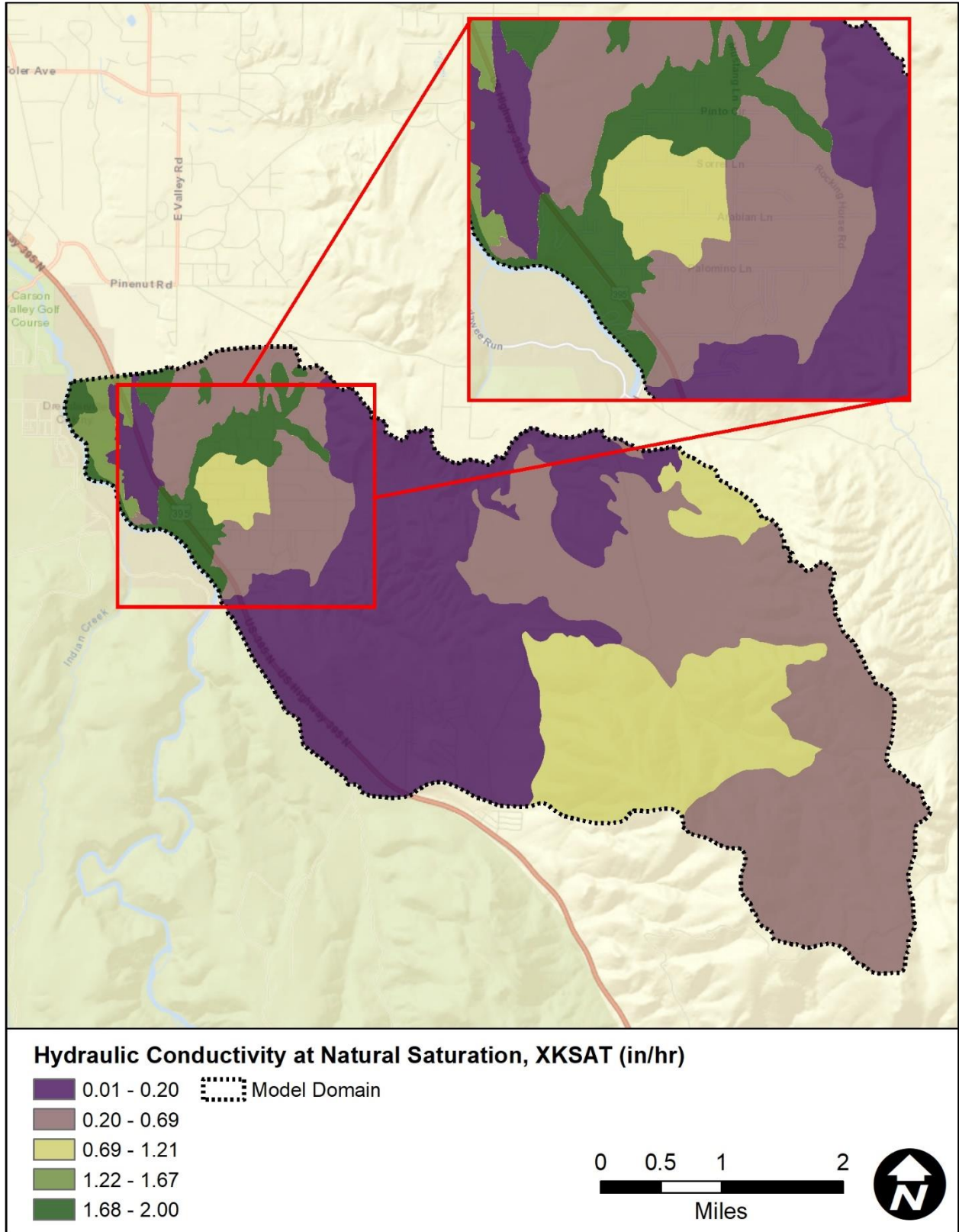


Figure 2-5. XKSAT values used in the FLO-2D modeling

Once the XKSAT values were determined, the values of DTHETA and PSIF were selected from Figure 2-6 and Figure 2-7, respectively. These charts are taken from Mohave County (2018), and they relate the DTHETA and PSIF values to a given XKSAT value. The DTHETA initial moisture condition was chosen based on the surface classification and is discussed in Section 2.2.6.2. The DTHETA and PSIF values that were used in the modeling are shown in Figure 2-8 and Figure 2-9, respectively.

Rock outcrop was set to zero, but percent impervious was used in the surface-based infiltration values (see Section 2.2.6.2). Limiting infiltration depth was set to 20 inches (or 1.67 feet) based on the minimum depth to restrictive layer of 19.69 inches that was extracted from the NRCS soils data. The spatial variability of the depth to a restrictive layer is shown in Figure 2-10, but again the minimum depth of 1.67 feet was used for the entire modeling domain.

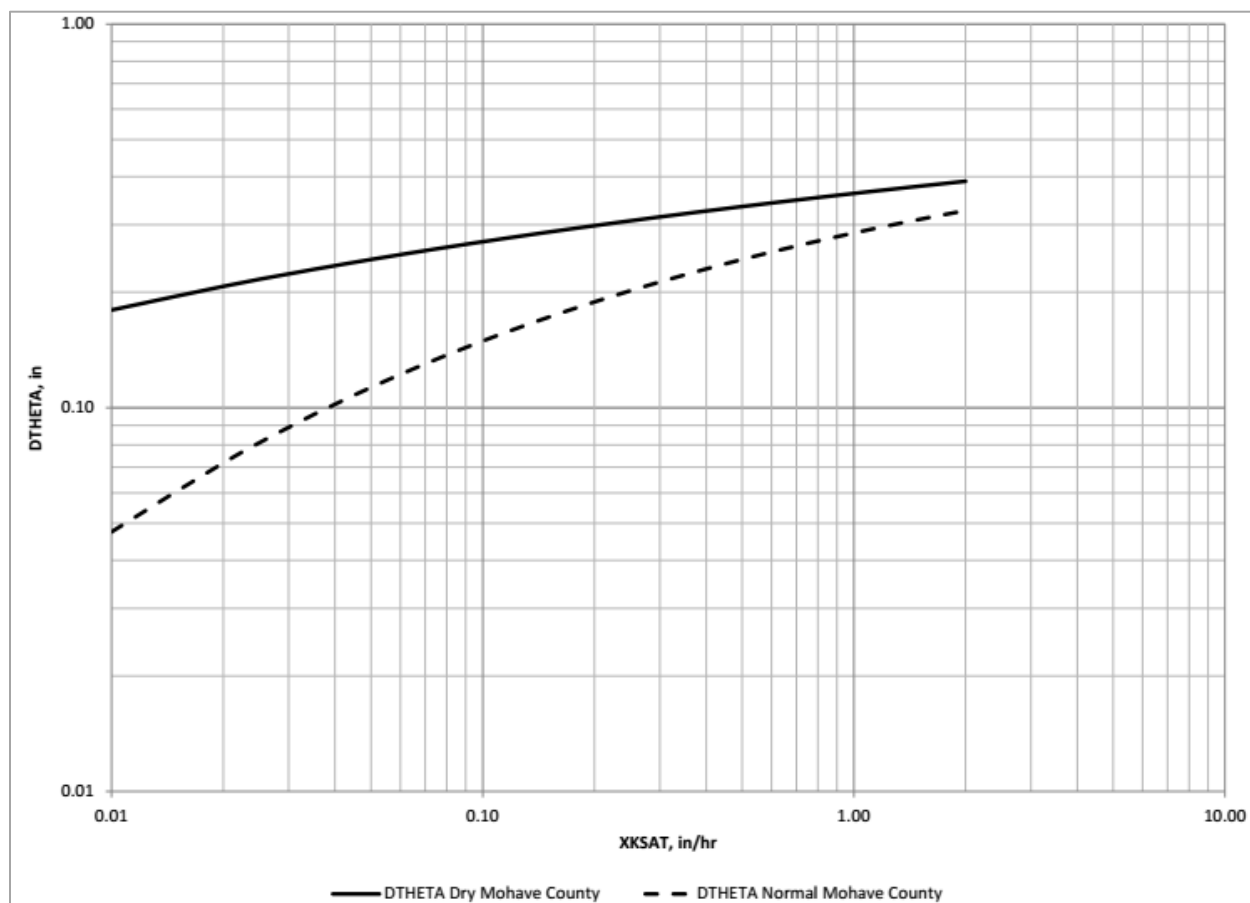


Figure 2-6. Values of DTHETA as a function of XKSAT, reproduced from Mohave County (2018).

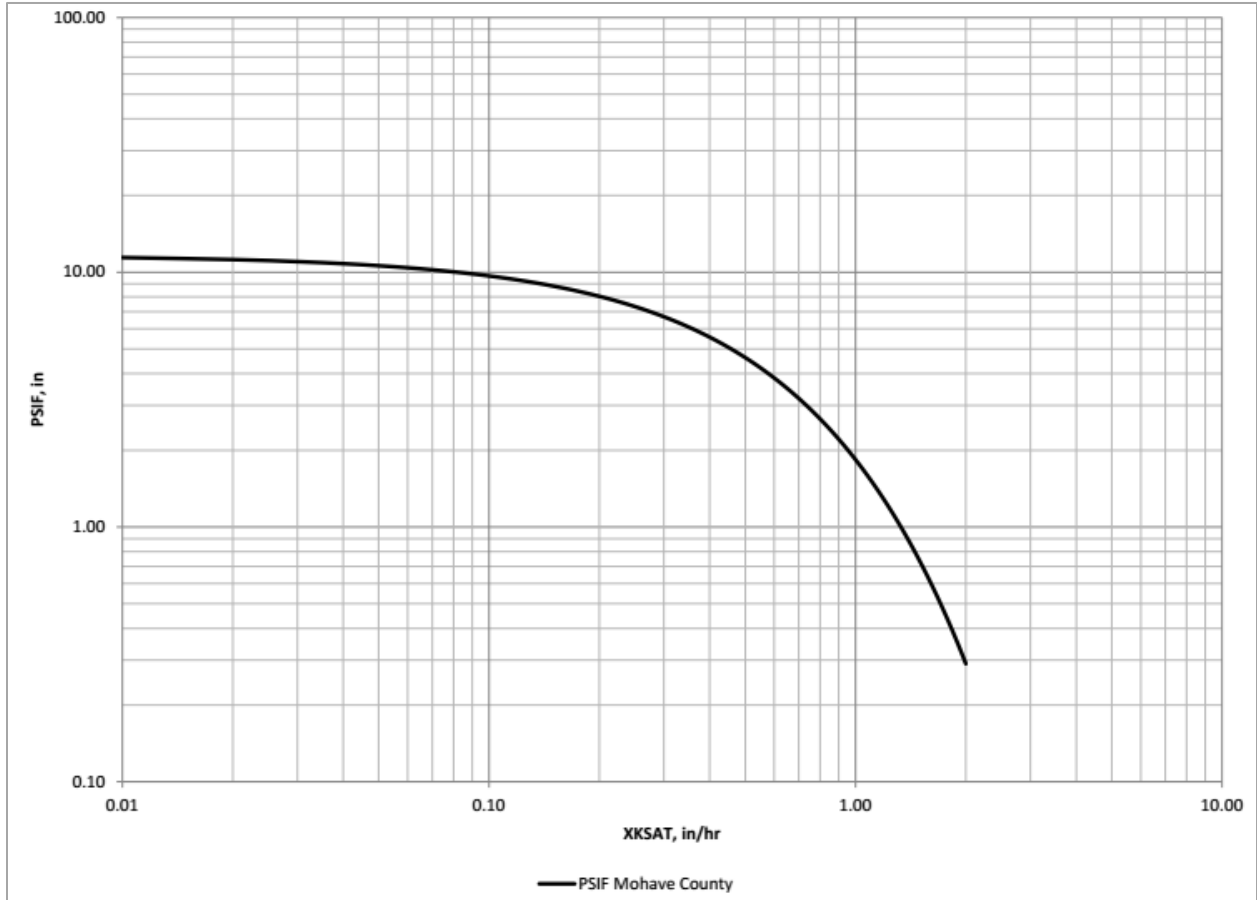


Figure 2-7. Values of PSIF as a function of XKSAT, reproduced from Mohave County (2018).

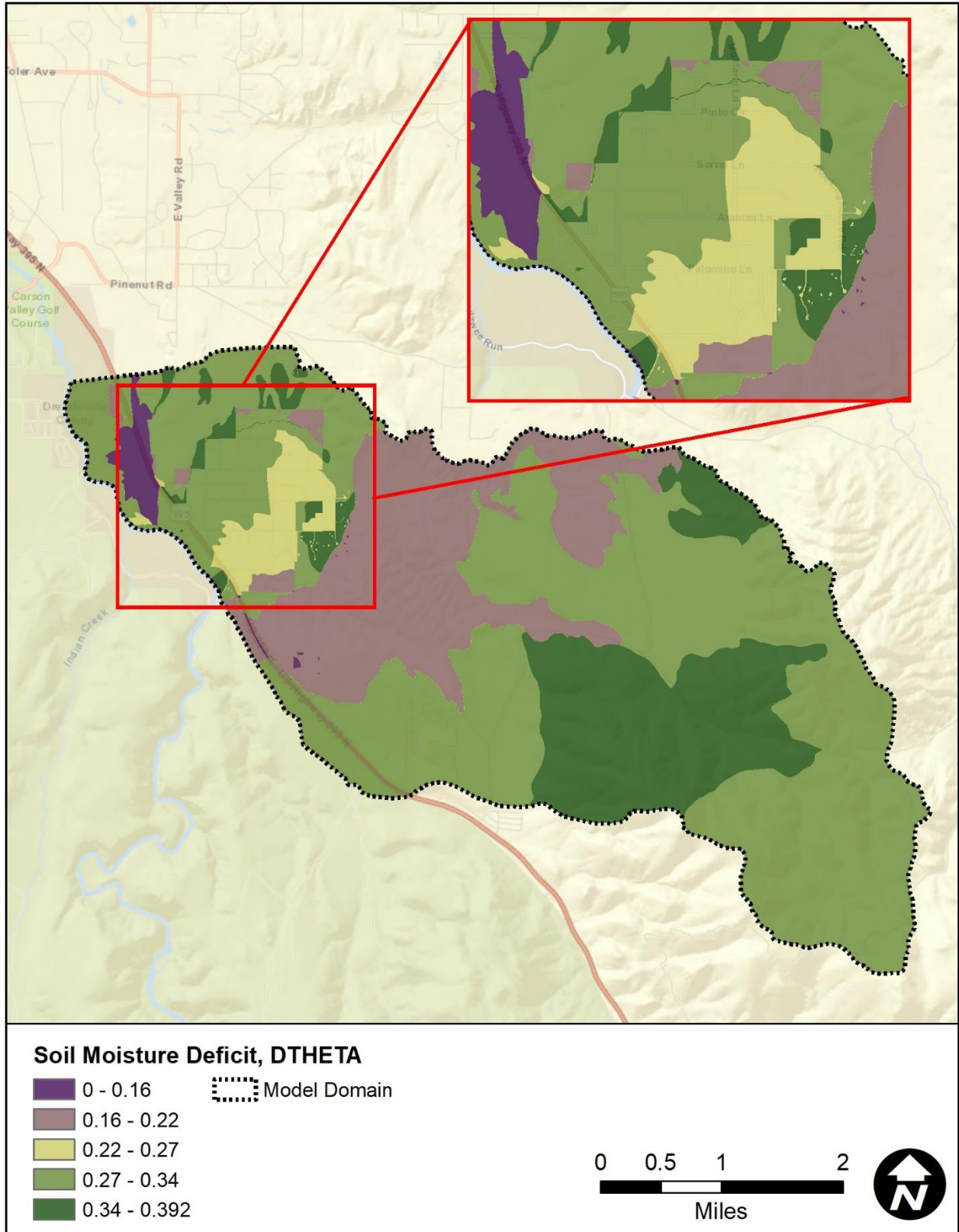


Figure 2-8. DTHETA values used in the FLO-2D modeling

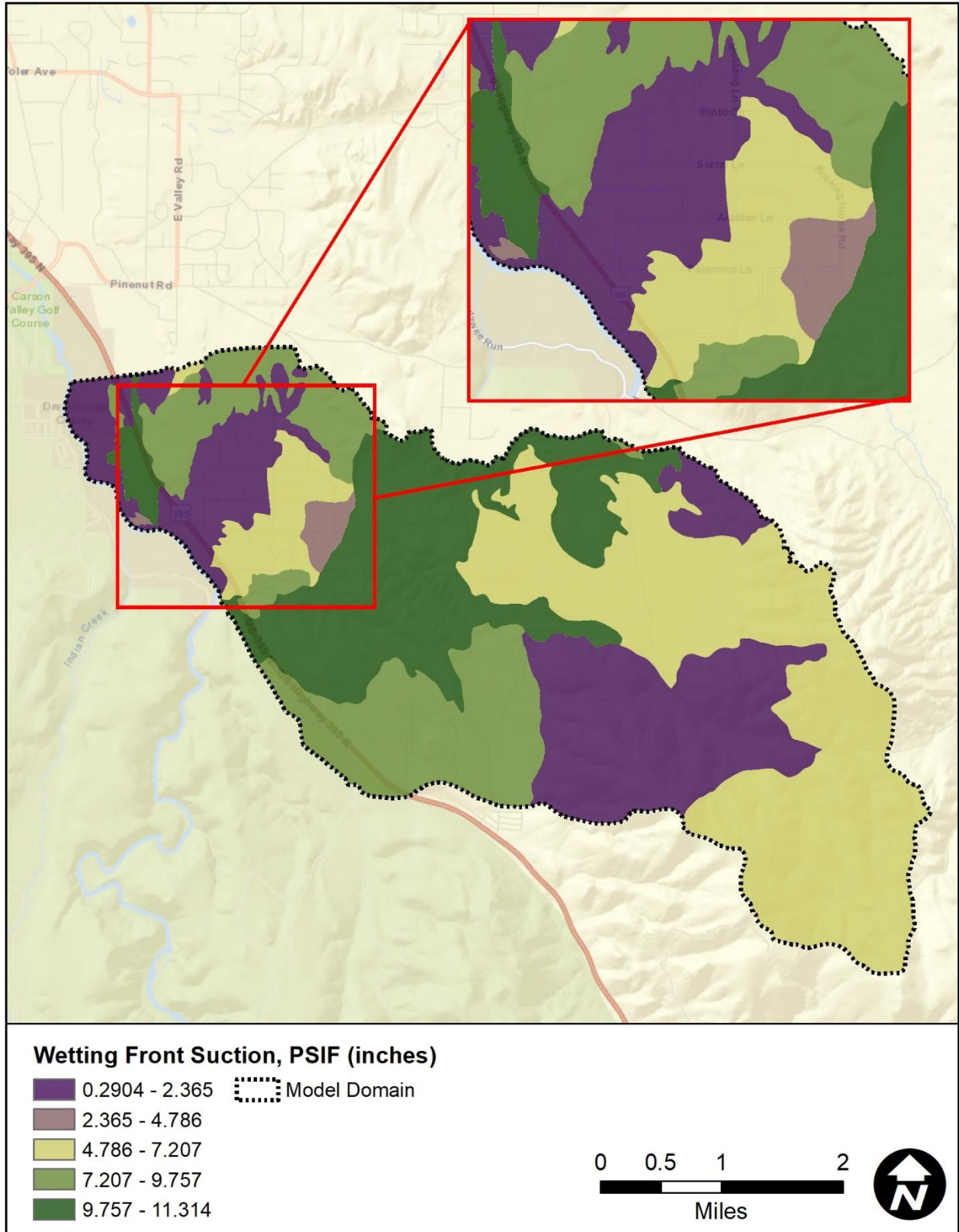


Figure 2-9. PSIF values used in the FLO-2D modeling

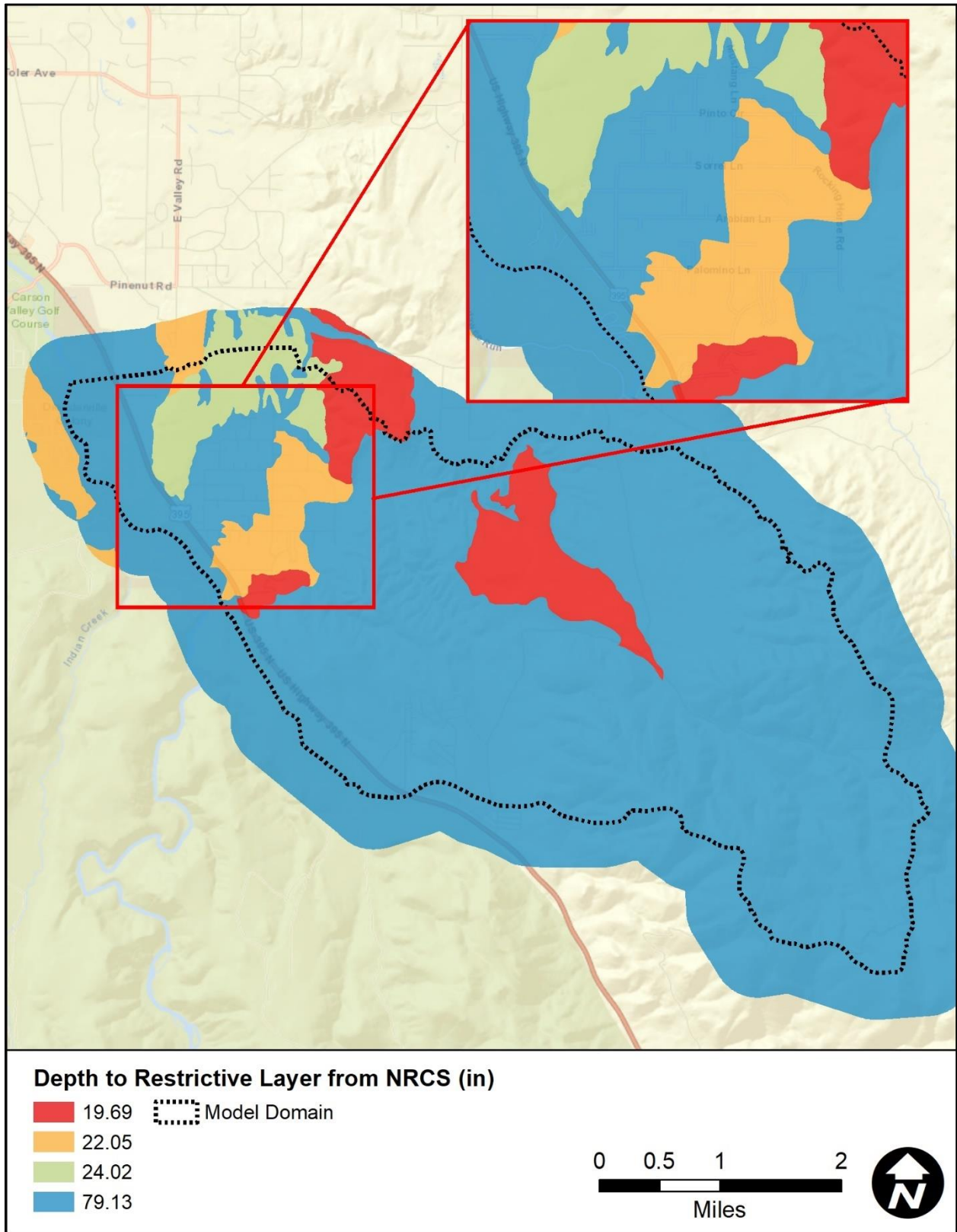


Figure 2-10. Spatial variability of the depth to a restrictive layer, from NRCS (2019)

2.2.6.2 *Surface-based*

The infiltration parameters which are dependent on the conditions and type of the ground surface are:

- Percent impervious, and
- Initial abstraction (IA) in inches.

Table 2-5 shows the surface classification and the corresponding percent impervious and the IA, while the spatial distribution of these land use categories is shown in Figure 2-3. These were selected based on experience in other studies, such as the Alpine View Estates ADMP (JEF 2019a) and the Dayton Valley ADMP (JEF, 2019b), field observations from both JEF and Douglas County staff, and aerial photograph interpretation of the study area. The unimproved roads were given a percent impervious value of 50% to account for added compaction through repeated vehicle use.

Table 2-5. Surface classification with corresponding percent impervious and initial abstraction

| Surface Classification | Percent Impervious (%) | Initial Abstraction ¹ (in) | DTHETA Condition |
|---|------------------------|---------------------------------------|------------------|
| Upper Watershed Rangeland | 0 | 0.45 | dry |
| Focus Areas Rangeland | 0 | 0.35 | dry |
| Maintained Turf | 0 | 0.10 | normal |
| Rural Residential | 15 | 0.15 | normal |
| Unimproved Road | 50 | 0.10 | dry |
| Agriculture | 0 | 0.50 | normal |
| Building | 95 | 0.05 | normal |
| Pavement | 95 | 0.05 | normal |
| Wash | 0 | 0.10 | dry |
| Water | 100 | 0.00 | saturated |
| 1. Note that the initial abstraction used in the modeling has been reduced by 0.048 inches to recognize that the TOL (surface detention) value used by FLO-2D acts as a part of initial abstraction | | | |

2.2.7 Hydraulic Structures

Both culverts and minor storm drains can be simulated with the hydraulic structure routine within the FLO-2D software. Please see the FLO-2D Data Input Manual (FLO-2D Software, Inc., 2019) and the FLO-2D Reference Manual (FLO-2D Software, Inc., 2018) for more details on the application of this routine and its associated modeling options.

All culverts (there are no storm drains within the study area) that were modeled as a part of this ADMP are shown in Figure 2-11. Douglas County provided the consultant team with GIS and as-built data for some structures within the study area and NDOT provided sizes and locations for culverts along US 395. Additionally, JEF staff conducted a field verification visit to the study area in January 2020 to locate additional structures and to verify the information developed from the collected data (e.g. locations, sizes, overall condition, etc.).

2.2.7.1 Culverts

In 2016, the Flood Control District of Maricopa County (FCDMC) produced a comprehensive FLO-2D verification report in which recommendations on modeling hydraulic structures were provided. Per those recommendations, the generalized culvert equation option in FLO-2D was used in the Ruhenstroth ADMP models for single barrel box and circular culverts as a first option. If a single culvert crossing used multiple barrels (or pipes), a rating table was developed assuming inlet control for the culvert. The modeling options that were used to model culverts are summarized in the list below.

- 1) Generalized culvert equations used for single barrel boxes and circular culverts with no tailwater influence (i.e., INOUTCONT parameter set to 0 because the generalized equations account for tailwater conditions).
- 2) If a culvert had multiple barrels (or pipes), a rating table was developed based on inlet control or the width in the generalized culvert equations was adjusted to match the equivalent area of the multiple barrels. Rating tables were used for this study.
- 3) If a culvert had significant sediment blockage, a rating table was developed based on inlet control with a reduced discharge based on the percent area clogged.
- 4) If a culvert had an irregular shape (i.e., ellipse or arch), a rating table was developed based on a simplified EPA-SWMM model (and the flow reduced if there was significant sediment blockage).
- 5) If tailwater conditions could affect flow, a rating table was used and the INOUTCONT parameter in FLO-2D was set to 1.
- 6) If there was potential for reverse flow in a culvert, a rating table was used and the INOUTCONT parameter in FLO-2D was set to 2.

2.2.7.1.1 Clogging Factors

If a culvert was observed to have significant sediment blockage during a field investigation, an appropriate reduction in flow was applied to the rating table or the open area (e.g., if a culvert was blocked by 50%, the flow or open area was reduced by 50%).

In general, smaller culverts (<36 inches) used a 50% clogging factor. Larger culverts (≥ 36 inches and box culverts) did not have a clogging factor except where sediment deposition was observed at the culvert or in the watersheds that exhibited high sediment transport rates. The culverts that used a clogging factor were denoted by adding a “clg” to the name of the structure in the FLO-2D HYSTRUC.DAT input file.

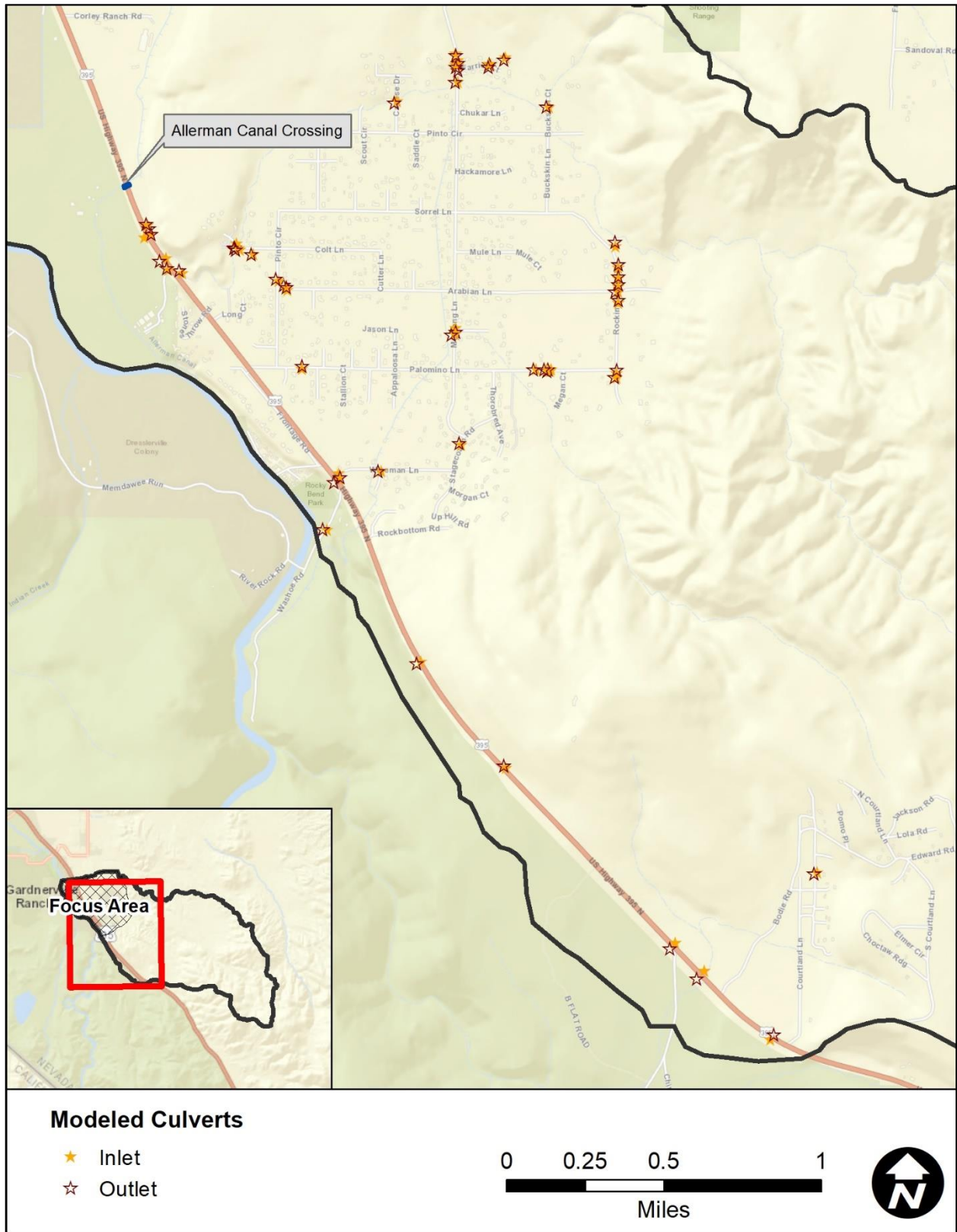


Figure 2-11. Locations of all modeled hydraulic culverts

2.2.7.1.2 Driveway Culverts

Within the focus area, almost every house has a small driveway culvert that allows small roadside ditch flows to pass underneath the driveway (see the example in Figure 2-12). These culverts usually range in size from 12- to 18-inches with the largest driveway culverts observed at 24-inches. Since these culverts are at nearly every house, there are hundreds of such structures within the study area – a number that is impracticable for field verification of every location. Therefore, a generalized rating table was developed for driveway culverts where a detailed measurement was not available. A comparison of the rating tables developed assuming inlet control and a 50% clogging factor for circular culvert sizes 12- to 24-inches and the generalized table is shown in Figure 2-13. The generalized rating table gives a good approximation of flow capacity for a typical driveway culvert at depths below 2 feet (i.e., depths that are commonly seen in roadside ditches). The generalized rating table also uses a 50% clogging factor.

2.2.7.1.3 Allerman Canal Crossing

Since the water surface slope in a canal is extremely flat, the Allerman Canal crossing of US 395 was modeled with lowered cell elevations that approximated the water surface upstream and downstream. This was done to prevent erroneous oscillations that can occur in a FLO-2D hydraulic structure when the headwater/tailwater conditions are nearly equal (e.g., at an equalizer pipe between two basins). The location of the crossing is shown in Figure 2-11.



Figure 2-12. Typical driveway culverts

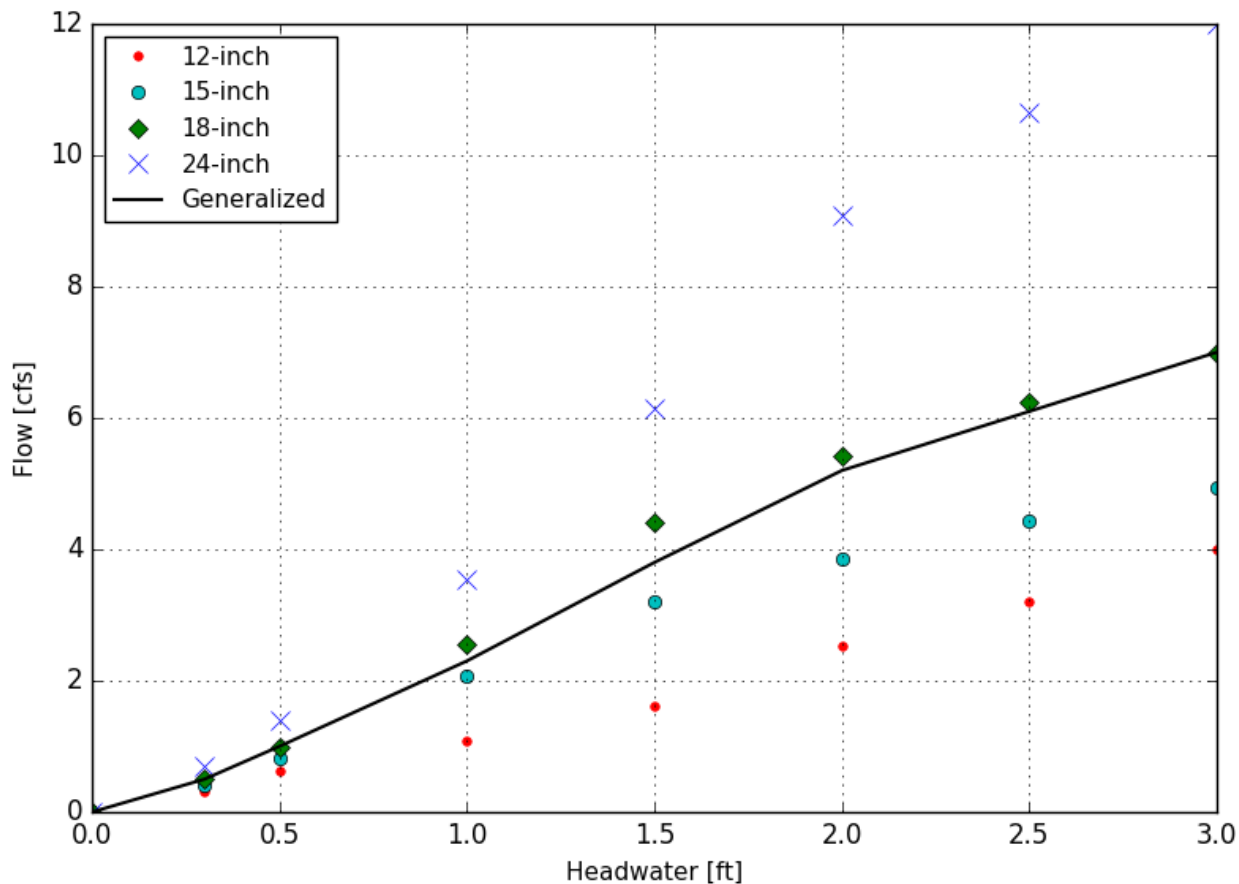


Figure 2-13. Rating table comparison

2.2.8 Buildings (as Flow Obstructions)

Douglas County provided a shapefile of building footprints as a part of initial data collection for this study. This shapefile was updated by the consultant team using the latest available aerial photography (dated late 2018) to reflect the most current conditions.

This updated shapefile was used to create a global area-weighted 10-foot pixel blocked obstruction raster (representing each FLO-2D grid element). The raster was then used to extract the percentage of area obstructed by buildings and assigned to area reduction factors (ARF) for each grid in the model. Cells that were 100% blocked used the FLO-2D totally blocked element routine. The buildings that were modeled with the ARF functionality are shown in Figure 2-3.

2.2.9 Model Control Parameters

CONT.DAT and TOLER.DAT contain numerical stability and simulation controls for the FLO-2D model. The CONT.DAT file controls simulation time, output report time interval, some numerical controls and model switches, such as infiltration and rain. The total simulation time was set to 15 hours for the 6-hour storm, while the total simulation time was set to 30 hours for the 24-hour simulations. These times were sufficient to ensure the floodwave has traveled through the entire study area.

2.2.9.1.1 CONT.DAT

In the CONT.DAT file, the global Manning's n value adjustment factor (AMANN) and the limiting Froude number (FROUDL) were the numerical controls that were used in the Ruhstroth ADMP. For this study, these controls were set to:

- AMANN = 0 (depth integrated roughness is used with the SHALLOWN parameter)
- FROUDL = 0.95
- SHALLOWN = 0.40 (spatially varied shallow Manning's n was also used, see Section 2.2.5)

For the limiting Froude number, a value of 0.95 was used in this study to be consistent with FEMA modeling procedures since the FLO-2D model may be used as the basis for future floodplain delineation and/or redelineation.

The global SHALLOWN parameter was set to 0.40 for the modeling area to account for the increased roughness due to large boulders, rocks, and vegetation at shallow depths. However, the spatially varied shallow n was applied per the detailed surface feature classification, so that a lower shallow n could be used where appropriate (e.g., on paved streets).

2.2.9.1.2 TOLER.DAT

The TOLER.DAT file contains the numerical tolerance settings specified for the model. These settings include: the flow exchange tolerance (TOL), percent allowed change in flow depth (DEPTOL), dynamic wave stability criteria (WAVEMAX), and Courant-Friedrich-Lewy numerical stability parameter for floodplain grid element flow exchange (COURANTFP). For the RADMP models, the settings applied were:

- TOL = 0.004 feet (the depth at which FLO-2D begins to route flow)
- DEPTOL = 0 (not used, model uses Courant number as stability criteria)
- WAVEMAX = 0 (not used, model uses Courant number as stability criteria)
- COURANTFP = 0.6 (main stability criterion used by FLO-2D)

These values have been used in similar studies, which yielded reasonable results. For this project, these values have produced good model stability and reasonable results.

2.3 MODEL RESULTS

2.3.1 Floodplain Cross-Sections

Floodplain cross-sections were developed and included in the FPXSEC.DAT file to query flow hydrographs, peak discharges, and flow volumes from the FLO-2D model at key locations, such as:

- Major flow concentration locations,
- Areas near potential mitigation sites, and
- Areas of interest to Douglas County

Major floodplain cross-section locations are shown on Figure 2-14. Hydrograph plots at the floodplain cross-sections for each storm event are included in Appendix B. The peak flow and volume for each floodplain cross-section are shown in Table 2-6.

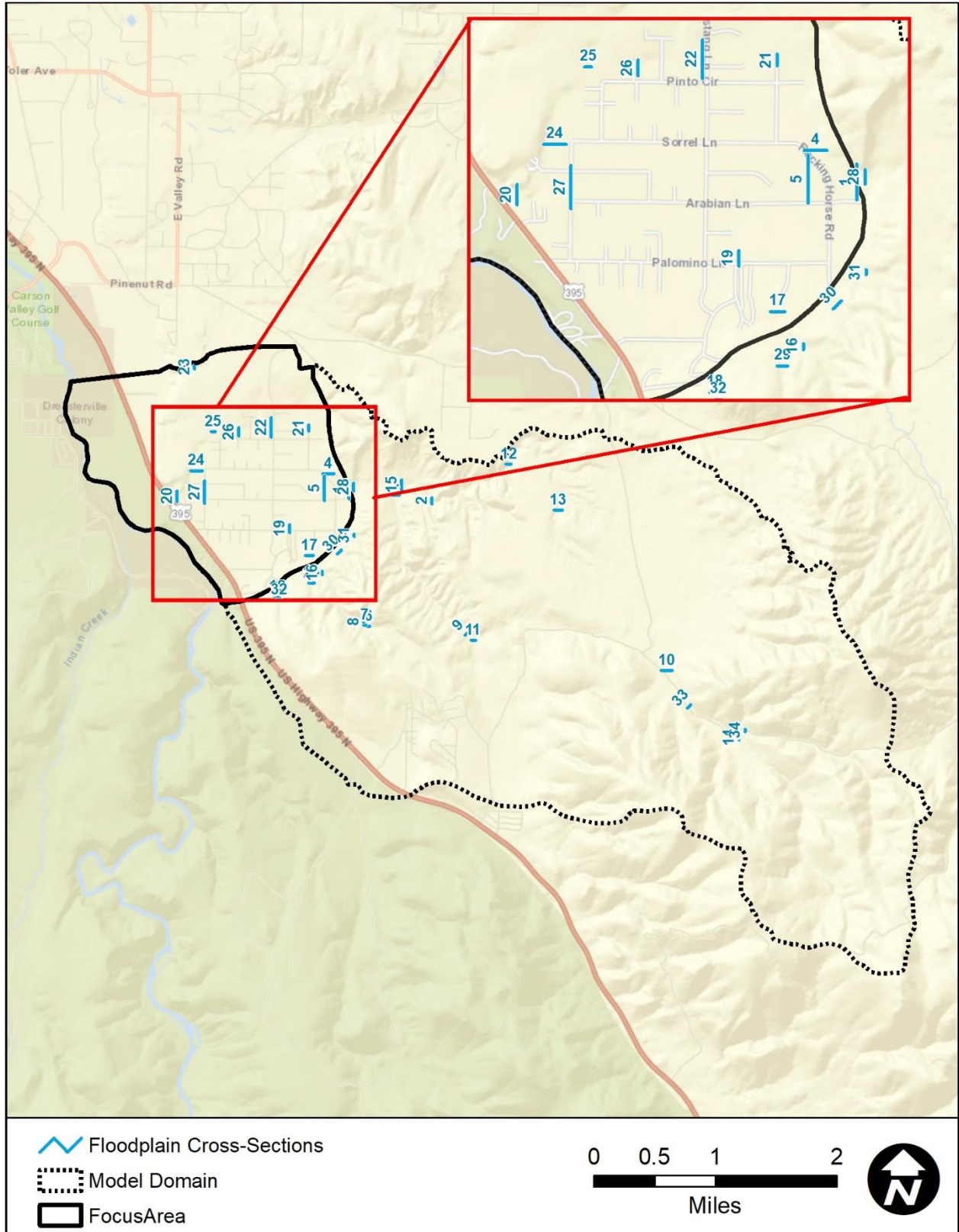


Figure 2-14. Floodplain cross-section locations

Table 2-6. Peak flow and volume results from the FLO-2D floodplain cross-sections

| ID | 100Y24H | | 100Y6H | | 25Y24H | |
|----|-----------|--------|-----------|--------|-----------|--------|
| | Peak Flow | Volume | Peak Flow | Volume | Peak Flow | Volume |
| | cfs | ac-ft | cfs | ac-ft | cfs | ac-ft |
| 1 | 1233 | 476 | 1393 | 232 | 636 | 241 |
| 2 | 793 | 255 | 1009 | 136 | 266 | 108 |
| 3 | 391 | 161 | 736 | 72 | 256 | 93 |
| 4 | 1232 | 475 | 1373 | 231 | 632 | 240 |
| 5 | 1 | 0 | 9 | 0 | 0 | 0 |
| 6 | 87 | 32 | 221 | 14 | 61 | 21 |
| 7 | 43 | 16 | 113 | 7 | 30 | 10 |
| 8 | 133 | 48 | 331 | 21 | 93 | 32 |
| 9 | 204 | 71 | 416 | 34 | 83 | 31 |
| 10 | 576 | 119 | 1323 | 78 | 97 | 15 |
| 11 | 119 | 31 | 114 | 14 | 15 | 6 |
| 12 | 726 | 212 | 1028 | 115 | 189 | 79 |
| 13 | 575 | 131 | 1005 | 81 | 87 | 24 |
| 14 | 310 | 64 | 658 | 38 | 66 | 11 |
| 15 | 840 | 288 | 981 | 150 | 327 | 130 |
| 16 | 212 | 78 | 464 | 34 | 151 | 52 |
| 17 | 236 | 86 | 528 | 37 | 168 | 58 |
| 18 | 51 | 19 | 91 | 8 | 37 | 13 |
| 19 | 266 | 93 | 527 | 38 | 172 | 59 |
| 20 | 1400 | 554 | 964 | 232 | 669 | 267 |
| 21 | 480 | 228 | 482 | 107 | 329 | 118 |
| 22 | 1221 | 472 | 997 | 221 | 599 | 233 |
| 23 | 0 | 0 | 3 | 0 | 0 | 0 |
| 24 | 1206 | 459 | 840 | 206 | 555 | 220 |
| 25 | 0 | 0 | 9 | 1 | 0 | 0 |
| 26 | 1219 | 468 | 932 | 216 | 587 | 229 |
| 27 | 244 | 91 | 345 | 27 | 128 | 44 |
| 28 | 1231 | 475 | 1389 | 232 | 634 | 241 |
| 29 | 25 | 9 | 111 | 4 | 19 | 6 |
| 30 | 32 | 12 | 138 | 5 | 23 | 8 |
| 31 | 15 | 6 | 66 | 2 | 11 | 4 |
| 32 | 49 | 18 | 88 | 8 | 36 | 12 |
| 33 | 580 | 119 | 1301 | 76 | 101 | 16 |
| 34 | 240 | 49 | 527 | 30 | 43 | 6 |

2.3.2 Depth and Discharge Results

Flow depth and discharge results from the existing conditions FLO-2D modeling are shown on Figure 2-15 through Figure 2-20. These figures are for general illustrative purposes and not practical for

obtaining detailed information at site-specific locations. For more detailed information, please see the digital data in Appendix B, which includes the grid-based results for maximum flow depth, maximum peak discharge, maximum velocity, and other FLO-2D output.

2.3.3 Animations

Google Earth animations of the Lower model have been included with the digital model results (see Appendix B). These animations are helpful for visualizing the dynamic nature of the flooding as it moves through the study area.

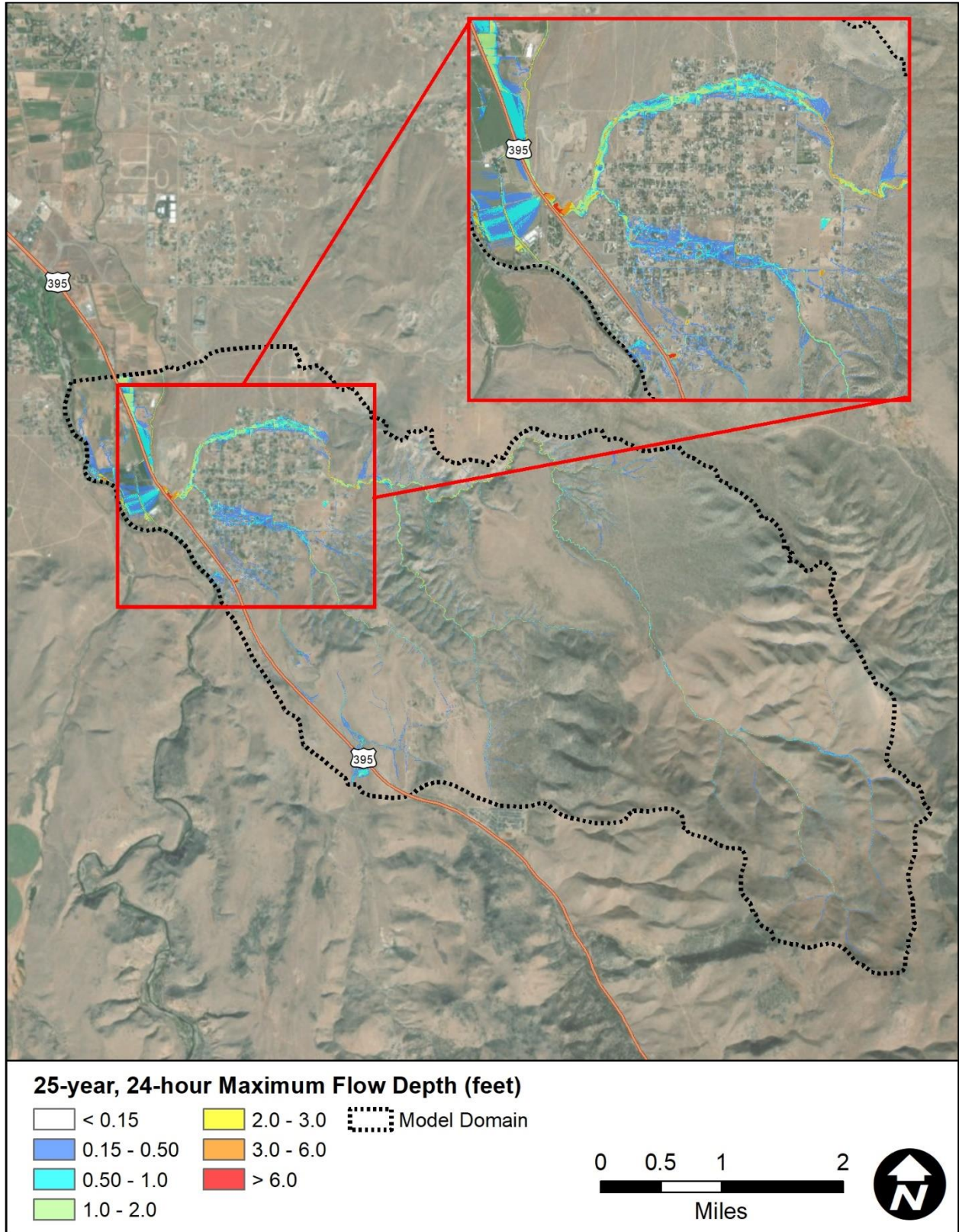


Figure 2-15. Existing conditions 25-year, 24-hour flow depth results

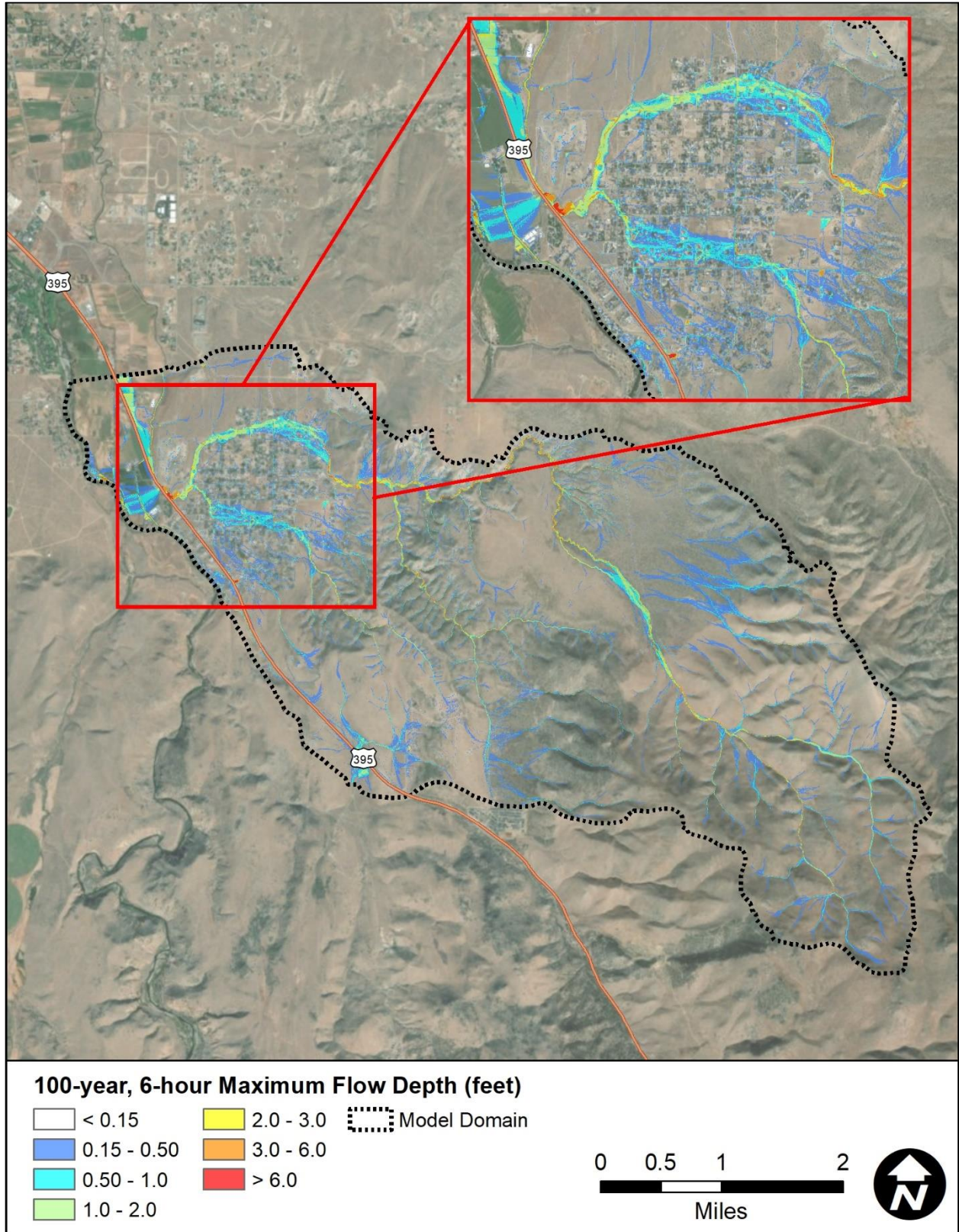


Figure 2-16. Existing conditions 100-year, 6-hour flow depth results

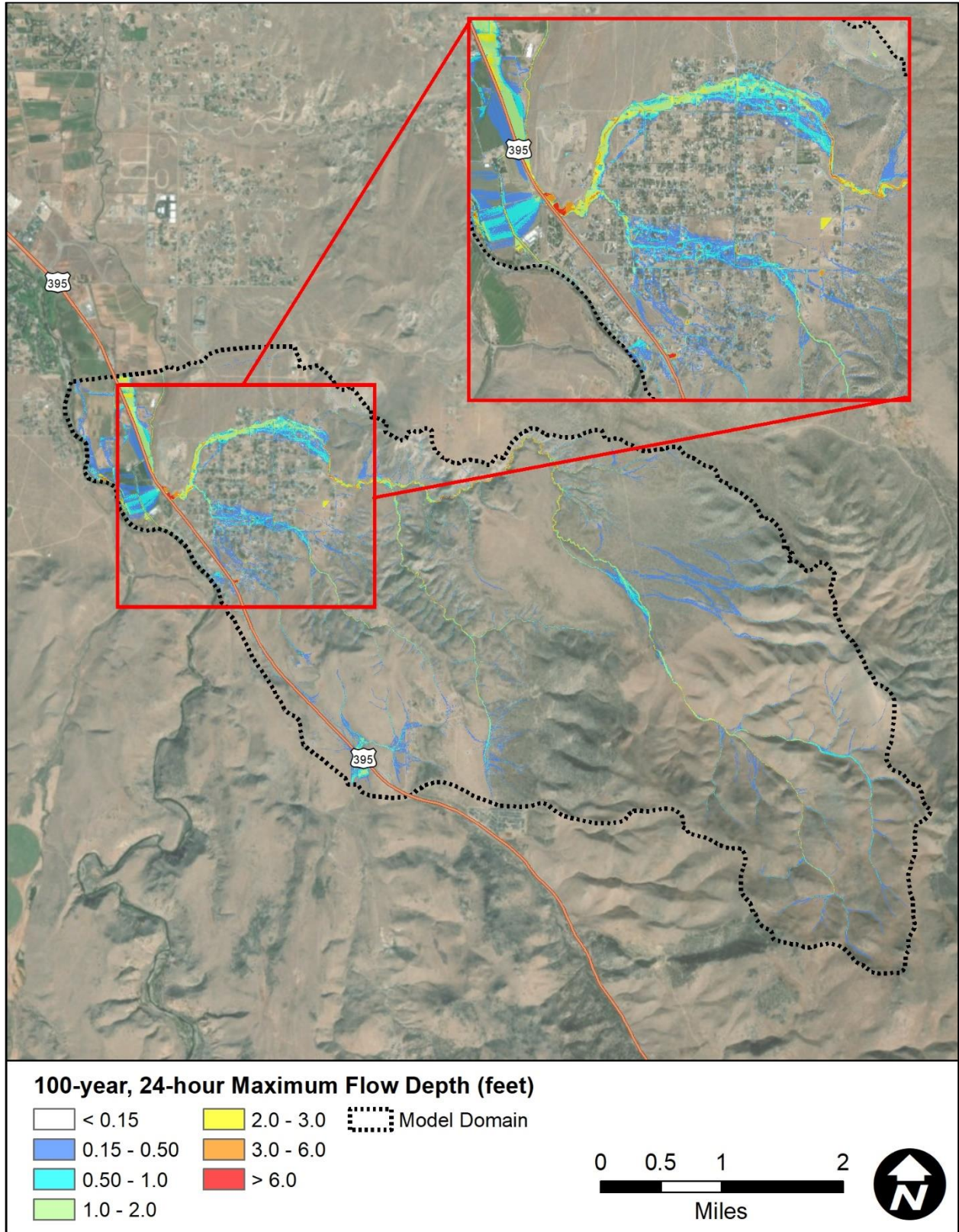


Figure 2-17. Existing conditions 100-year, 24-hour flow depth results

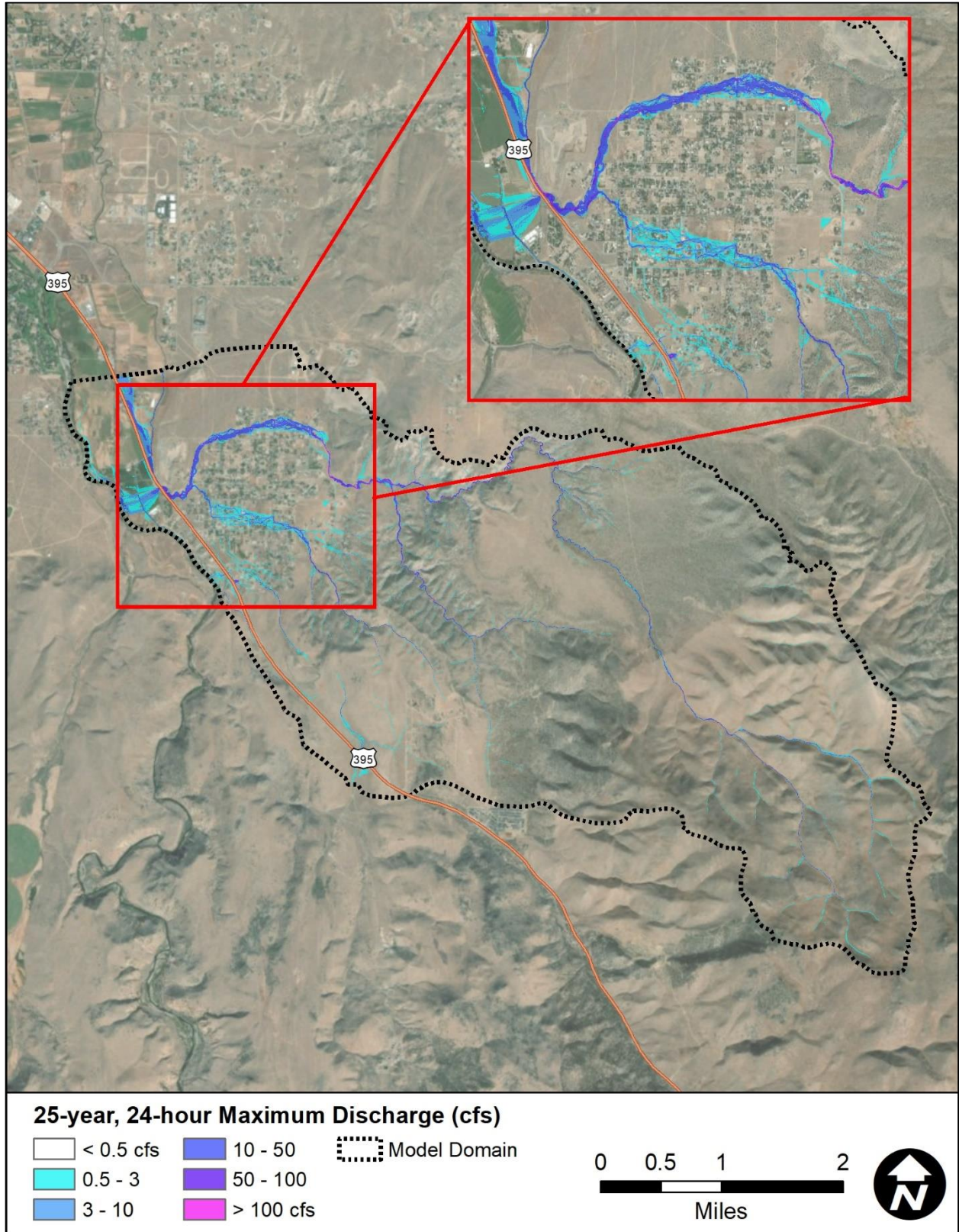


Figure 2-18. Existing conditions 25-year, 24-hour discharge results

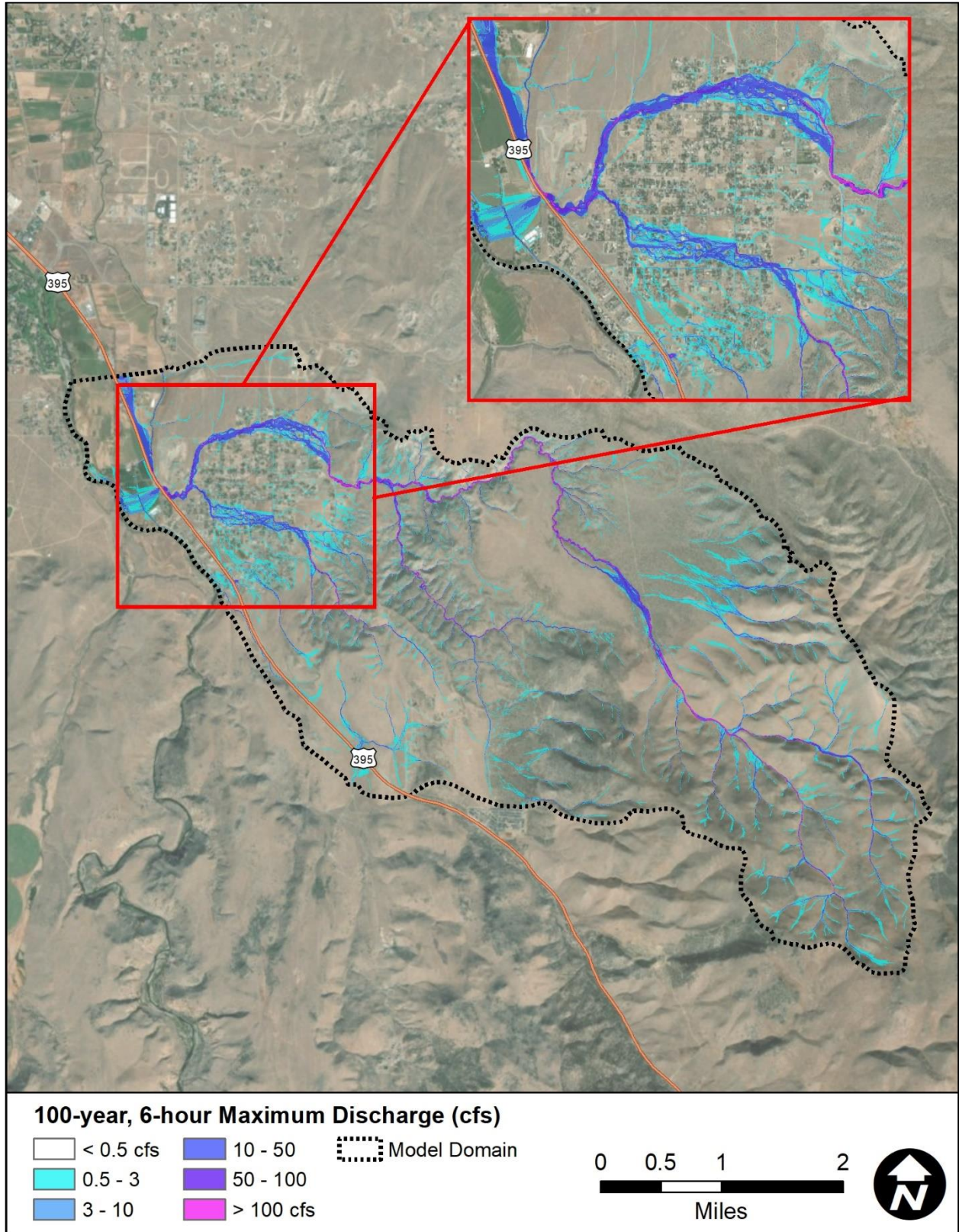


Figure 2-19. Existing conditions 100-year, 6-hour discharge results

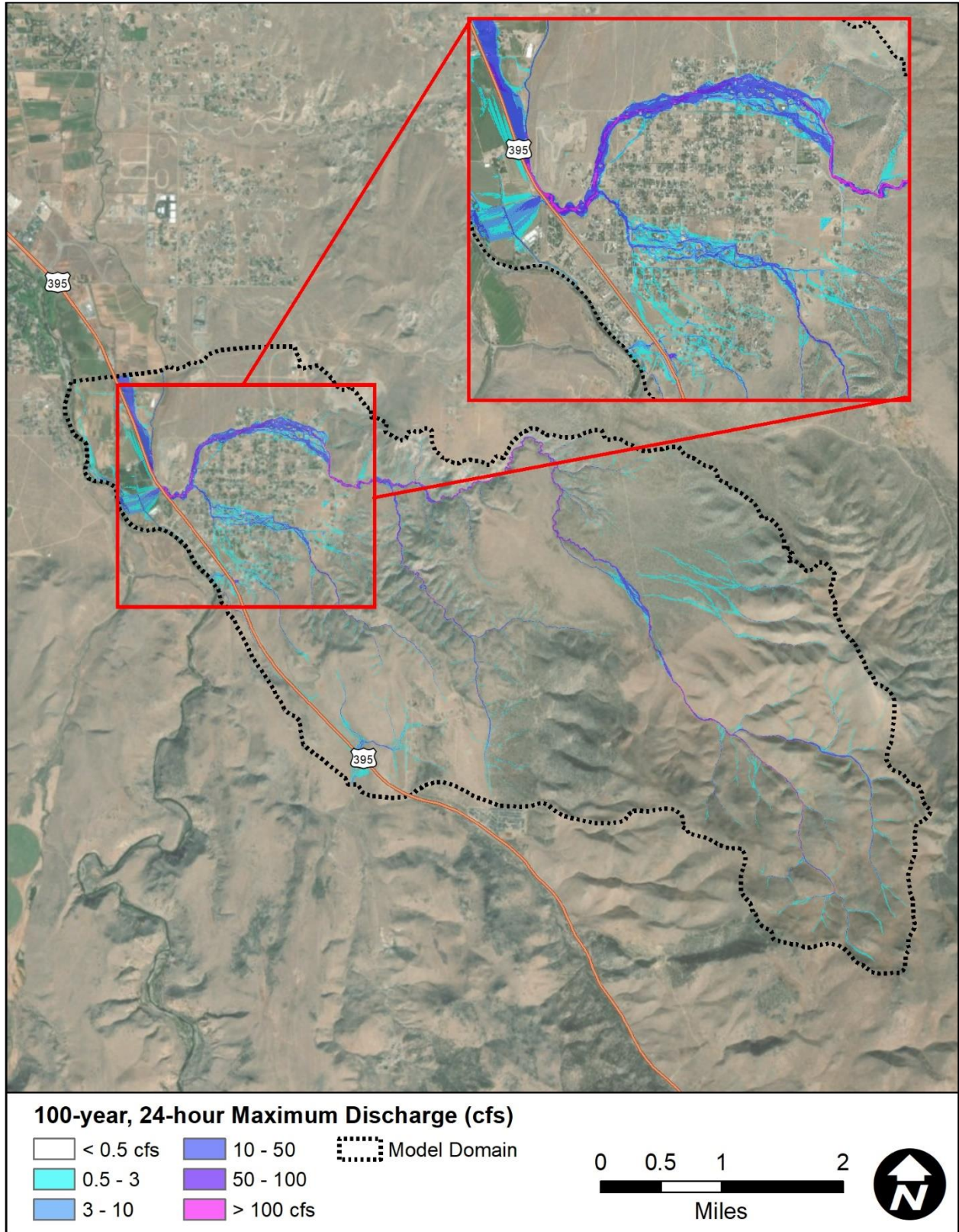


Figure 2-20. Existing conditions 100-year, 24-hour discharge results

2.4 VERIFICATION OF RESULTS

2.4.1 Comparison with USGS Regression Equations

As a verification of model results, the 100-year 6- and 24-hour results at seven drainage basins were compared with the 100-year USGS regression equation, shown as Equation (1), for the Eastern Sierras Region 5 (USGS, 1997).

$$Q_{100} = 7000AREA^{0.782}(ELEV/1000)^{-2.18}(LAT - 28)^{4.6} \quad (2)$$

Where:

- Q_{100} is the 100-year peak discharge (cfs)
- $AREA$ is the drainage area (square miles)
- $ELEV$ is mean basin elevation (ft)
- LAT is the latitude of site (decimal degrees)

The results from this comparison are shown in Table 2-7 and Figure 2-21, while the basin locations used for this comparison are shown in Figure 2-22.

Table 2-7 shows both the 100-year 6-hour (labeled as 100Y6H) and the 100-year 24-hour (labeled as 100Y24H) peak flow results from the FLO-2D modeling compared with the 100-year flow from the regression equation. The unit discharges for each basin and the median values are also calculated and shown in the table.

The comparison indicates that the FLO-2D results for the entire study area are generally reasonable. In Figure 2-21, all results fall below the USGS envelope curve and within the cloud of values, and both the 100-year 6-hour and 100-year 24-hour results follow the low- to middle-elevation study area line (which includes USGS Regression Regions 2-16, not just Region 5). However, both storm values are above the 100-year discharge relation for Region 5, but it should be noted that the USGS used mean values for variables other than drainage area when plotting this line. Therefore, this plot may not appear to fit the data.

In general, the results appear reasonable. The 100-year 24-hour median unit discharge compare extremely well with the median generated from Equation (1). However, the 100-year 6-hour median unit discharge is much larger than the regression median, but the 6-hour results are dominated by basins that are much smaller than 1 square mile where localized intense storm events can generate very high peak flows.

Table 2-7. Comparison with 100-year USGS regression equation

| Basin ID | Basin Area | Regression Peak Flow | Regression Unit Discharge | 100Y6H Peak Flow | 100Y6H Unit Discharge | 100Y24H Peak Flow | 100Y24H Unit Discharge |
|----------|-----------------|----------------------|---------------------------|------------------|-----------------------|-------------------|------------------------|
| | mi ² | cfs | cfs/mi ² | cfs | cfs/mi ² | cfs | cfs/mi ² |
| 1 | 11.828 | 1,473 | 125 | 1,389 | 117 | 1,231 | 104 |
| 2 | 3.451 | 449 | 130 | 1,301 | 377 | 580 | 168 |
| 3 | 2.930 | 552 | 189 | 736 | 251 | 391 | 134 |
| 4 | 0.605 | 179 | 296 | 464 | 768 | 212 | 350 |
| 5 | 0.128 | 54 | 419 | 88 | 691 | 49 | 385 |
| 6 | 0.084 | 40 | 480 | 138 | 1,645 | 32 | 379 |
| 7 | 0.065 | 33 | 503 | 111 | 1,713 | 25 | 390 |
| 8 | 0.040 | 23 | 579 | 66 | 1,643 | 15 | 377 |
| | | Median: | 358 | - | 729 | - | 363 |

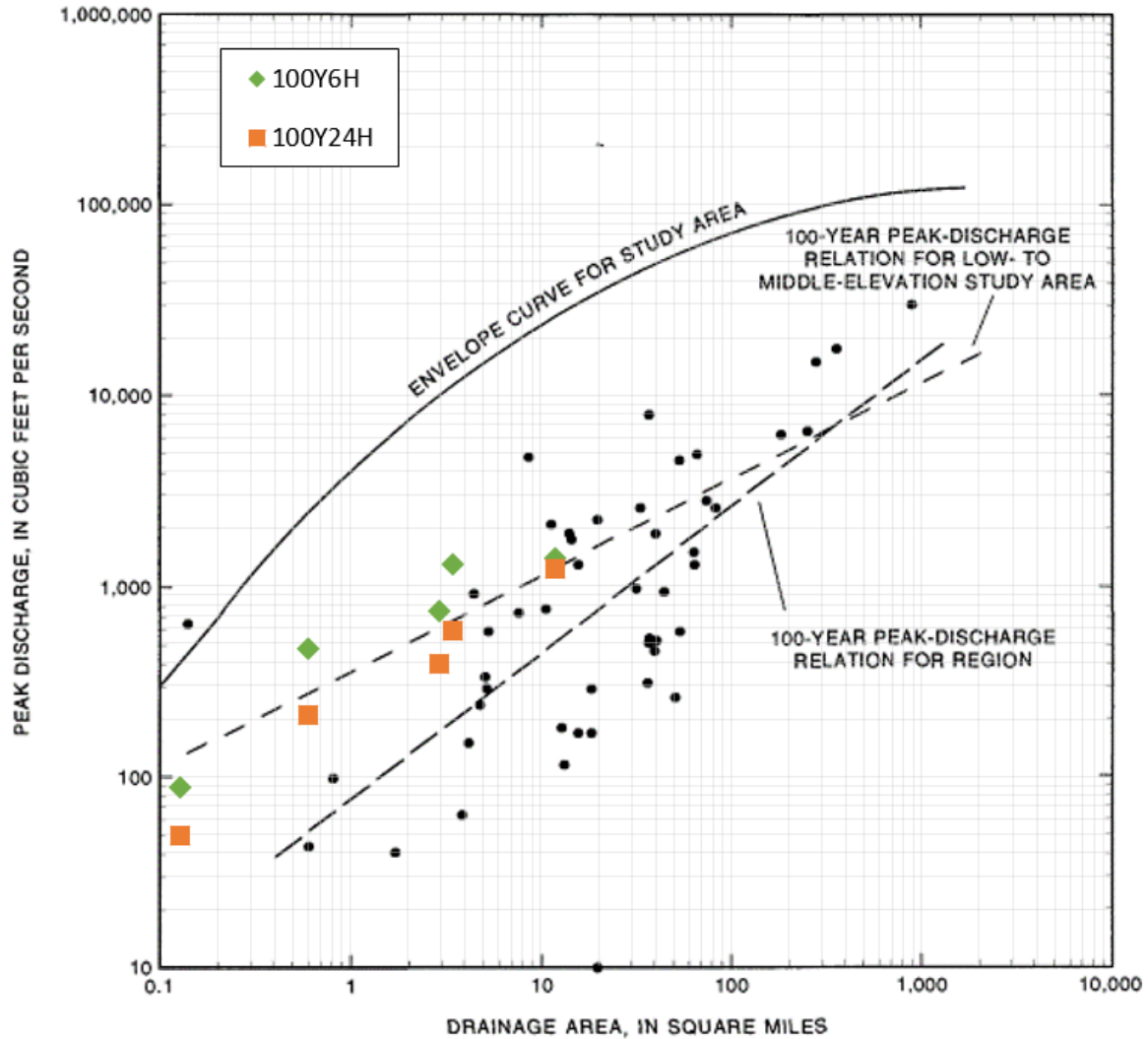


Figure 2-21. Comparison of FLO-2D results with the relations between 100-year peak discharge and drainage area and plot of maximum peak discharge of record and drainage area for gaged sites in the Eastern Sierras Region 5, adapted from USGS (1997)

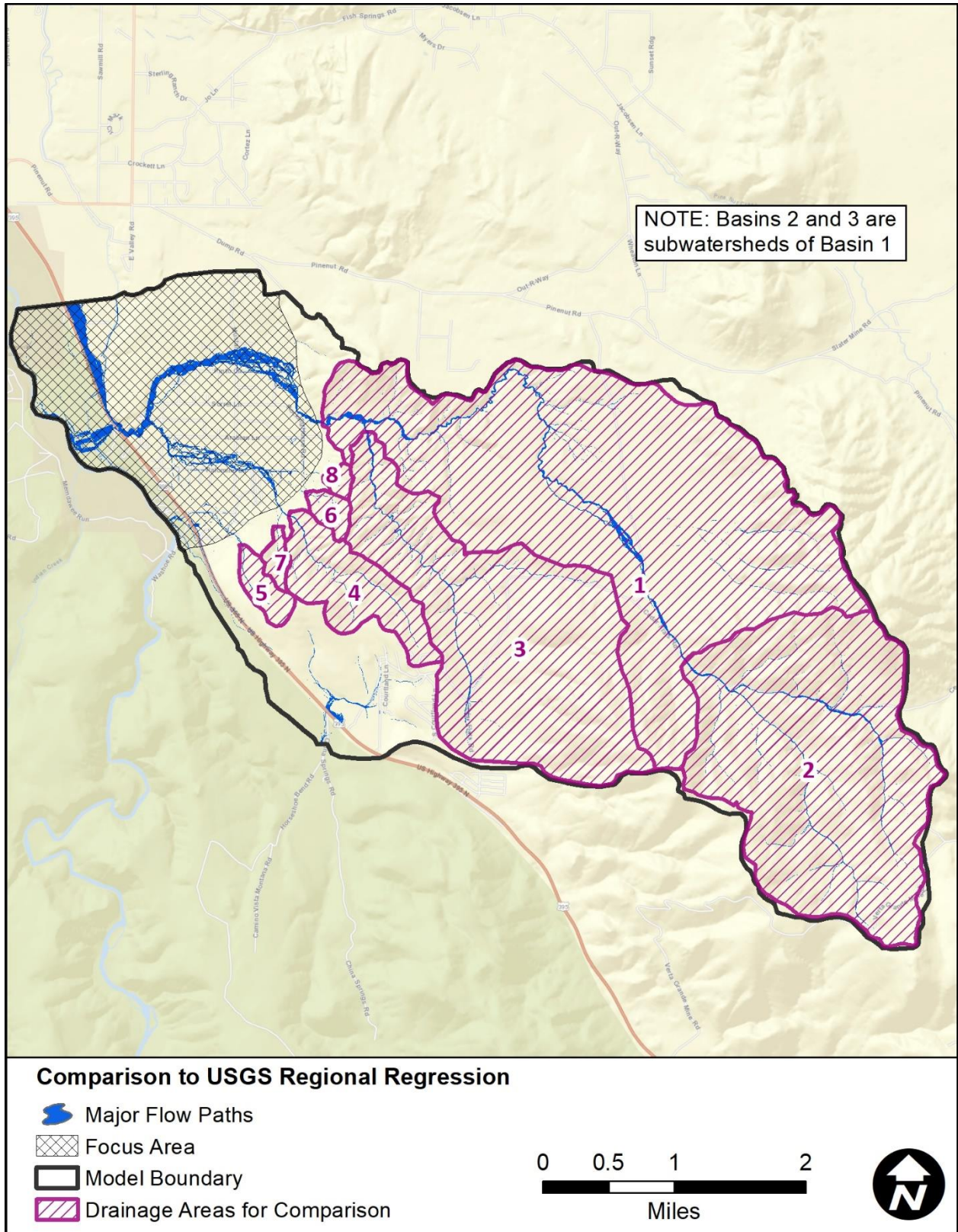


Figure 2-22. Drainage basins used for comparison of FLO-2D results to the USGS 100-year regression equations

2.4.2 Additional USGS Data

As part of another hydrology update project, NDOT recently obtained peak flow estimates for both inactive and active crest stage sites. Since these were crest gages, they contained only peak flow estimates rather than entire hydrographs.

The maximum peak of record for each gage was parsed from the USGS data peak flow data, while the drainage area was collected from each gage’s site description on the USGS website. However, not all gages listed the drainage area in the site description. Of the 216 total sites, forty-five did not list the drainage area, and these sites were excluded from the comparison to the ADMP peak results. A summary of the drainage area statistics for all 216 sites is shown in Figure 2-23, and the spatial location of the sites is shown in Figure 2-24.

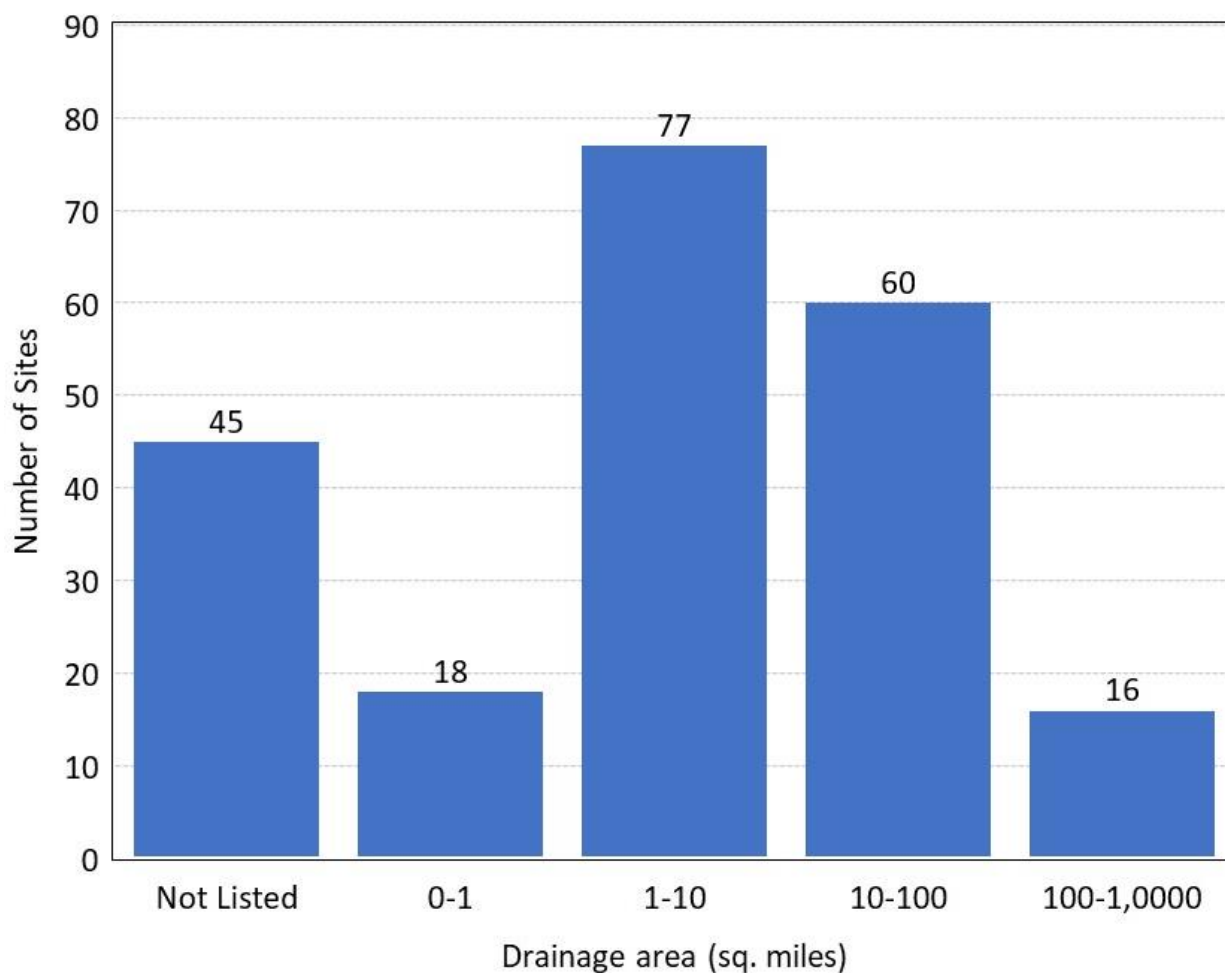


Figure 2-23. Drainage area statistics for USGS crest stage sites

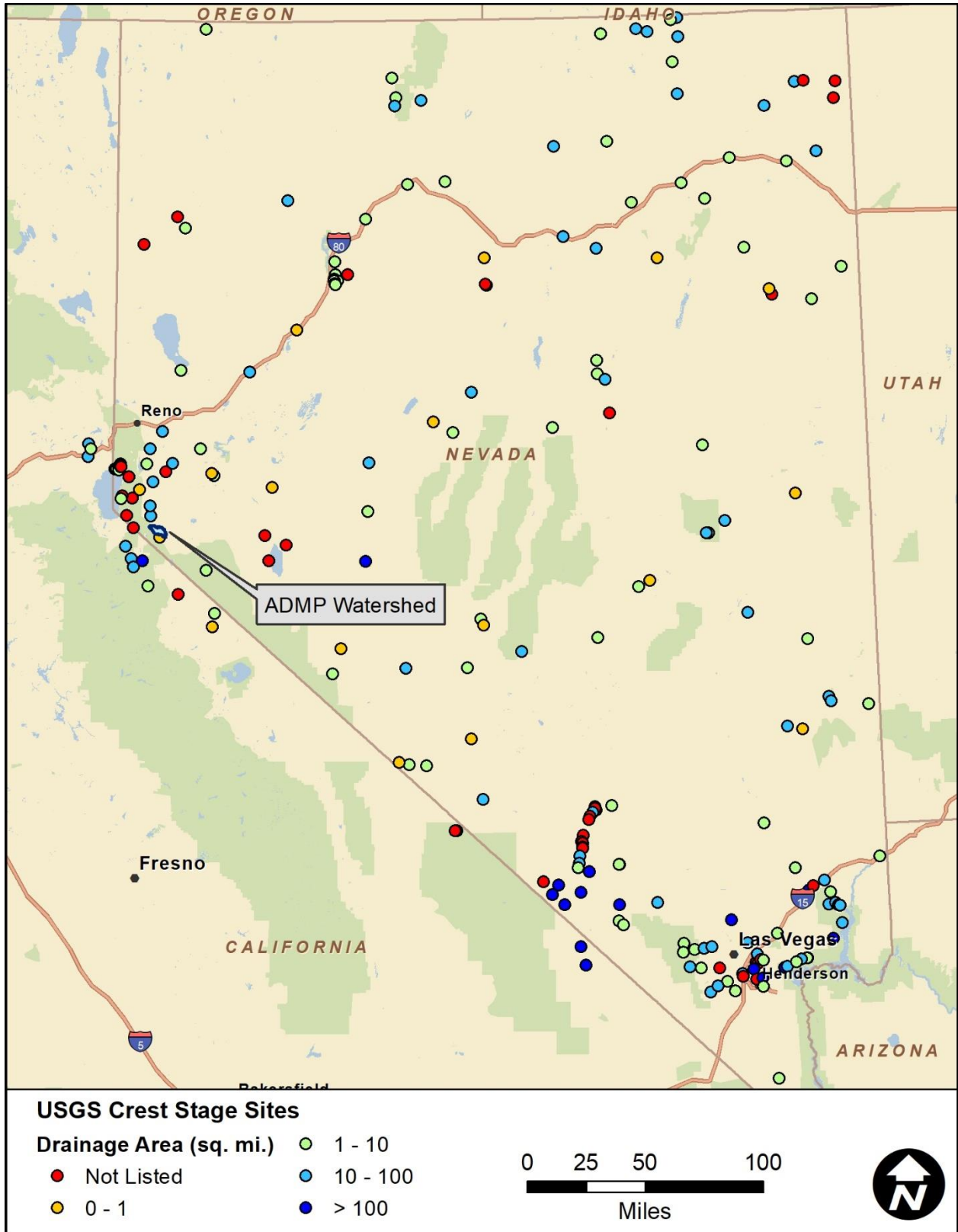


Figure 2-24. Location and drainage areas of USGS crest stage sites

As an additional verification of the peak flow estimates for the ADMP, the crest stage flow peak estimates were compared with the 100-year, 24-hour and 100-year, 6-hour FLO-2D results and peak flow estimates from the 1997 100-year regression equation (Equation 1). This comparison is shown as Figure 2-25. As before, both the FLO-2D and the 100-year regression estimates fall within the cloud of data, which provides another indicator that the RADMP results are reasonable.

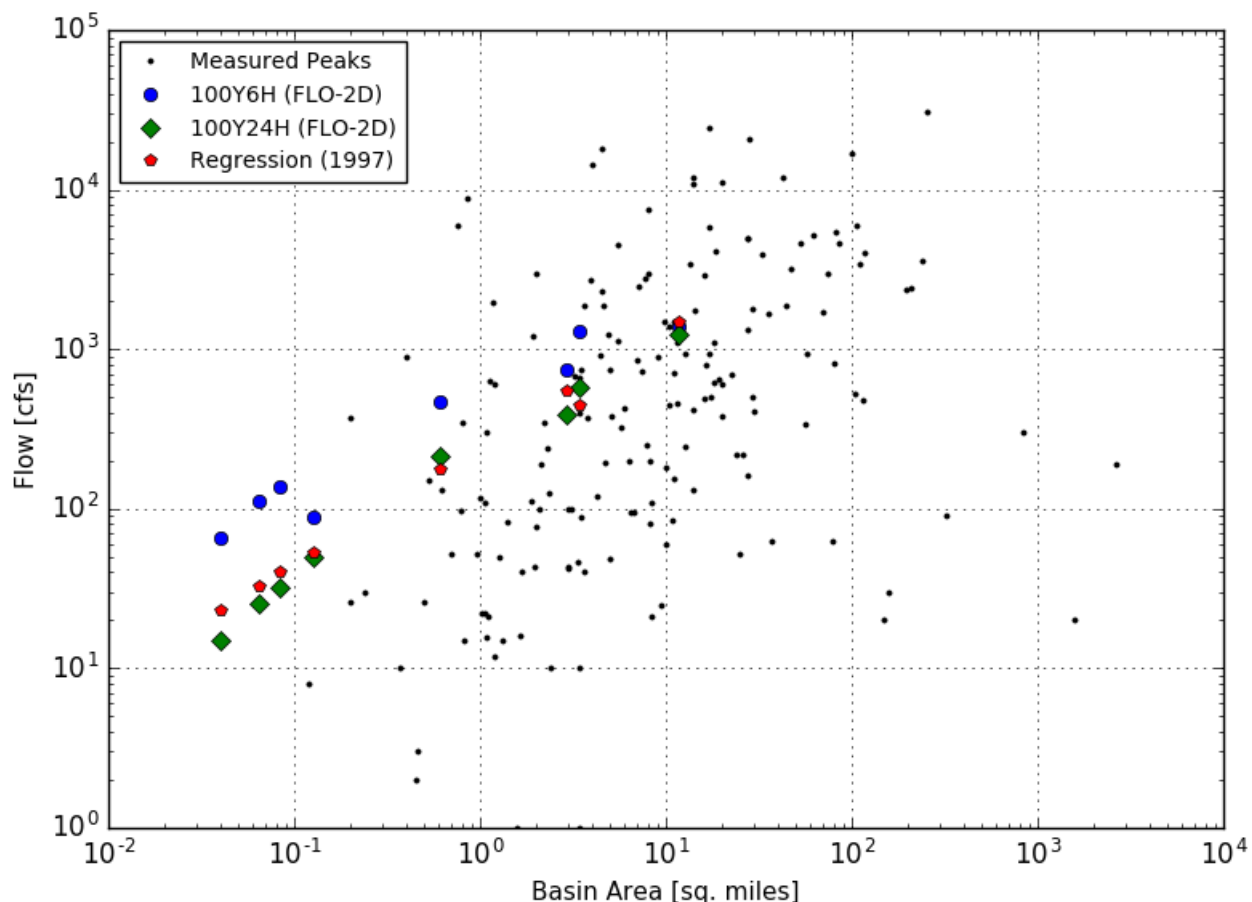


Figure 2-25. Comparison of FLO-2D results, 1997 100-year regression equation, and peak flow estimates from crest stage sites

2.4.3 Historical Flooding Documentation

As a part of the public outreach effort, the consultant team collected photographs, videos, and anecdotal information of historical flooding from residents within the ADMP study area as well as Douglas County staff. This information was used to help verify and adjust the FLO-2D model if needed. In general, the model results corresponded well with the historical information. Four locations where documentation was submitted are listed below and are illustrated in Figure 2-26 through Figure 2-29 to show the correlation between model results and actual flooding accounts.

- Buckskin Court crossing
- Horseman Court crossing
- Near Lacey Court and Mustang Lane
- Near Bennett Court and Pinto Circle

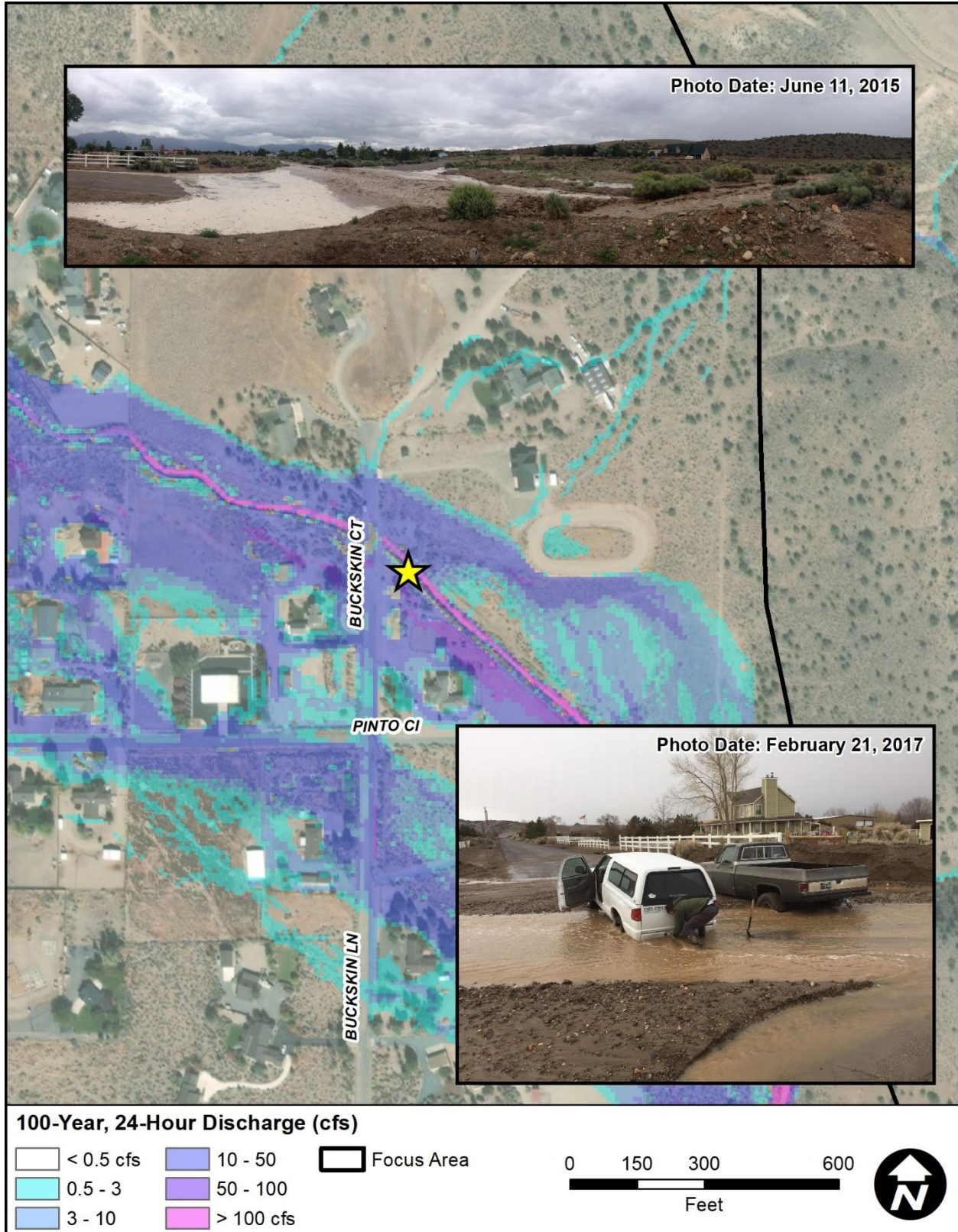


Figure 2-26. Verification for the Buckskin Court crossing area

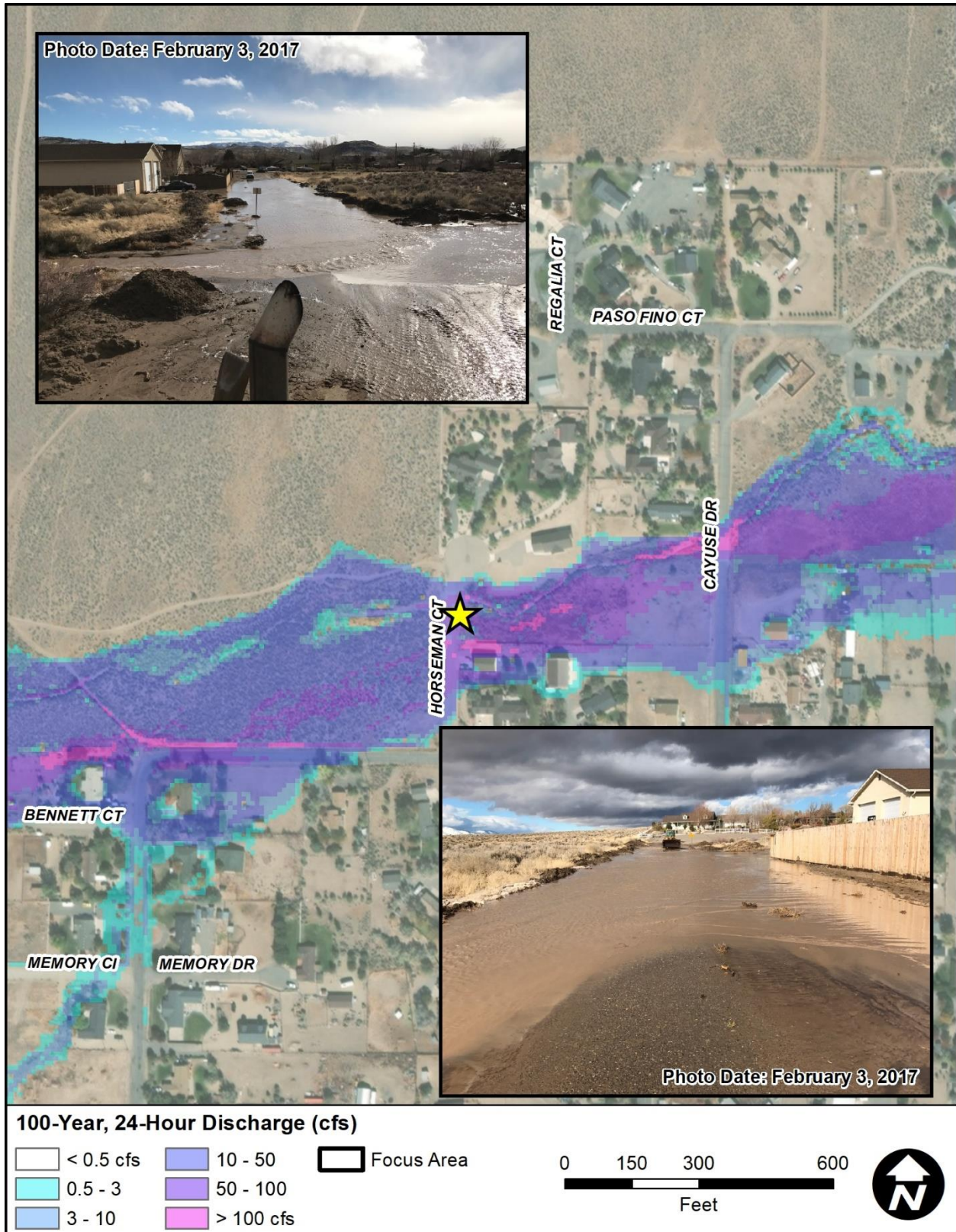


Figure 2-27. Verification for the Horseman Court crossing area

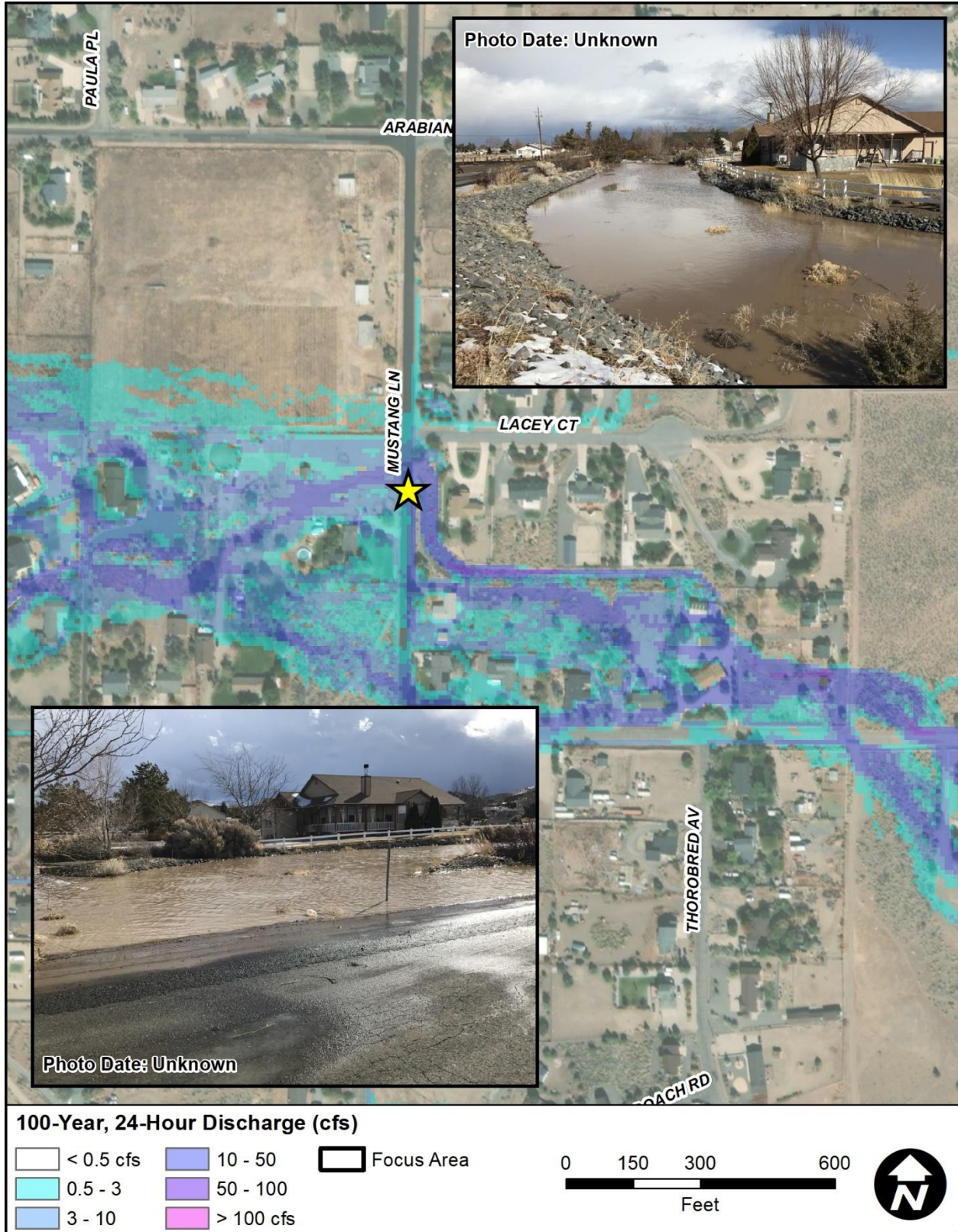


Figure 2-28. Verification for the Lacey Court/Mustang Lane area

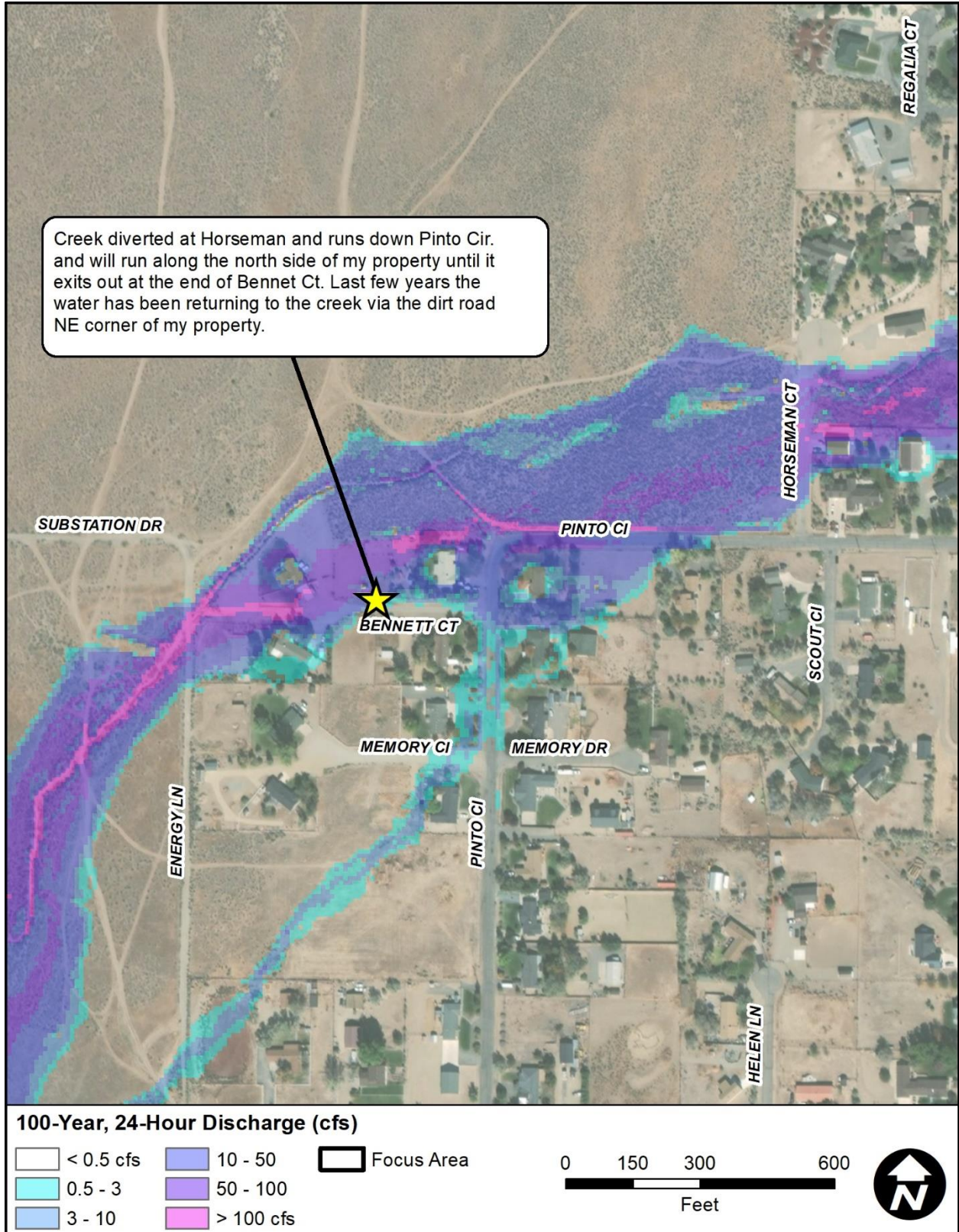


Figure 2-29. Verification for the Bennett Court/Pinto Circle area (resident-provided comment)

2.5 SUMMARY

The existing conditions FLO-2D models were created using the best available information for land cover, surface classification, topography, and hydrology. Every effort was made to ensure the models represented existing conditions as of the date of the LiDAR survey.

Photographs and anecdotal information collected from both Douglas County and the residents within the community were used to help calibrate and verify the modeling results. Like all models, the RADMP FLO-2D models are a simulation of potential conditions that could occur during a range of storm events. The models cannot exactly replicate actual, observed storm events at all locations within the community due to the vast number of variables that change with each unique storm event.

The modeling results reflect the complex flooding and sedimentation hazards that exist within the Ruhenstroth study area. The results provide valuable, quantitative, detailed information from which future planning and development decisions can be based. The existing conditions models also serve as a foundation from which potential mitigation alternatives can be assessed (Section 5).

Although the ADMP FLO-2D modeling effort was not intended to replicate an actual historical flood event, the comparison of the modeling results with USGS regression equations, anecdotal flood information, and independent hydraulic calculations indicate the project FLO-2D models suitably depict storm runoff conditions – indicating that the underlying input parameters are reasonable. Given the distributary nature of the flooding within the community, and the high sediment transport rates, flooding characteristics (e.g., depth, discharge, location) are likely to change from one flood event to the next. Even small anthropogenic changes to the landscape (e.g. dirt piles, berms, construction of outbuildings, landscaping debris piles, etc.) will result in sediment accumulation, channel scour, and changes in flowpath directions that may not be represented in the project FLO-2D modeling. In other words, the results of the modeling represent potential flooding conditions as of the date of the project topographic mapping. Updated mapping and FLO-2D modeling are recommended if major changes to the landscape occur in the future.

3 SEDIMENTATION ANALYSES

3.1 SEDIMENT SAMPLING AND TRANSPORT ANALYSIS

3.1.1 Sediment Sampling

Since the ADMP study area has known sedimentation issues (see example of sediment deposition at a culvert in Figure 3-1), a sediment transport analysis was conducted to help evaluate the source and identify mitigation solutions. Seven sediment samples were collected in September 2020 by JEF staff to help classify the type of sediment being transported to (and through) the ADMP focus area. The sampling locations are shown along with the sample IDs in Figure 3-2. All sediment samples were analyzed by mechanical sieve, and the gradation curves from each of these samples are shown in Figure 3-3, while major characteristics of the sediment are tabulated in Table 3-1.



Figure 3-1. Example of sediment deposition at culvert

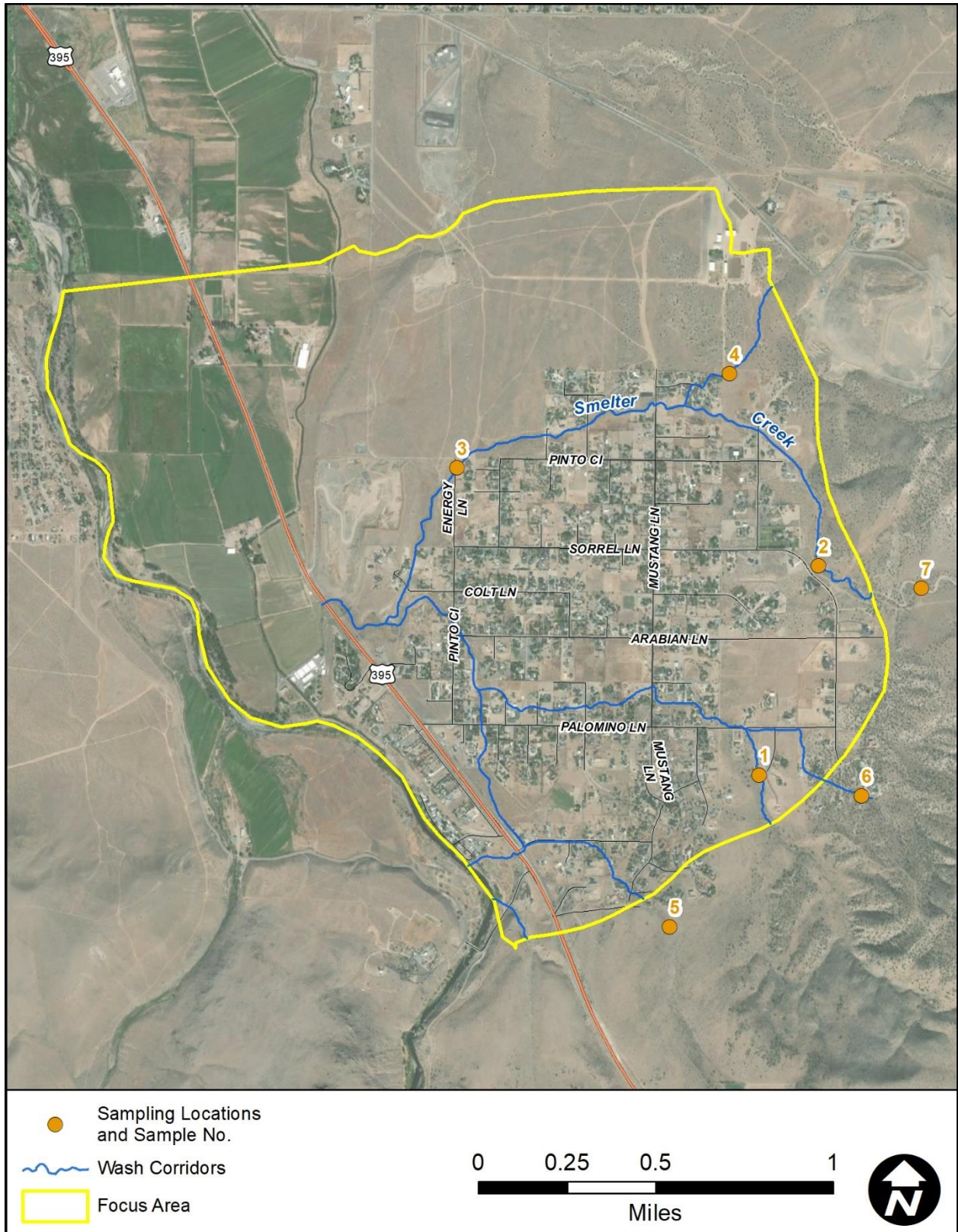


Figure 3-2. Sediment sample locations and sample ID

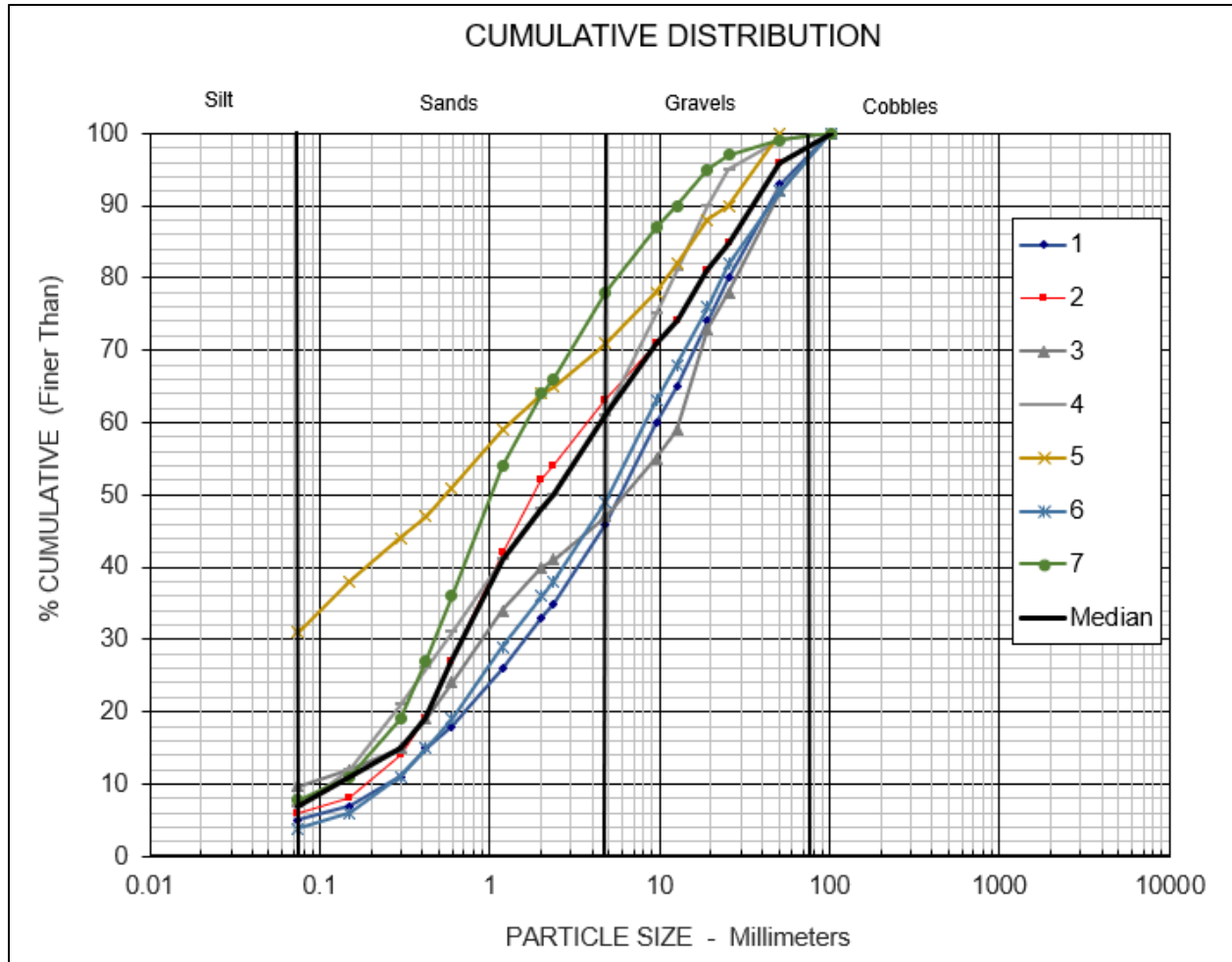


Figure 3-3. Gradation curves for the collected sediment samples

Table 3-1. Major characteristics of the sediment within the lower watershed

| ID | Type | D16 (mm) | D50 (mm) | D84 (mm) | G |
|----------------|----------------|----------|----------|----------|-------|
| 1 | Sieve Analysis | 0.48 | 6.12 | 33.22 | 14.58 |
| 2 | Sieve Analysis | 0.35 | 1.84 | 23.80 | 14.61 |
| 3 | Sieve Analysis | 0.33 | 6.54 | 36.29 | 20.39 |
| 4 | Sieve Analysis | 0.22 | 2.38 | 14.80 | 13.83 |
| 5 | Sieve Analysis | - | 0.55 | 14.80 | - |
| 6 | Sieve Analysis | 0.46 | 5.10 | 30.48 | 13.57 |
| 7 | Sieve Analysis | 0.24 | 1.06 | 7.93 | 9.49 |
| Median | - | 0.34 | 2.38 | 23.80 | 14.21 |
| Average | - | 0.35 | 3.37 | 23.04 | 14.41 |

3.1.2 Sediment Transport Analyses

The FLO-2D hydraulic modeling was used to assess the trends of both flooding and sedimentation throughout the study area. Hydraulic data from FLO-2D inherently includes both discharge and flow depth at each grid element. This hydraulic data was used to estimate sedimentation using the Yang sediment transport equation (1973, 1984) on a cell-by-cell scale. The median values from Table 3-1 were used in the sediment calculations.

For each modeled storm event, the total accumulated (i.e., throughout the entire storm event) sediment transport capacities were calculated at each cell. These accumulated capacities can identify areas where deposition or scour may be expected. The detailed results will be discussed in Section 0.

3.1.2.1 Yang Equation

Sediment transport was calculated using the Yang sediment transport methodology. This approach followed the calculation outline found in the HEC-RAS Hydraulic Reference Manual (USACE, 2016). The grain size distribution was discretized into three equal mass components where sediment transport capacity was computed separately for each component and the results were combined while weighting the capacity of each component by its relative mass contribution. The governing equation for estimating sediment concentration for each grain size using the Yang approach is as follows:

$$\log C_t = 5.435 - 0.286 \log \frac{\omega d_m}{\nu} - 0.457 \log \frac{u_*}{\omega} + \left(1.799 - 0.409 \log \frac{\omega d_m}{\nu} - 0.314 \log \frac{u_*}{\omega} \right) \log \left(\frac{VS}{\omega} - \frac{V_{cr}S}{\omega} \right) \quad (3)$$

$$\log C_t = 6.681 - 0.633 \log \frac{\omega d_m}{\nu} - 4.816 \log \frac{u_*}{\omega} + \left(2.874 - 0.305 \log \frac{\omega d_m}{\nu} - 0.282 \log \frac{u_*}{\omega} \right) \log \left(\frac{VS}{\omega} - \frac{V_{cr}S}{\omega} \right) \quad (4)$$

Where:

- C_t is the total sediment concentration (ppm)
- ω is the particle fall velocity (ft/s)
- d_m is the median particle diameter (ft)
- ν is the kinematic viscosity (ft²/s)
- u_* is the shear velocity (ft/s)
- V is the average channel velocity (ft/s)
- S is the energy gradient (ft/ft)

Equation 3 is used for sand with a median diameter < 2mm, while Equation 4 is for gravel with a median diameter is ≥ 2mm. Within a model spanning 2-dimensions in plan-view, such as FLO-2D, the Yang methodology differentiates itself through application of vectorized parameters – average channel velocity and slope, notably. Using time-varying output from FLO-2D, the direction of maximum velocity at each time step was determined and the terms utilized in the Yang equation were applied in that direction. This method allows the sediment transport capacity analysis to adapt to changes in peak flow direction which is especially valuable in areas of flowpath uncertainty such as coalescing alluvial fans and areas subject to flooding sources that can change over time (e.g., distributary flooding patterns).

3.2 RESULTS

3.2.1.1 *Sediment Rasters*

Since the total accumulated transport is calculated at each cell, an overall map of the study area with sediment transport capacities can be produced similar to the FLO-2D results presented in Section 2.3. Since the 100-year, 24-hour storm produces the largest amount of volume and sediment, it is used as a representative example. The relative total accumulated sediment transport within the focus area calculated with the Yang equation is shown in Figure 3-4. Note - The colors in both these figures represent relative transport capacity to each other, so green is relatively low compared to red, but green is higher than areas without color.

In general, the results are as expected. Higher sediment transport rates appear in the channels, while rates decrease as the flow leaves the mountain channels and spreads out over the landscape. Unsurprisingly, Smelter Creek produces the most sediment because it has the largest drainage area with the longest drain time.

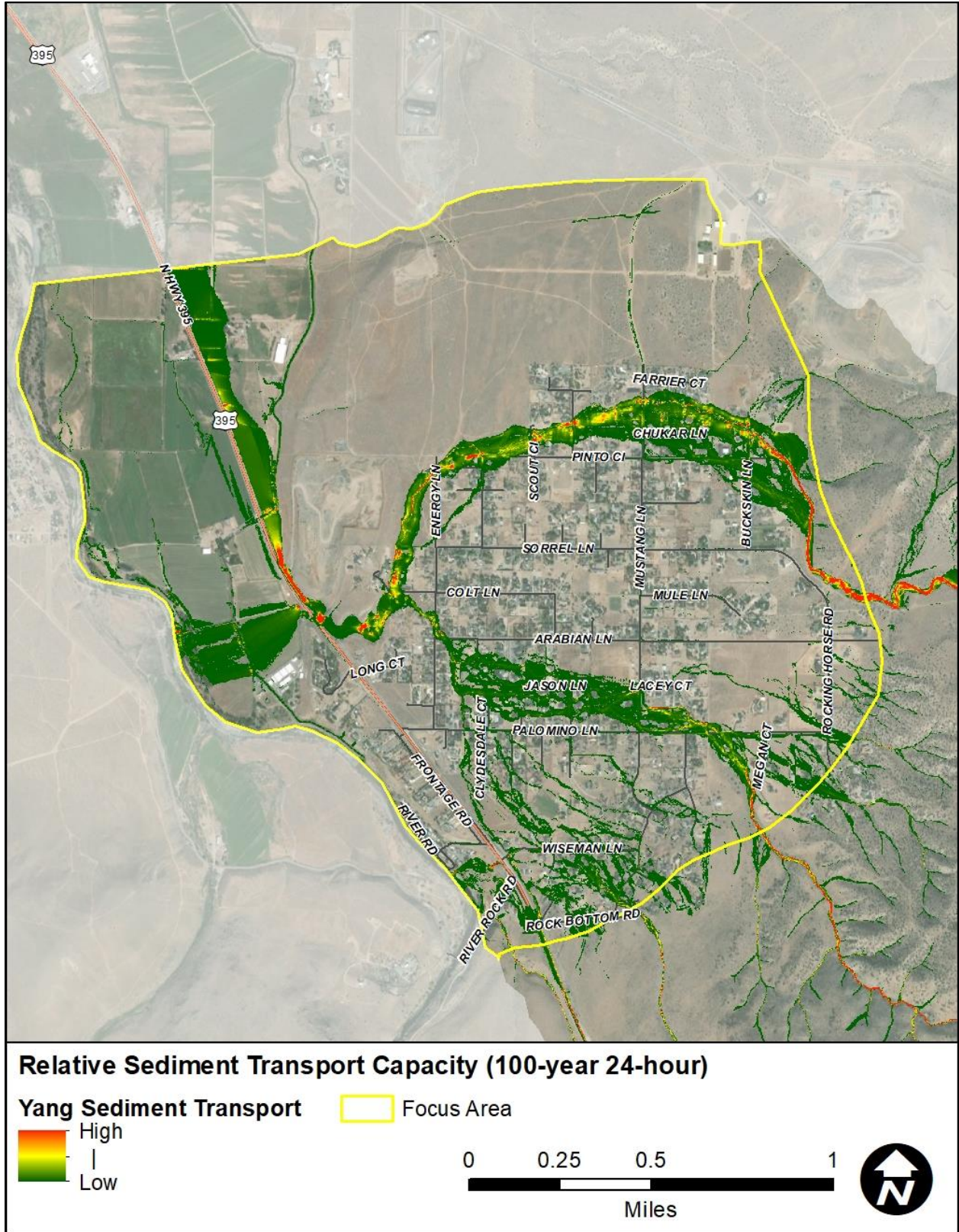


Figure 3-4. Total accumulated sediment transport capacity by the Yang methodology for the 100-year, 24-hour event

3.2.2 Sediment Profiles

Two sediment transport profiles were developed for the major contributing flow paths within the ADMP focus area because alternatives will most likely be developed to control these sediment inflow points. The sediment delivery along the profiles are shown for the three modeled storm events, i.e., 100-year 24-hour (100Y24H), 100-year 6-hour (100Y6H), and the 25-year 24-hour (25Y24H). The 100Y24H Yang sediment raster is shown in the background to reference the areas of transport.

To develop these profiles, the total accumulated sediment transport through each station (or cross-section) over the entire storm event was calculated for the Yang equation. The transport profiles are plotted and shown in Figure 3-5. These plotted profiles used a moving average to smooth the noise in the data so that general trends can be identified.

In this study, these profiles were used in two ways. First, the profiles can be used to identify areas where sediment transport is not in equilibrium or out of balance. This is important because when sediment transport is out of balance, erosion (degradation) or deposition (aggradation) is occurring within the wash. When sediment transport is increasing (i.e., the slope change is positive), the wash is gathering sediment through degradation. Conversely, when the sediment transport profile is decreasing, and the slope change is negative, the wash is losing sediment through aggradation.

Areas where there can be significant erosion or deposition are highlighted on the profile. Basically, as flow exits the mountains on the righthand (or upstream) area of the profiles, the transport capacity is the highest. This means that sediment is generally deposited within the focus area as flow moves through the Ruhenstroth area. This phenomenon can be clearly seen in the Unnamed Wash profile.

In the Smelter Creek profile, other areas of erosion and deposition are highlighted. As Smelter Creek exits the mountains, the sediment transport capacity clearly decreases. However, there are additional areas where there is significant erosion and deposition. For any potential mitigation alternatives, it is necessary to either capture or smooth this profile so that the sediment is passed through the system without erosion or deposition, but sediment basins may be required to mitigate any potential increase in sediment delivered to downstream property owners.

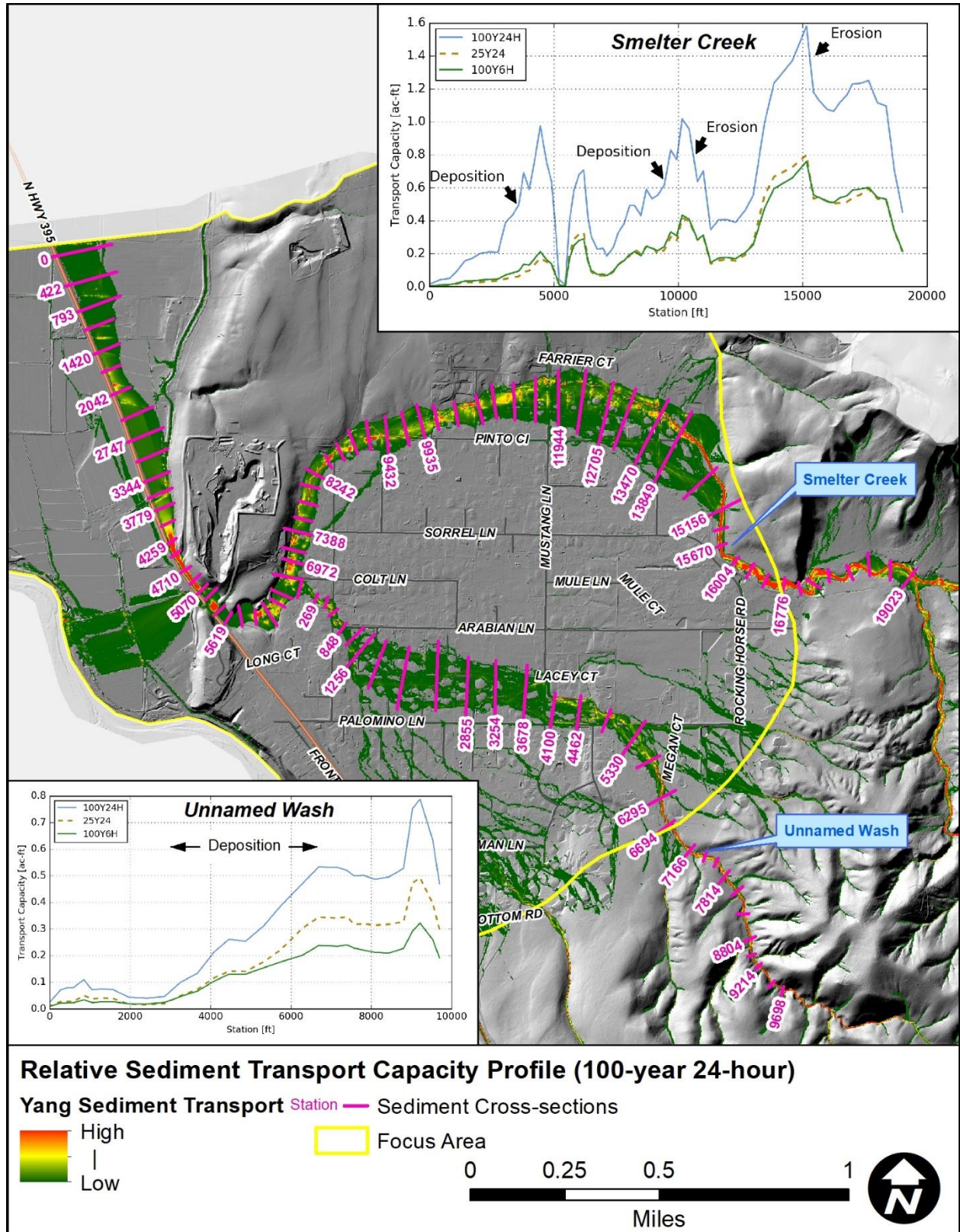


Figure 3-5. Cumulative sediment transport profile for the primary overland flow path throughout the 100-year 24-hour event

4 FLOOD HAZARD CLASSIFICATION

4.1 PURPOSE

During a severe storm event, flood waters flow throughout the Ruhenstroth ADMP study watershed. Not all flood hazards pose a risk to people or to their properties. Flood risk depends on the presence of both a flood hazard and a person, their property, or vehicle. As an example, flow in a constructed flood control channel does not present a risk until someone enters the channel. Identifying areas where flood waters may cause risks that potentially harm people, vehicles, or property is an important objective of the ADMP. Identification of potential flood risks in the study area helps the consultant team prioritize which flood problems should be addressed and in what order and provides valuable information to Douglas County personnel on where to focus response efforts during a flood event.

For the purposes of this study, flood hazards were defined based on the physical characteristics of the flood water – that is, the location, depth, and velocity associated with those flood waters. The hydrology and hydraulic modeling results were used to define flood hazards for three storms:

- The 25-year, 24-hour event
- The 100-year, 24-hour event
- The 100-year, 6-hour event

The flood risk assessment involved selecting criteria and quantifying flood risks throughout the study watershed using the FLO-2D model results. Three types of potential flood risks were assessed – flooding risks to pedestrians, passenger vehicles, and buildings.

The building flood inundation assessment is a planning-level analyses to estimate the number of habitable structures potentially inundated by flow depths greater than six inches. This Phase I analysis was done considering existing conditions. A proposed conditions assessment will be conducted during the Phase II (separate study) portion of the ADMP.

The following sections describe the flood classification criteria, methodology, and description of provided electronic files for each potential flood risk assessment.

4.2 FLOODING HAZARDS TO PEDESTRIANS

Pedestrian flood hazards were classified using the depth-velocity relationship outlined in the United States Bureau of Reclamation (USBR) Technical Memorandum 11 (TM 11) (1988). The depth-velocity relationships presented in TM 11 are a good basis for flood hazard classification since the criteria are widely accepted. TM 11 presents two possible classifications for pedestrians: flood danger levels for adults and for children. This study considers the flood danger classification for children throughout the entire watershed to simplify the methodology and to be conservative. The depth-velocity flood danger level relationship from TM 11 is shown as Figure 4-1.

The following three categories exist for pedestrian flood hazards:

- *Low*: These are areas with depths and velocities corresponding to the Low Danger Zone as shown in Figure 4-1. Low pedestrian hazards are not displayed on the map exhibits because, per

TM11, low hazard zones do not present a threat to children of almost any size (excluding infants) and cover all areas not classified with a higher flood hazard.

- *Moderate*: Areas with depths and velocities corresponding to the Judgment Zone in Figure 4-1 have been labeled as having a moderate potential flood hazard to pedestrians.
- *High*: Areas with depths and velocities corresponding to the High Danger Zone in Figure 4-1 have been labeled as having a high potential flood hazard to pedestrians.

The flood hazards to pedestrians have been digitized in GIS in the form of a raster. The rasters generated for the risk analysis coincide with the FLO-2D grid elements with a 10-foot by 10-foot pixel size. The raster contains values of 1, 2, and 3 which correlates to a low, moderate, and high hazard classification, respectively. Since the 100-year, 6-hour storm produces the largest peak runoff for most areas (see Table 2-6, the flooding hazard from this storm event is shown as Figure 4-2.

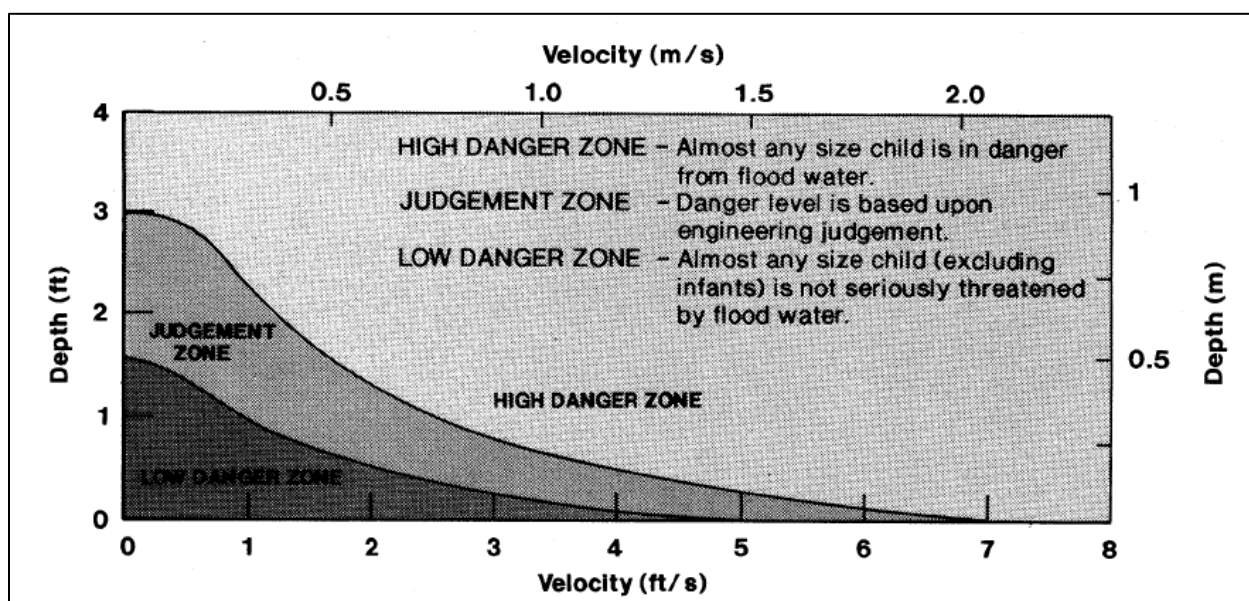


Figure 4-1. Depth-Velocity flood danger level relationship for children, from USBR (1988)

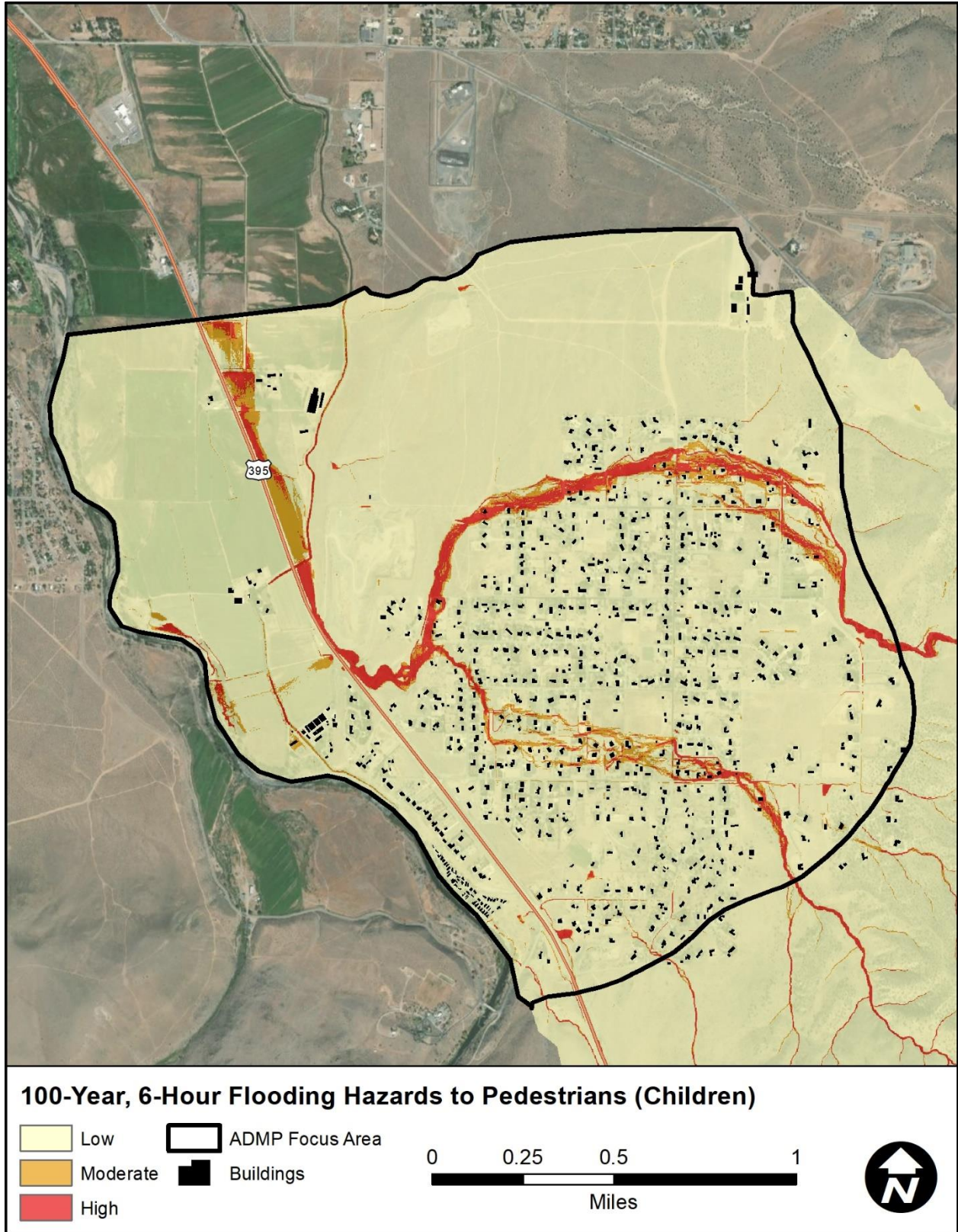


Figure 4-2. USBR criteria flooding hazards to pedestrians based on the 100-year, 6-hour results

4.3 FLOODING HAZARDS TO PASSENGER VEHICLES

Potential hazards to passenger vehicles were classified using a combination of minimum depth criteria and the depth-velocity relationship in TM 11 as shown in Figure 4-3. The following four categories exist for passenger vehicle flood hazards:

- **Low:** This hazard category is based solely on minimum depth criteria and is for roadway crossings with depths less than half a foot. Low passenger vehicle hazards are not displayed on the map exhibits because low hazard zones indicate areas where vehicles “are not seriously in danger” and, as such, almost any size passenger vehicle can safely pass. Also, this hazard classification covers all areas not classified with a higher flood hazard. This classification is not explicitly shown in the Figure 4-3.
- **Moderate:** This hazard category is based on a combination of minimum depth criteria and the depth-velocity relationship in TM 11. Specifically, these are roadway crossings with depths and velocities falling into the Low Danger Zone (as shown in Figure 4-3 that also have greater than a half a foot of depth. The threshold depth of half a foot was chosen because half a foot of water will reach the bottom of most passenger cars and can cause loss of control and possible stalling.
- **High:** Roadway crossings with depths and velocities corresponding to the Judgment Zone in have been labeled as having a high potential flood hazard for passenger vehicles.
- **Very High:** Roadway crossings with depths and velocities corresponding to the High Danger Zone in Figure 4-3 have been labeled as having a very high potential flood hazard for passenger vehicles.

The flood hazards to passenger vehicles have also been digitized in GIS in the form of a raster. The raster contains values of 1, 2, 3, and 4. These values correlate to low, moderate, high, and very high classification, respectively. The TM 11 flooding hazards to vehicles for the 100-year, 6-hour storm is shown in Figure 4-4.

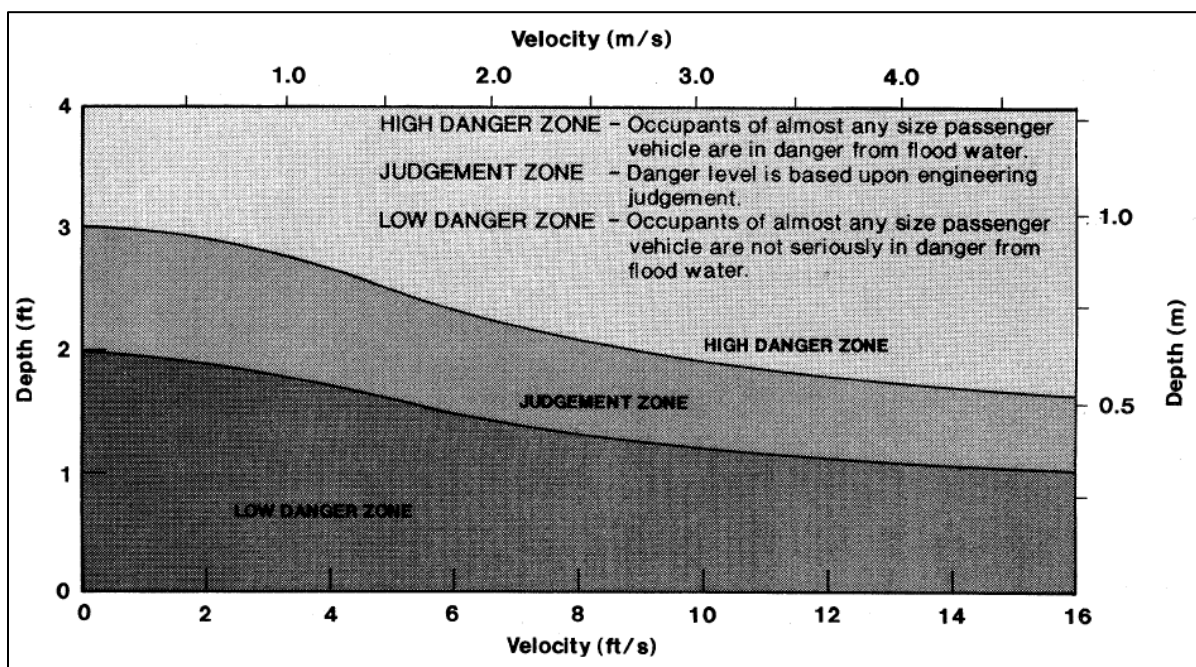


Figure 4-3. Depth-Velocity flood danger level relationship for passenger vehicles, from USBR (1988)

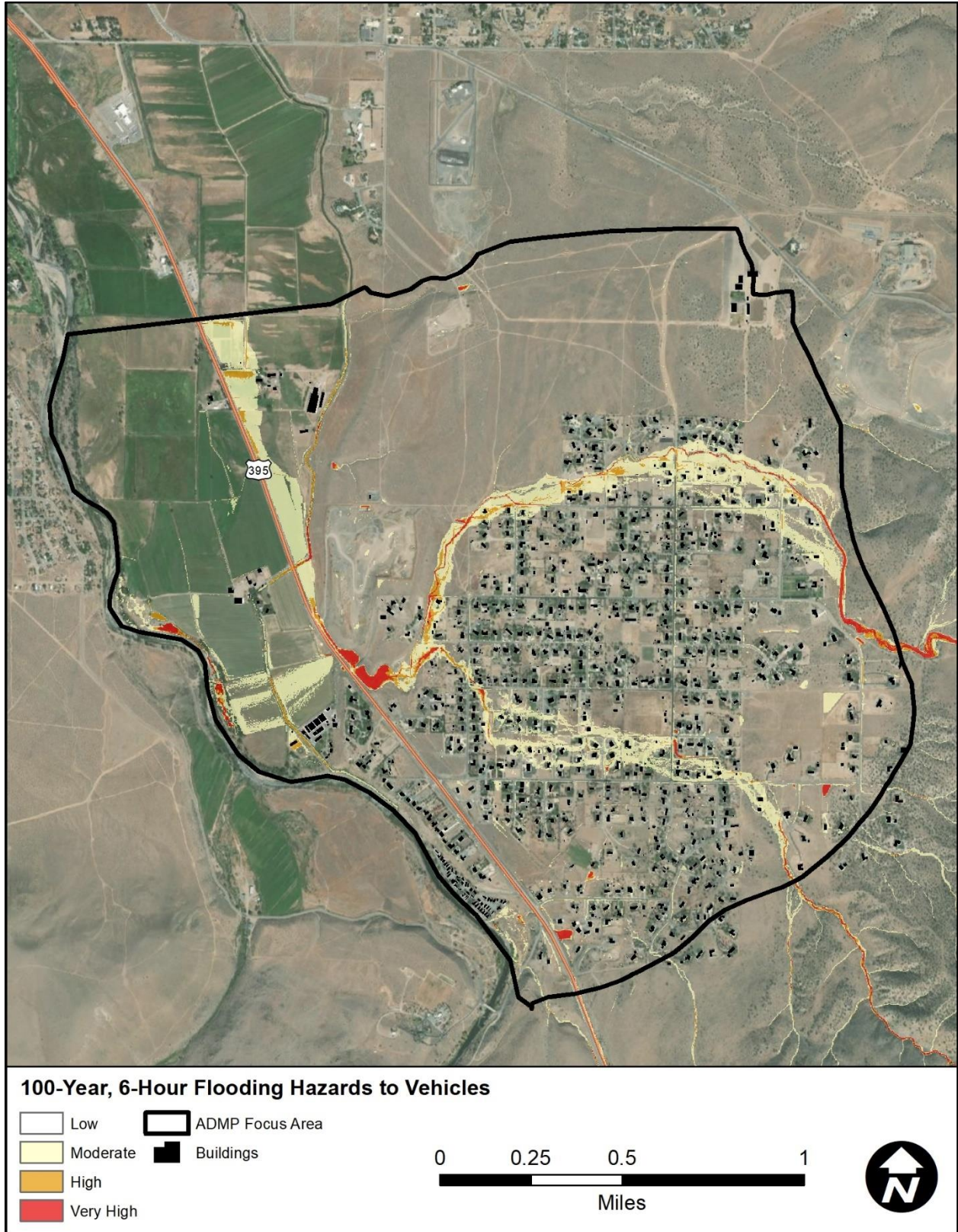


Figure 4-4. USBR criteria flooding hazards to vehicles based on the 100-year, 6-hour results

To isolate the actual risk to vehicles, the County’s street centerlines GIS layer was intersected with the hazards zones to produce a “Potential Risk to Passenger Vehicles” map. This isolates the road crossings that pose a risk to vehicles during a storm event. All three storm events produce conditions of “High” or “Very High” risk using the USBR criteria. The flood risk road crossing locations are shown in Figure 4-5 through Figure 4-7, respectively.

The road crossing locations are listed below by storm event (numbering corresponds to Figure 4-5 through Figure 4-7). By identifying these specific locations in the ADMP, Douglas County has the information needed to respond during flood events by dispatching road crews to close the high flood risk crossings. It also provides a list of locations to potentially be considered for future road improvements in the County’s capital improvement planning.

25-Year, 24-Hour

1. Smelter Creek at Energy Lane (Very High)
2. Smelter Creek at Horseman Court (High)
3. Smelter Creek at Cayuse Drive (High)
4. Smelter Creek at Mustang lane (High)
5. Smelter Creek at Buckskin Lane (High)
6. Smelter Creek at Unnamed Access Road (High)

100-Year, 6-Hour

1. Smelter Creek at Energy Lane (Very High)
2. Smelter Creek at Horseman Court (High)
3. Smelter Creek at Cayuse Drive (High)
4. Smelter Creek at Mustang Lane (High)
5. Smelter Creek at Buckskin Lane (High)
6. Palomino Lane between Rocking Horse Court and Megan Court (High)
7. Smelter Creek at Unnamed Access Road (High)

100-Year, 24-Hour

1. Smelter Creek at Energy Lane (Very High)
2. Smelter Creek at Horseman Court (High)
3. Smelter Creek at Cayuse Drive (High)
4. Smelter Creek at Mustang lane (Very High)
5. Smelter Creek at Buckskin Lane (High)
6. Colt Lane and Sullivan Drive (High)
7. Smelter Creek at Unnamed Access Road (Very High)

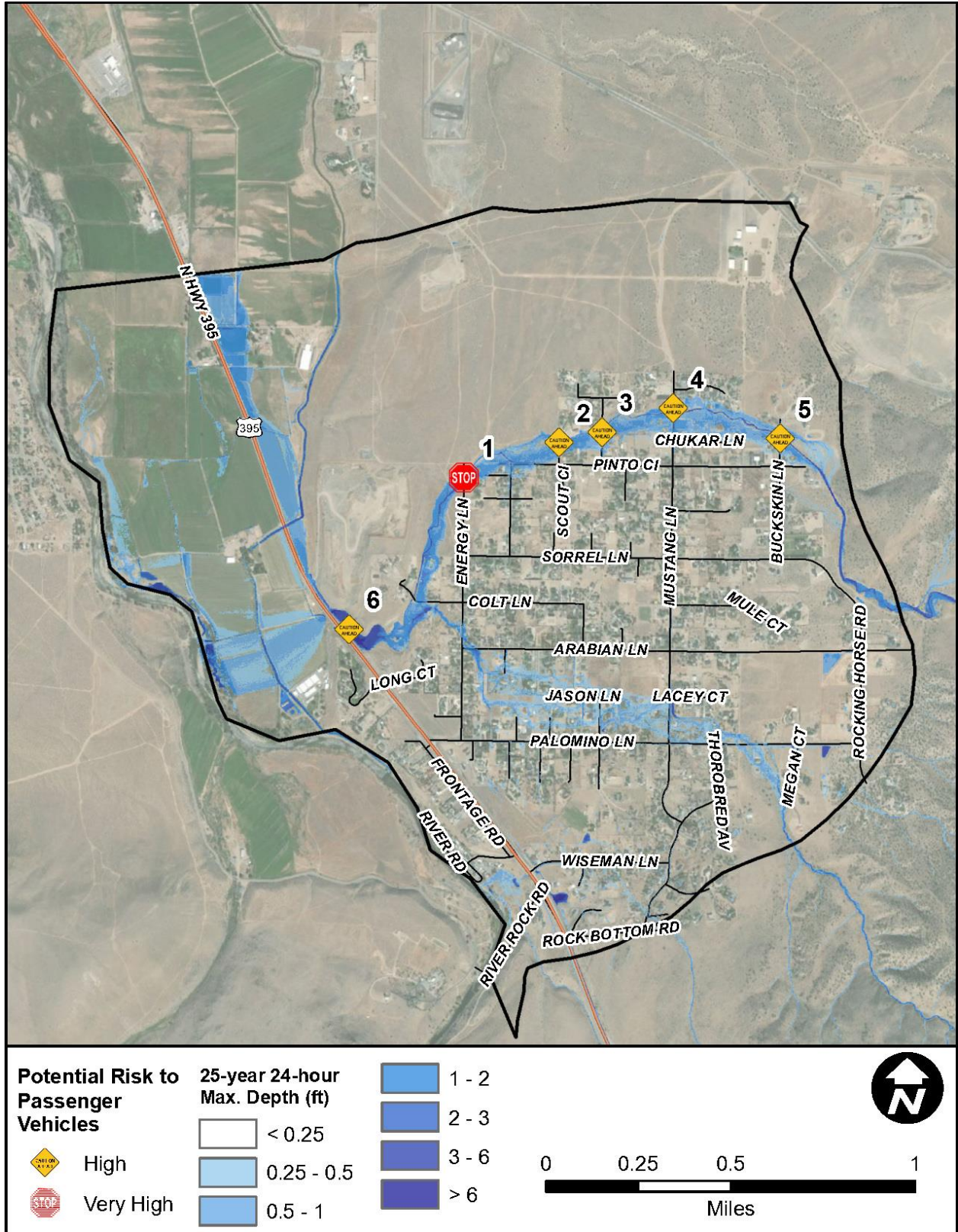


Figure 4-5. Hazardous road crossings during a 25-year, 24-hour storm (USBR criteria)

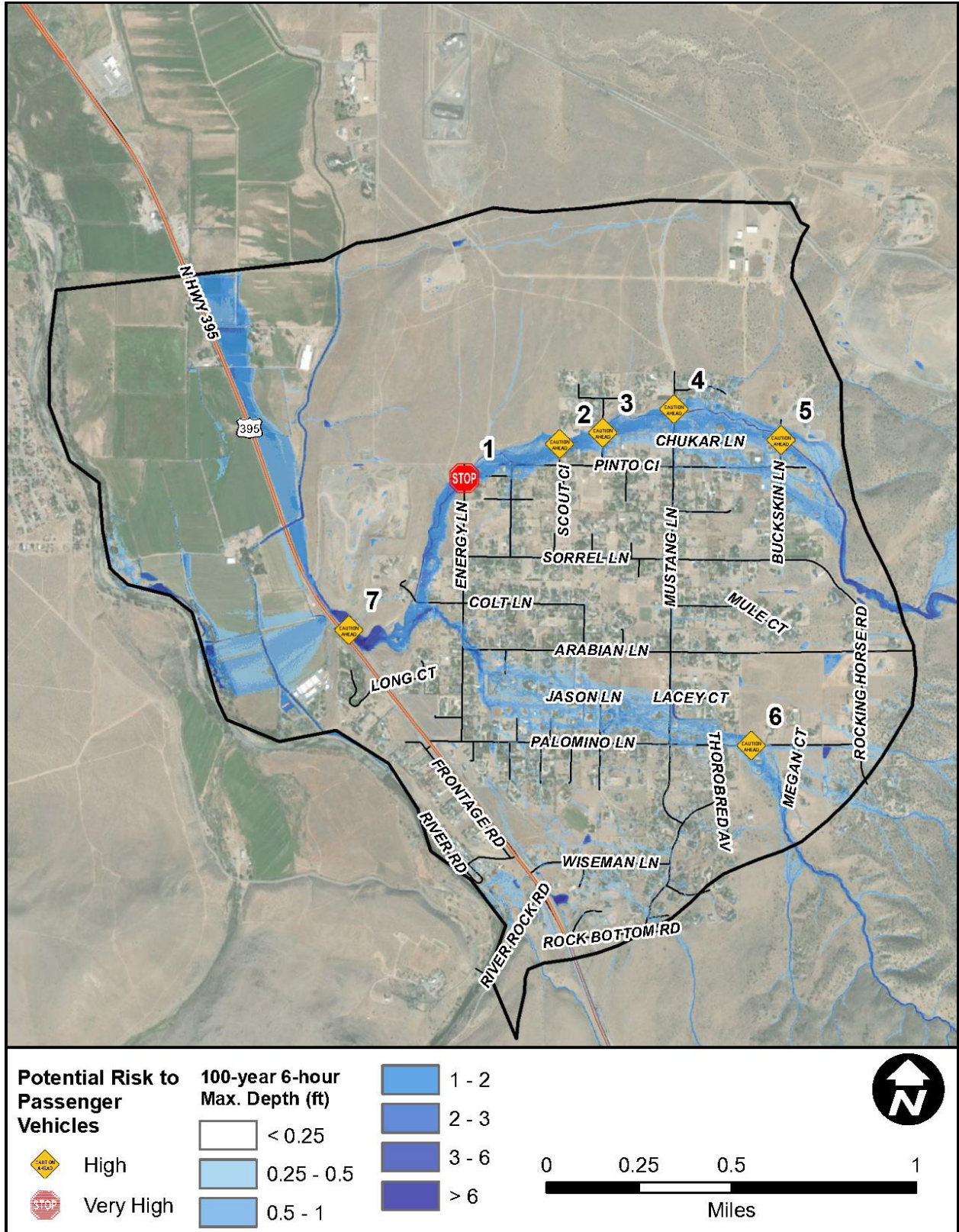


Figure 4-6. Hazardous road crossings during a 100-year, 6-hour storm (USBR criteria)

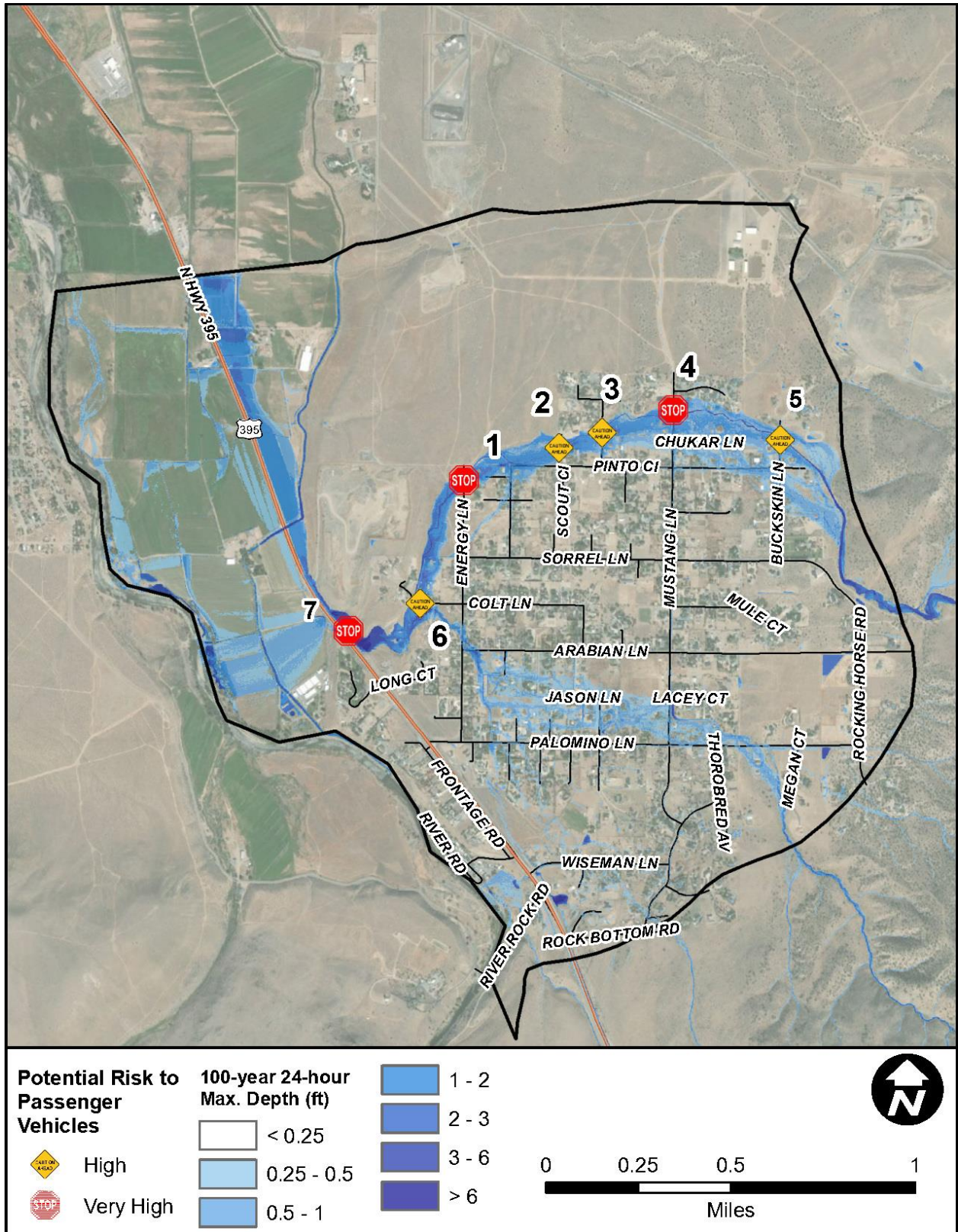


Figure 4-7. Hazardous road crossings during a 100-year, 24-hour storm (USBR criteria)

4.4 FLOODING HAZARDS TO STRUCTURES

Potential hazards to buildings were classified using the depth-velocity relationship from TM 11. The depth-velocity relationship from TM 11 is shown as Figure 4-8. The following three categories exist for potential flood hazards to structures:

- *Low*: Buildings that have contact with at least one FLO-2D grid element that has a depth-velocity relationship corresponding to the low danger zone in Figure 4-8 have been designated as having a low potential flood hazard.
- *Moderate*: Buildings that have contact with at least one FLO-2D grid element that has a depth-velocity relationship corresponding to the judgment danger zone in Figure 4-8 have been designated as having a moderate potential flood hazard.
- *High*: Buildings that have contact with at least one FLO-2D grid element that has a depth-velocity relationship corresponding to the high danger zone in Figure 4-8 have been designated as having a high potential flood hazard.

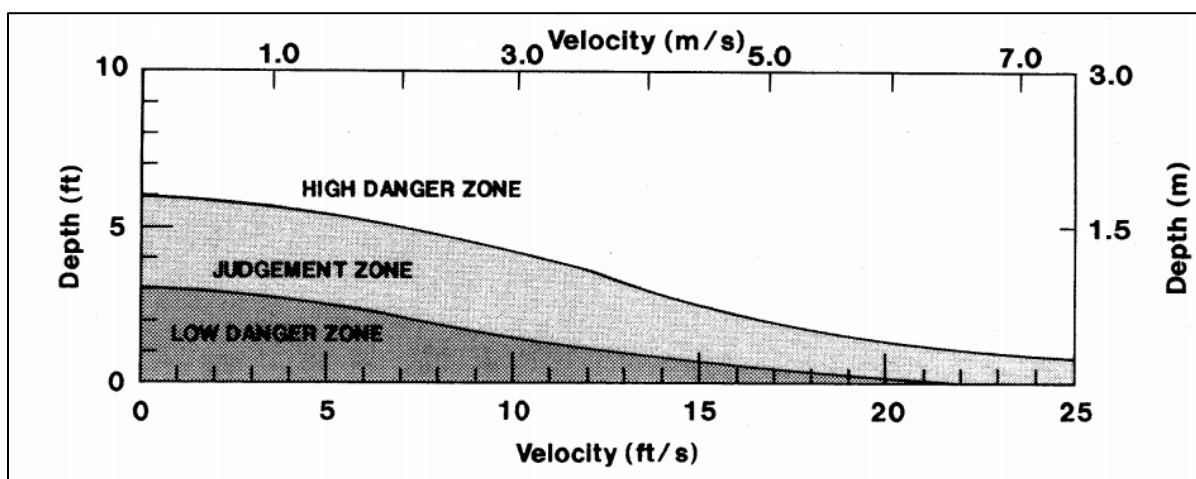


Figure 4-8. Depth-Velocity flood danger level relationship for structures built on foundations, from USBR (1988)

To create the building flood hazard classification, the building polygon shapefile is intersected with the flood hazard layer using GIS software tools. When multiple grid cells from the flood hazard layer intersect one building polygon, the maximum hazard classification is assigned to the building. Buildings with less than 600 square feet (e.g., unattached garages or sheds) were not considered because they were assumed to be uninhabited due to their size. The result is a building polygon shapefile with a hazard attribute classifying low, moderate, or high flood hazards.

The tabulated building hazard results are shown in Table 4-1. Due to the relatively shallow flooding in the project area and how the TM criteria were developed (i.e. to assess conditions downstream of a dam during a dam failure), there is only one building with a moderate hazard classification during the 100-year 6-hour event. All other buildings are classified as having a low hazard classification during the studied events. As a representative example, the 100-year 6-hour flooding hazards to buildings raster is shown in Figure 4-8.

Table 4-1. Building flooding hazard classification results (USBR criteria)

| Existing Conditions | | | | |
|----------------------------|-----------------------|-----------------------|-----------------------|-----------------------------|
| Recurrence Interval | Building Count | Building Count | Building Count | Total Building Count |
| | Low | Moderate | High | |
| 25Y24H | 953 | 0 | 0 | 953 |
| 100Y24H | 953 | 0 | 0 | 953 |
| 100Y6H | 952 | 1 | 0 | 953 |

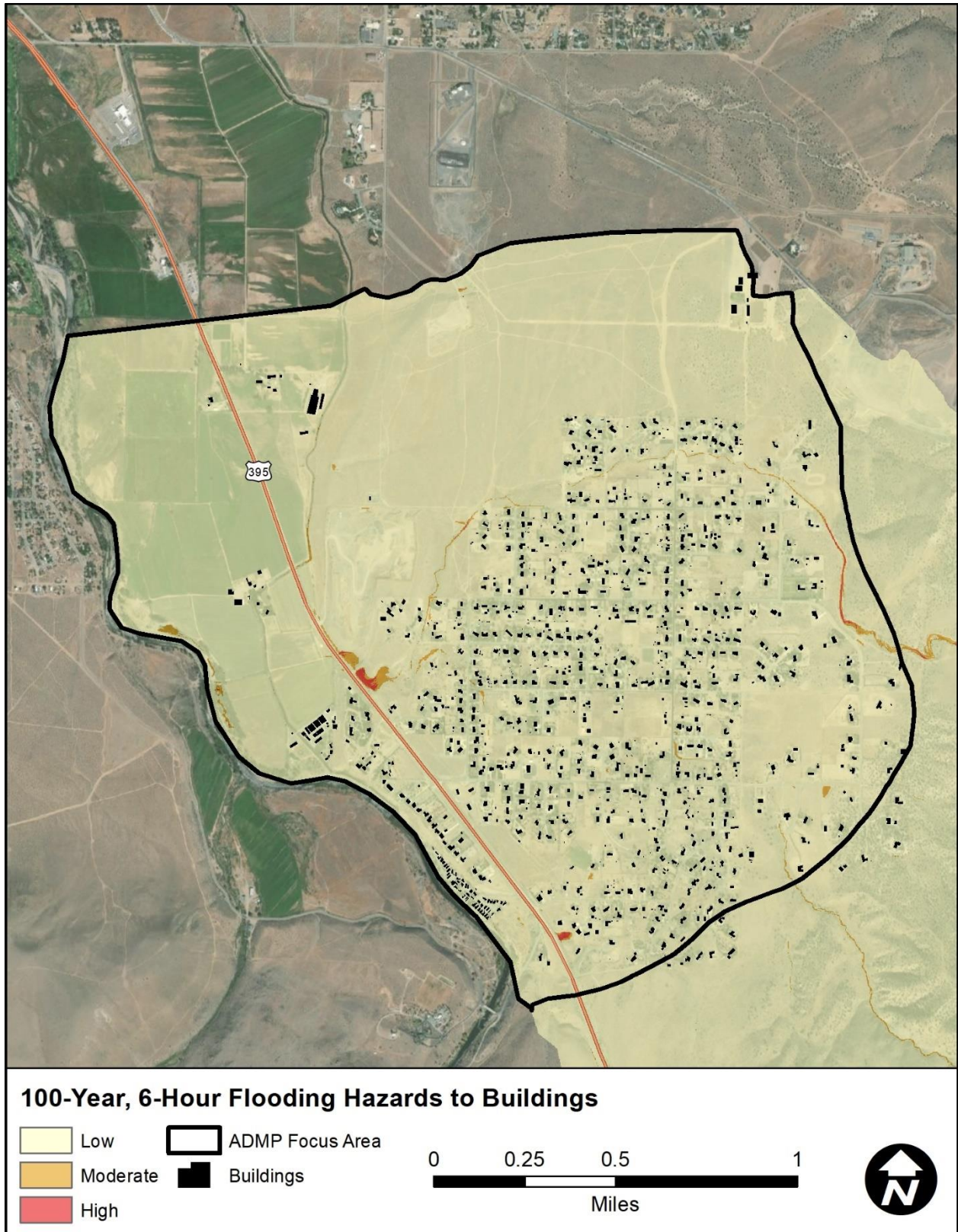


Figure 4-9. USBR criteria flooding hazards to buildings based on the 100-year, 6-hour results

4.5 BUILDING INUNDATION ASSESSMENT

4.5.1 Methodology

The USBR TM 11 procedures are commonly used within the engineering community for assessing flood risk. However, TM 11 was developed “for estimating the downstream area susceptible to flooding due to a dam failure” (USBR, 1988). As such, lower flood depths may produce a “Low” risk classification for buildings when using TM 11 but may be of a sufficient depth to justify a higher risk classification. To both verify the TM 11 results and to provide a lower threshold risk assessment, a separate building impact analysis was run using the building footprint data and the maximum depth results from the FLO-2D modeling for the base conditions. The maximum depth layers only consider the maximum depth that occurred during the model simulation.

From the building footprint data, there are 1,319 structures within the study area; however, not all these structures are habitable structures (e.g. - water tanks or sheds). For this analysis, the same 600 square foot filter that was used in the Flooding Hazard to Structures (Section 4.4) analysis was applied. After applying this filter there are 953 structures in the study area.

4.5.2 Existing Conditions

Each building was classified based on the maximum depth that fell within the structure outline. The structures were tabulated into four groups:

- 1) 0.25 ft < Depth (inclusive of groups 2 through 4 below)
- 2) 0.25 ft < Depth ≤ 0.5 ft – Low
- 3) 0.5 ft ≤ Depth ≤ 1.0 ft – Moderate
- 4) 1.0 ft < Depth – High

The results for existing conditions are tabulated in Table 4-2, while the results for the 100-year 6-hour storm are shown in Figure 4-10.

Table 4-2. Buildings that are impacted by various depths (base conditions)

| Existing Conditions | | | | |
|---------------------|---------------------------|---------------------------|---------------------------|----------------------|
| Recurrence Interval | Building Count Flow Depth | Building Count Flow Depth | Building Count Flow Depth | Total Building Count |
| | 0.25' < h ≤ 0.5' | 0.5' < h ≤ 1' | 1' < h | 0.25' < h |
| 25Y24H | 135 | 68 | 17 | 220 |
| 100Y24H | 162 | 106 | 32 | 300 |
| 100Y6H | 281 | 149 | 43 | 473 |

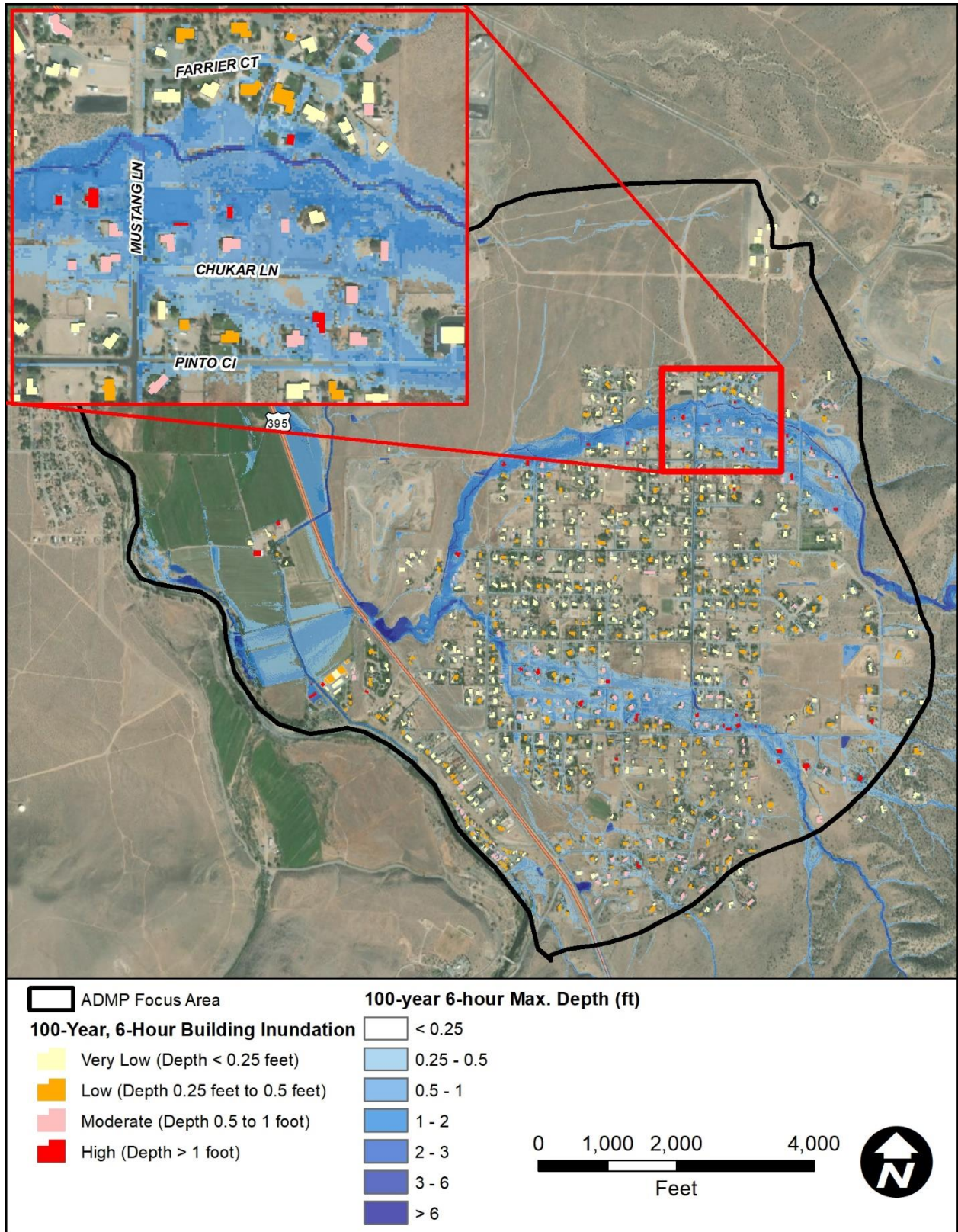


Figure 4-10. Building inundation assessment (100-Year, 6-Hour) result example

4.6 SUMMARY

In this section the methodologies and results from four separate hazard assessments were presented. These included:

- Flood hazards to children
- Flood hazards to vehicles
- Flood hazards to buildings
- Building inundation assessment

These analyses help identify areas that have a higher risk of flooding and which property and infrastructure are most susceptible to damage. Having this information helps focus the mitigation alternative to areas where they are most needed. Additionally, the building inundation assessment will provide a baseline from which potential future mitigation projects can be assessed for flood risk and cost effectiveness.

5 ALL-WEATHER ACCESS

5.1 INTRODUCTION

As a part of Phase 1, alternatives that provide all-weather access for both the 25-year and 100-year flood events for four road crossings of Smelter Creek were developed. The crossings are:

- Buckskin Lane
- Mustang Lane
- Cayuse Drive
- Horseman Lane

A map that shows the locations of these crossings with the FLO-2D 100-year 6-hour results is show as Figure 5-1. In Douglas County, all-weather access is defined as a 12-foot wide dry lane that shall be maintained centered on the roadway. Since the roadway crossings are perpendicular to flow, all-weather access for this Task is defined as all flow contained in the culvert with no roadway overtopping.

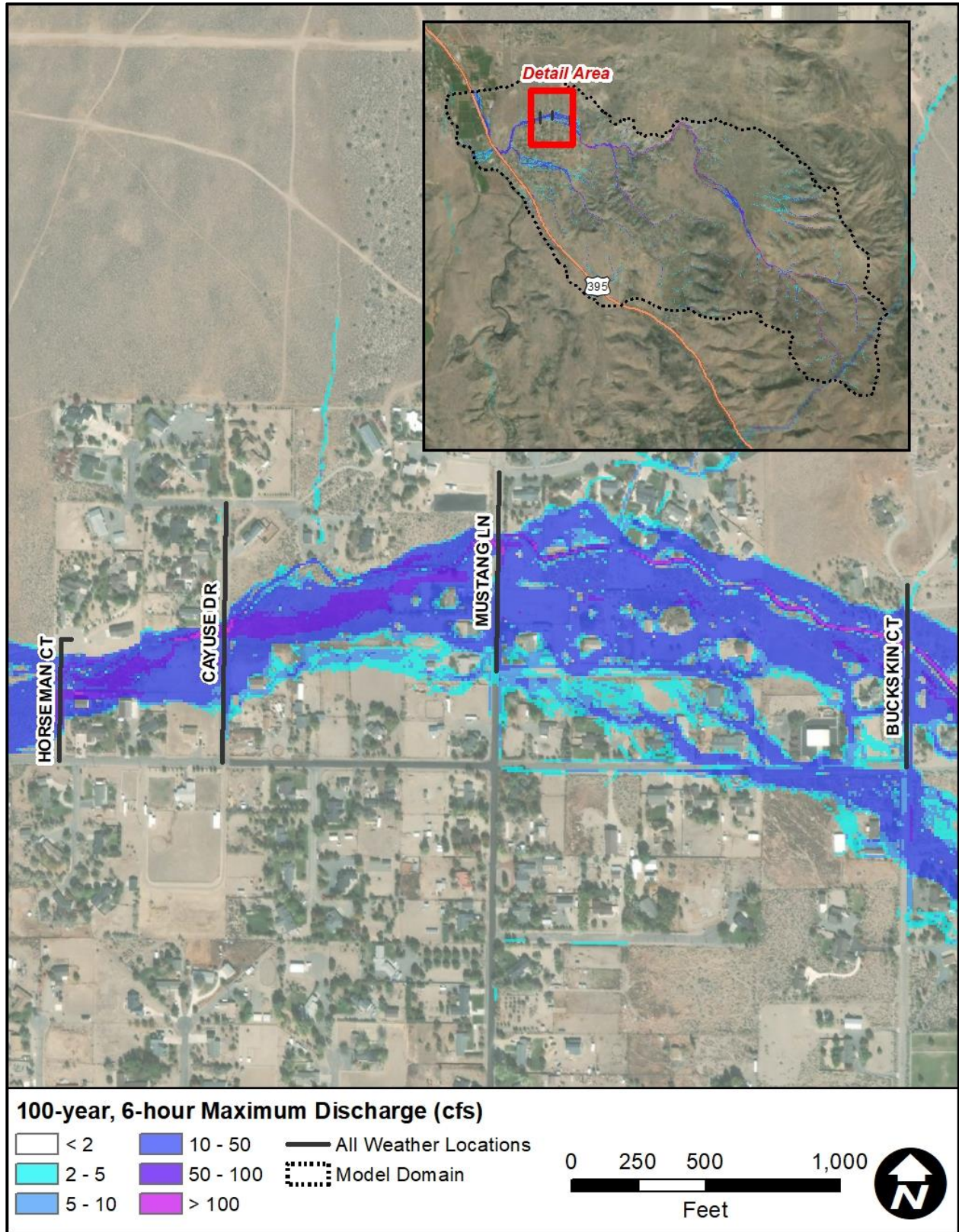


Figure 5-1. Location of all-weather access roadway crossings, shown with 100-year 6-hour maximum discharges

5.2 METHODOLOGY AND RESULTS

Although the historical alignment of Smelter Creek is mostly preserved, reaches of the present channel do not have capacity to convey the 100-year, 6-hour or the 25-year, 24-hour peak flows without overtopping and flooding adjacent properties. If only the four road crossings were improved without corresponding improvements to the adjacent Smelter Creek channel, these breakouts would be exacerbated and adverse impacts would occur (i.e., flow in the channel would pond behind the new culverts and roadway embankments and be diverted outside the channel corridor). Therefore, it is recommended that the existing channel be improved within the Ruhenstroth community to prevent breakouts and to contain flow at the new crossings. The concept elements are described below.

5.2.1 Smelter Creek Conveyance Improvements

5.2.1.1 Design Parameters

Using normal depth calculations, two concept channels (25-year and 100-year) were developed to prevent flow breakouts along the channel and at the proposed culvert locations. The design characteristics are:

- 25-Year Design
 - Flow (cfs): 640
 - Slope (ft/ft): 0.01
 - Manning's n value: 0.06 (same as FLO-2D modeling)
- 100-year Design
 - Flow (cfs): 1380
 - Slope (ft/ft): 0.01
 - Manning's n value: 0.06 (same as FLO-2D modeling)

5.2.1.2 Typical Sections

Based on the design parameters, two typical sections were developed. The 25-year typical section is shown as Figure 5-2, and the 100-year section is shown as Figure 5-3. In the 25-year section, the bottom width is 35 feet, side slopes are 3:1 (H:V), and 1-foot of freeboard is provided. Similarly, the bottom width is 45 feet, side slopes are 3:1 (H:V), and 1-foot of freeboard is provided in the 100-year section. These dimensions were chosen based on 1) the geometry of the existing upstream channel where it has capacity, 2) the estimated headwater elevation at the new culverts, and 3) the width of the new culverts was approximately the same as the bottom width of the channel.

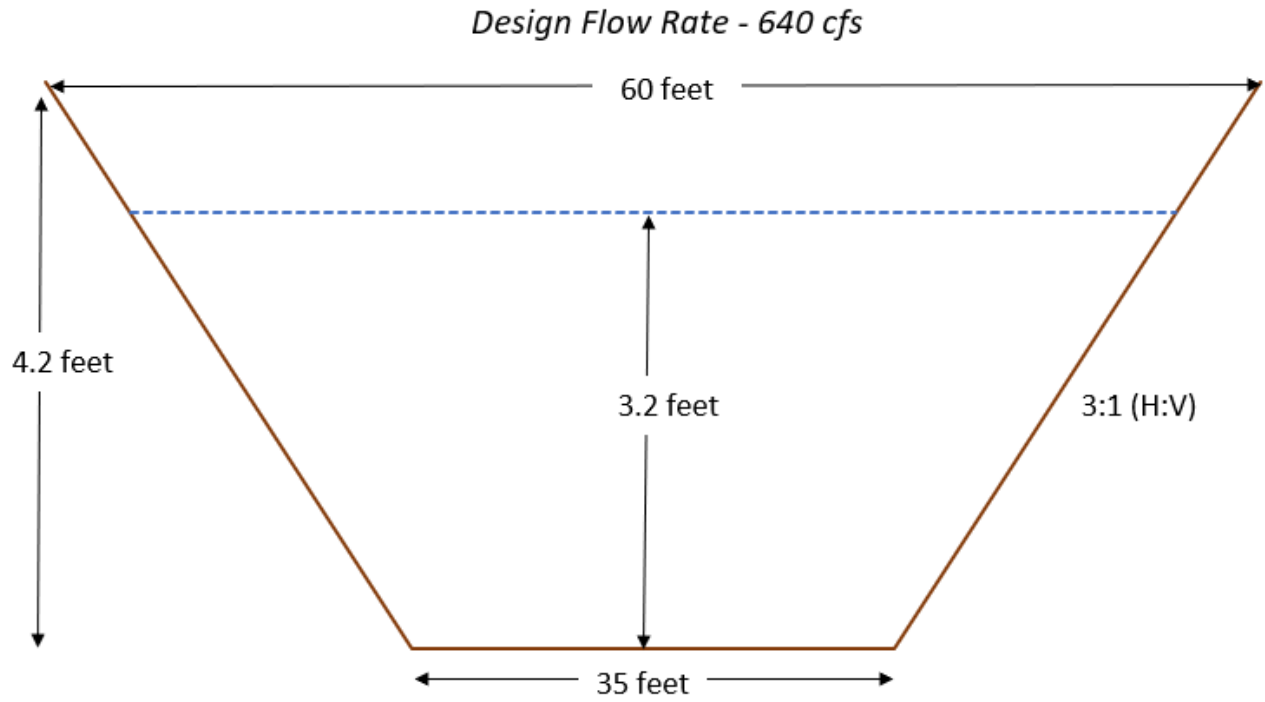


Figure 5-2. 25-year typical section

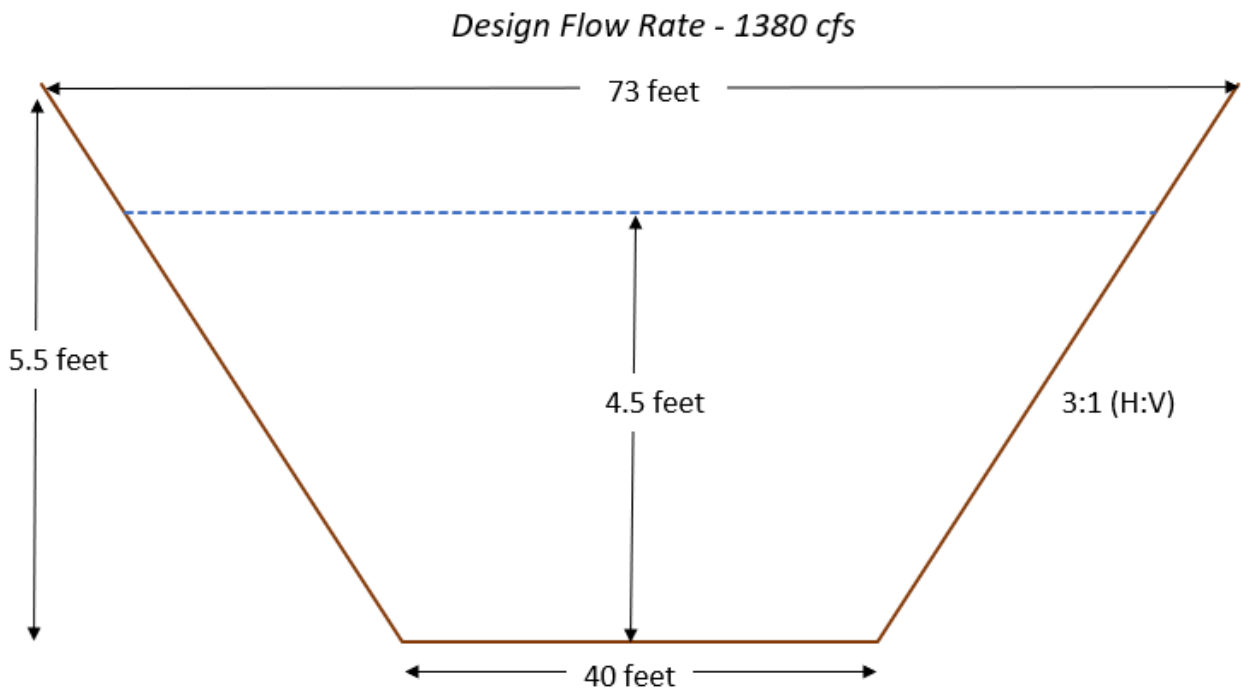


Figure 5-3. 100-year typical section

5.2.2 New Culverts

Using HY-8 and standard NDOT box culvert sizes, multiple culvert configurations were analyzed to estimate which configuration better aligned with the new channel. That is, headwater depths were reduced to be contained within the estimated freeboard of the new channels, and the width of the installed culverts approximately matched the upstream channel. The suggested culvert configurations are shown below:

- 25-Year Design
 - 4 barrel 8-ft by 5-ft reinforced concrete box culvert (RCBC)
- 100-year Design
 - 5 barrel 8-ft by 5-ft RCBC

The 25-year suggested improvements and existing conditions 25Y24H storm discharges are shown Figure 5-4, while the 100-year improvements and existing conditions 100Y24H storm discharges are shown in Figure 5-5.

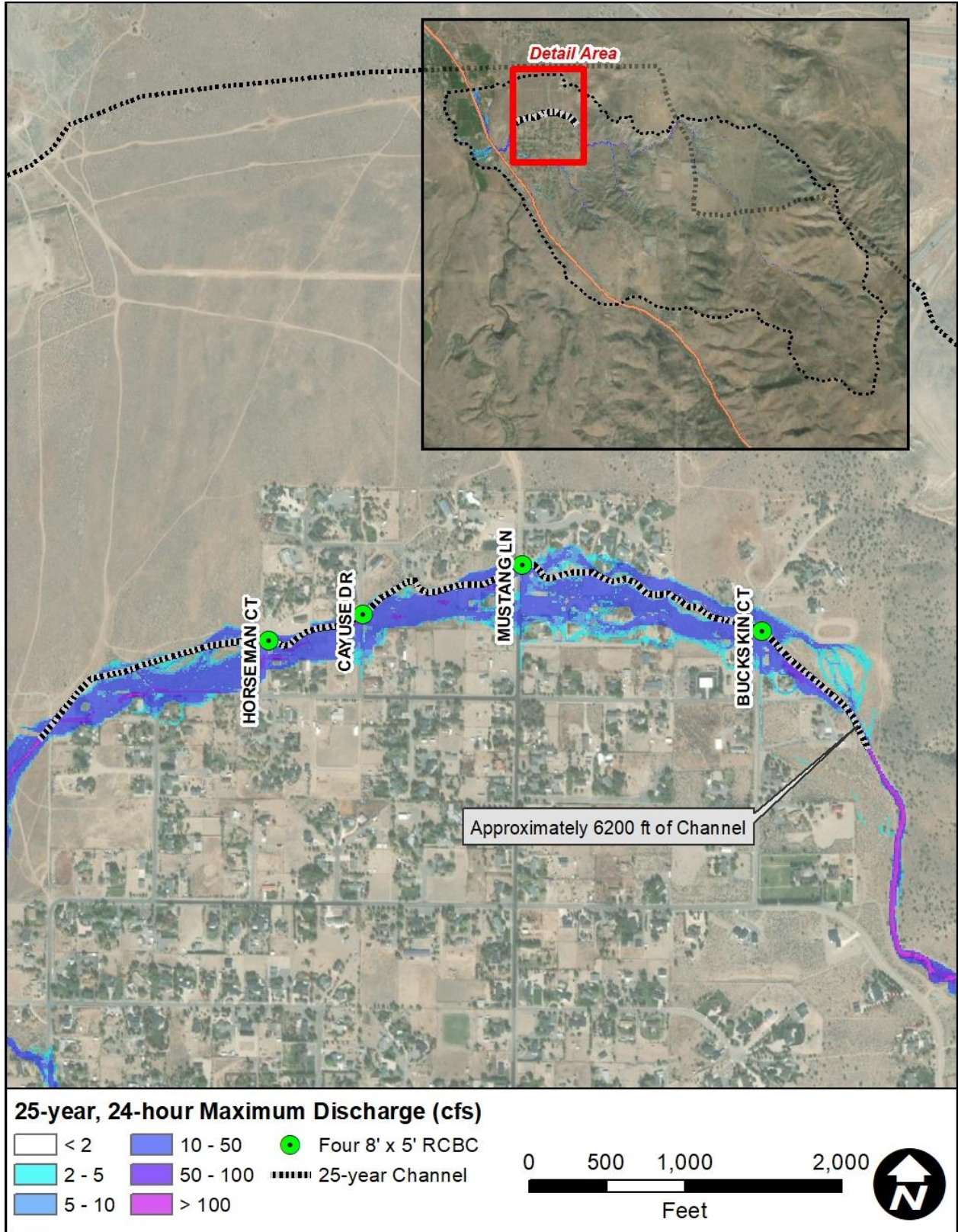


Figure 5-4. 25-year concept improvements

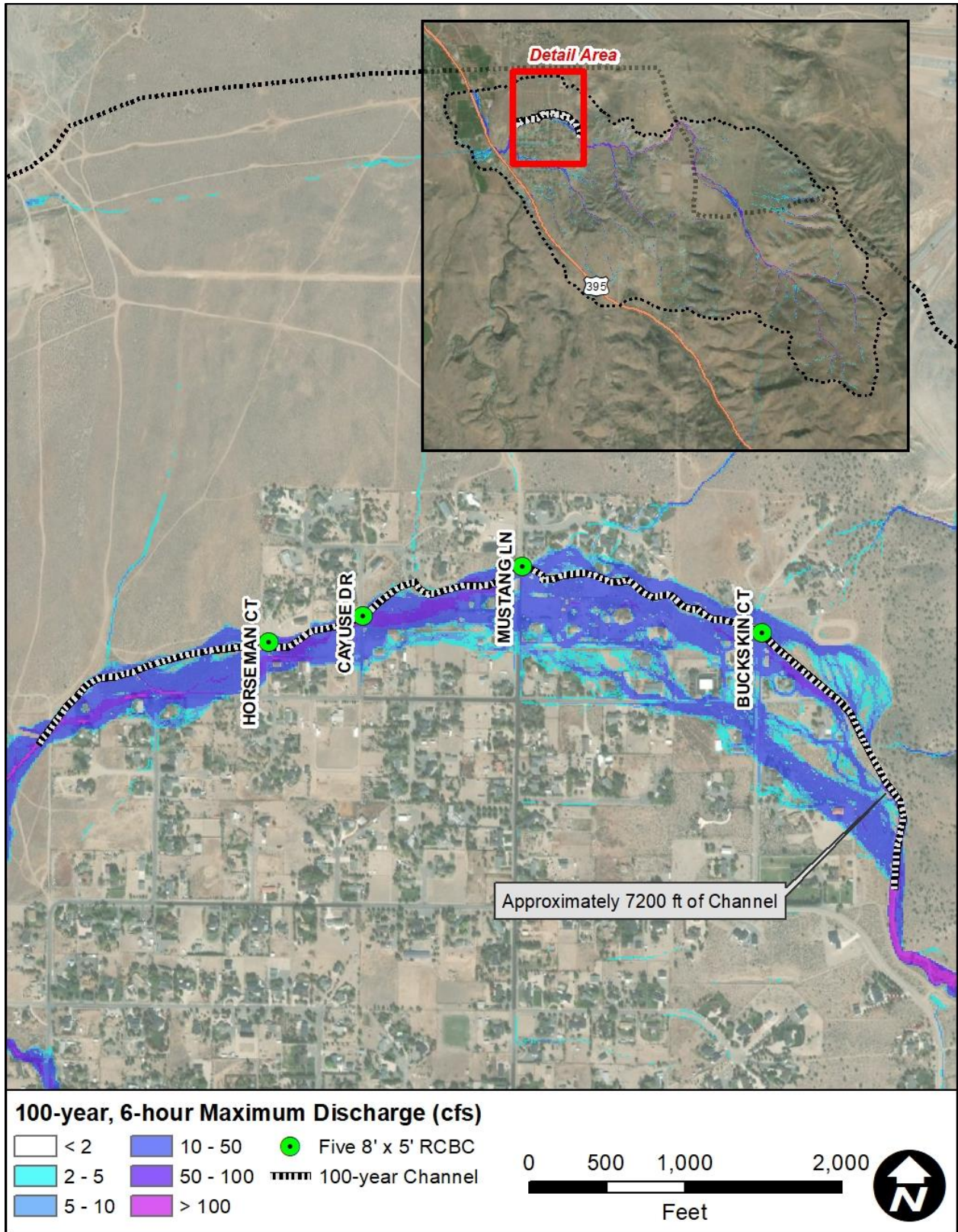


Figure 5-5. 100-year concept improvements

5.2.3 Cost Estimates

Approximate cost estimates for each of the concept elements are listed in Table 5-1 and Table 5-2. These costs were developed based on the cost per lineal foot basis that was used in the South Dayton ADMP (JEF, 2020b). However, these estimates do not consider detailed costs for right-of-way (ROW) acquisition, drainage easements, permit fees, FEMA CLOMR/LOMR development. As such, a 30% contingency was added to the total cost to account for unforeseen items.

Table 5-1. 25-year concept cost estimates

| Item | 25-Year Storm Cost Estimate |
|-------------------------------|------------------------------------|
| Existing Channel Improvements | \$4,490,000 |
| New Crossings (4 total) | \$680,000 |
| Contingency (30%) | \$1,550,000 |
| Total | \$6,720,000 |

Table 5-2. 100-year concept cost estimates

| Item | 100-Year Storm Cost Estimate |
|-------------------------------|-------------------------------------|
| Existing Channel Improvements | \$5,540,000 |
| New Crossings (4 total) | \$840,000 |
| Contingency (30%) | \$1,910,000 |
| Total | \$8,290,000 |

6 REFERENCES

Douglas County, 2017, Design Criteria and Improvement Standards.

FEMA, 1999, Flood Insurance Study for Douglas County, Nevada Unincorporated Areas.

_____, 2010, Flood Insurance Study for Douglas County, Nevada Unincorporated Areas.

_____, 2016, Flood Insurance Study for Douglas County, Nevada Unincorporated Areas.

Flood Control District of Maricopa County (FCDMC), 2018, Drainage Design Manual for Maricopa County, Arizona - Hydrology, December 2018. Can be downloaded from:

<https://www.maricopa.gov/DocumentCenter/View/2370/Drainage-Design-Manual-for-Maricopa-County-Volume-I-Hydrology---revised-121418-PDF>

_____, 2016, Drainage Policies and Standards for Maricopa County, Supplemental Technical Document, FLO-2D Verification Report, May 2016. Can be downloaded from:

http://apps.fcd.maricopa.gov/pub/docs/scanfcdlibrary/1004_045DrainagePoliciesandStandardsforMaricopaCountySupplementalTechnicalDocumentationFLO2DVerificationReport.pdf

FLO-2D Software, Inc., 2018, FLO-2D Reference Manual, Build No. 18 2018.

_____, 2019, FLO-2D Data Input Manual, August 2019 – Build 19.

Floyd, B., 2017, Alluvial Fan Mapping for the Carson River Watershed Methodology, U.S. Army Corps of Engineers, Sacramento District.

Jarrett, R. D., 1985. Determination of Roughness Coefficients for Streams in Colorado, USGS Water Resources Investigations Report 85-4004.

JE Fuller, Inc. (JEF), 2018, Johnson Lane Area Drainage Master Plan Technical Study Data Notebook, Douglas County, Nevada.

_____, 2019a, Alpine View Estates Area Drainage Master Plan Technical Study Data Notebook. Douglas County, Nevada.

_____, 2019b, Dayton Valley Area Drainage Master Plan Technical Study Data Notebook. Lyon and Storey Counties, Nevada.

- _____, 2020a, Sun Valley ADMPU Roughness Determination. Memorandum prepared for the Flood Control District of Maricopa County, dated April 30, 2020.
- _____, 2020b, South Dayton Valley Area Drainage Master Plan Technical Study Data Notebook. Lyon County, Nevada.
- Mohave County, 2018, Drainage Design Manual for Mohave County, Third Edition, May 2018.
- Natural Resources Conservation Service (NRCS), 2019, Web Soil Survey, retrieved from <https://websoilsurvey.sc.egov.usda.gov/App/WebSoilSurvey.aspx> on December 10, 2019.
- National Weather Service (NWS), 2018, NOAA Atlas 14 Precipitation Frequency Estimates, retrieved from https://hdsc.nws.noaa.gov/hdsc/pfds/pfds_gis.html, on June 18, 2018.
- Nevada Department of Transportation (NDOT), 2015, Streamlining Hydrologic Prediction Processes Using New and More Accurate Techniques and Methods, NDOT Research Report, Report No. 530-13-803.
- Quantum Spatial, Inc. (QSI), 2019, Ruhestroth, Nevada LiDAR Technical Data Report, December 13, 2019.
- RO Anderson Engineering, Inc., 2015, Smelter Creek Regional Flood Control Project, Douglas County, Nevada, Feasibility Engineering Study. Minden, NV.
- US Bureau of Reclamation (USBR), 1988, Downstream Hazard Classification Guidelines, Acer Technical Memorandum No. 11.
- US Geological Survey (USGS), 1997, Methods for Estimating Magnitude and Frequency of Floods in the Southwestern United States, Water-Supply Paper 2433.
- Wolman, M. G., 1954, A Method of Sampling Coarse River-Bed Material, *Transactions, American Geophysical Union*, Vol. 35, No. 6, pp. 951-956.
- Yang, C. T., 1973, Incipient motion and sediment transport, *Journal of the Hydraulics Division, ASCE*, 99 (HY10), pp. 1670-1704.
- _____, 1984, Unit stream power equation for gravel. *Journal of Hydraulic Engineering, ASCE*, 110(HY12), pp. 1783-1797.

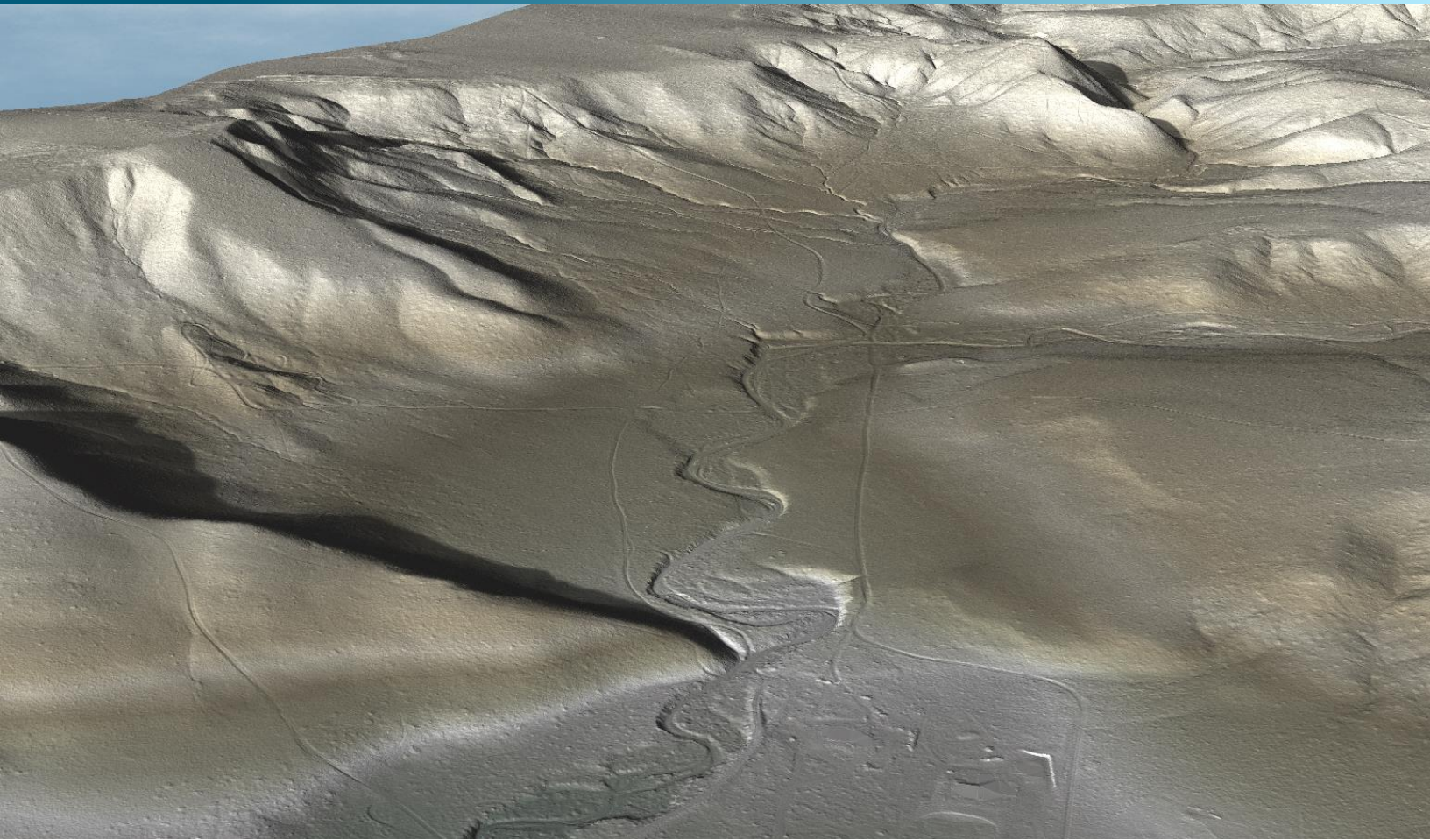
Yochum, S.E., Comiti, F., Wohl, E., David, G.C.L., Mao, L. 2014. Photographic Guidance for Selecting Flow Resistance Coefficients in High-Gradient Channels. USDA, Forest Service, Rocky Mountain Research Station, General Technical Report, RMRS-GTR-323

DRAFT

APPENDIX A

QSI LiDAR Report

December 13, 2019



Ruhenstroth, Nevada LiDAR

Technical Data Report

Prepared For:



JE Fuller
Mike Kellogg
8400 S. Kyrene Road
Suite 201
Tempe, AZ 85284
PH: 480-222-5712

Prepared By:



QSI Corvallis
1100 NE Circle Blvd, Ste. 126
Corvallis, OR 97330
PH: 541-752-1204

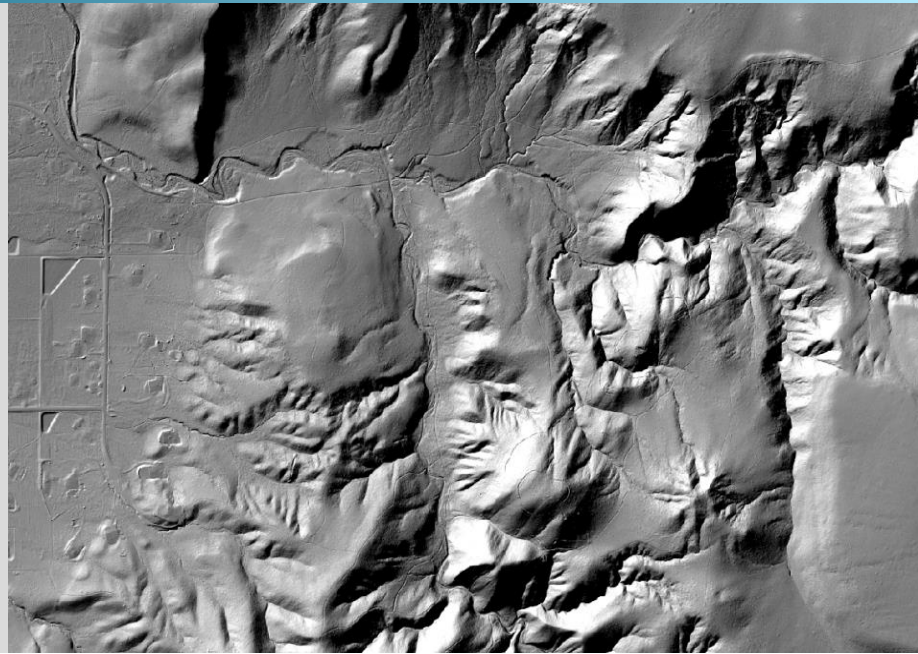
TABLE OF CONTENTS

- INTRODUCTION 1
 - Deliverable Products 2
- ACQUISITION 4
 - Planning..... 4
 - Airborne LiDAR Survey 5
 - Ground Survey..... 6
 - Base Stations..... 6
 - Ground Survey Points (GSPs)..... 7
- PROCESSING 9
 - LiDAR Data..... 9
- RESULTS & DISCUSSION..... 11
 - LiDAR Density 11
 - LiDAR Accuracy Assessments 14
 - LiDAR Non-Vegetated Vertical Accuracy 14
 - LiDAR Relative Vertical Accuracy 17
 - LiDAR Horizontal Accuracy 18
- CERTIFICATIONS 19
- GLOSSARY 20
- APPENDIX A - ACCURACY CONTROLS 21

Cover Photo: A view looking east over the Ruhenstroth project area. The image was created from the LiDAR bare earth model colored by elevation.

INTRODUCTION

A top down view of a hillshade digital elevation model showing the terrain east of Ruhestroth



In October 2019, Quantum Spatial (QSI) was contracted by JE Fuller (JEF) to collect Light Detection and Ranging (LiDAR) data in the fall of 2019 for the Ruhestroth site in Nevada. Data were collected to aid JEF in assessing the topographic and geophysical properties of the study area to support the creation of the Ruhestroth Area Drainage Master Plan.

This report accompanies the delivered LiDAR data and documents contract specifications, data acquisition procedures, processing methods, and analysis of the final dataset including LiDAR accuracy and density. Acquisition dates and acreage are shown in Table 1, a complete list of contracted deliverables provided to JEF is shown in Table 2, and the project extent is shown in Figure 1.

Table 1: Acquisition dates, acreage, and data types collected on the Ruhestroth site

| Project Site | Contracted Acres | Buffered Acres | Acquisition Dates | Data Type |
|--------------------|------------------|----------------|-------------------|-----------|
| Ruhestroth, Nevada | 12,420 | 13,250 | 10/24/2019 | LiDAR |

Deliverable Products

Table 2: Products delivered to JEF for the Ruhenstroth site

| Ruhenstroth, Nevada LiDAR Products | |
|-------------------------------------|--|
| Projection: Nevada State Plane West | |
| Horizontal Datum: NAD83 (2011) | |
| Vertical Datum: NAVD88 (GEOID12B) | |
| Units: US Survey Feet | |
| Points | LAS v 1.4 <ul style="list-style-type: none">All Classified Returns |
| Rasters | 3.0 Foot ESRI Grids <ul style="list-style-type: none">Bare Earth Digital Elevation Model (DEM) |
| Vectors | Shapefiles (*.shp) <ul style="list-style-type: none">Project BoundaryTile Index |

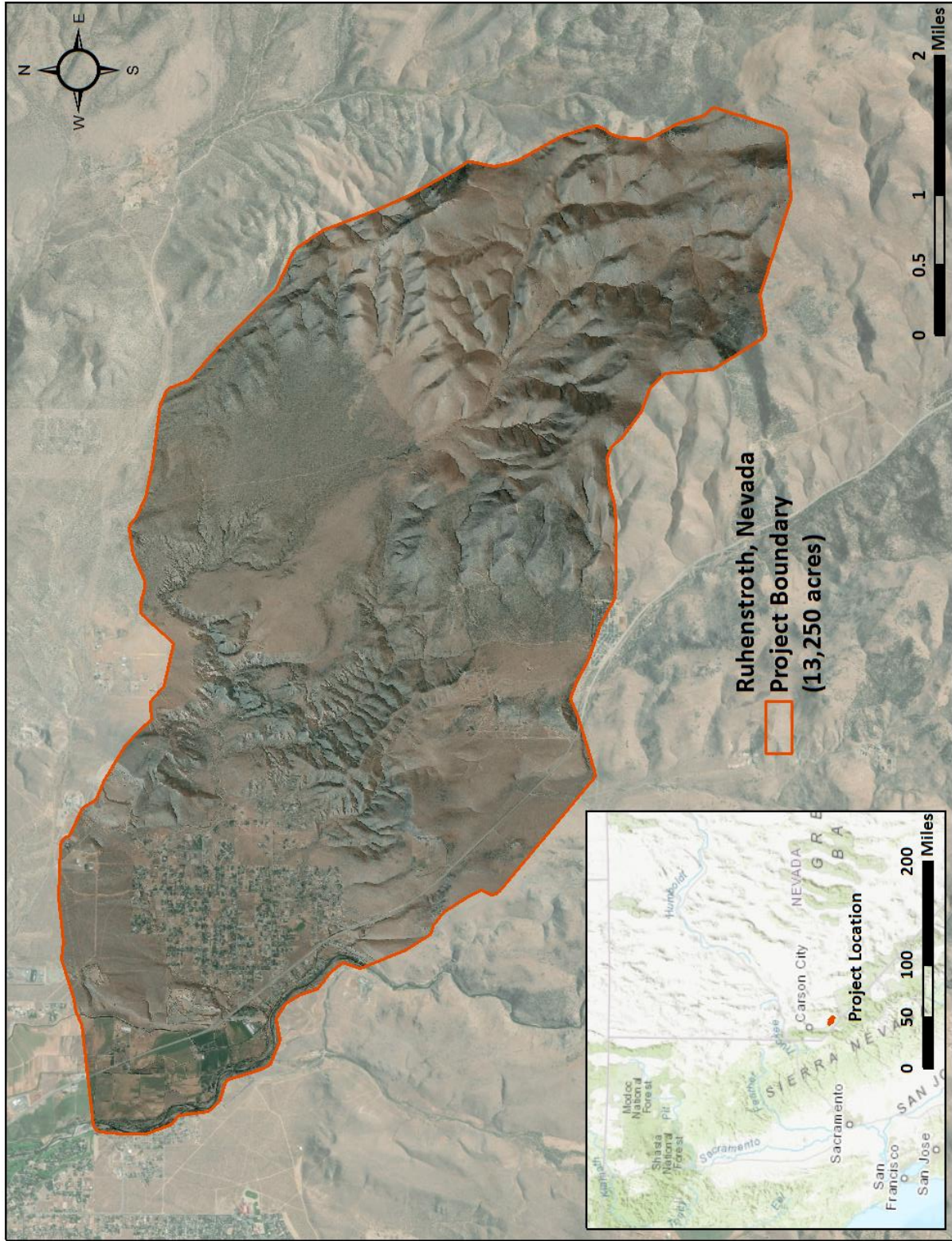


Figure 1: Location map of the Ruhenstroth site in Nevada

QSI's Cessna Caravan



Planning

In preparation for data collection, QSI reviewed the project area and developed a specialized flight plan to ensure complete coverage of the Ruhestroth LiDAR study area at the target point density of ≥ 8.0 points/m² (0.74 points/ft²). Acquisition parameters including orientation relative to terrain, flight altitude, pulse rate, scan angle, and ground speed were adapted to optimize flight paths and flight times while meeting all contract specifications.

Factors such as satellite constellation availability and weather windows must be considered during the planning stage. Any weather hazards or conditions affecting the flight were continuously monitored due to their potential impact on the daily success of airborne and ground operations. In addition, logistical considerations including private property access and potential air space restrictions were reviewed.

Airborne LiDAR Survey

The LiDAR survey was accomplished using a Riegl VQ-1560i system mounted in a Cessna Caravan. Table 3 summarizes the settings used to yield an average pulse density of ≥ 8 pulses/m² over the Ruhenstroth, Nevada project area. The Riegl VQ-1560i laser system can record unlimited range measurements (returns) per pulse. It is not uncommon for some types of surfaces (e.g., dense vegetation or water) to return fewer pulses to the LiDAR sensor than the laser originally emitted. The discrepancy between first return and overall delivered density will vary depending on terrain, land cover, and the prevalence of water bodies. All discernible laser returns were processed for the output dataset.

Table 3: LiDAR specifications and survey settings

| LiDAR Survey Settings & Specifications | |
|--|---|
| Acquisition Dates | October 24, 2019 |
| Aircraft Used | Cessna Caravan 208B |
| Sensor | Riegl |
| Laser | VQ-1560i |
| Maximum Returns | Unlimited |
| Resolution/Density | Average 8 pulses/m ² |
| Nominal Pulse Spacing | 0.35 m |
| Survey Altitude (AGL) | 1825 m |
| Survey speed | 145 knots |
| Field of View | 58.5° |
| Mirror Scan Rate | 117 lines/sec per channel |
| Target Pulse Rate | 700 kHz per channel |
| Pulse Length | 3 ns |
| Laser Pulse Footprint Diameter | 32.85 cm |
| Central Wavelength | 1064 nm |
| Pulse Mode | Multiple Times Around (MTA) |
| Beam Divergence | 0.18 mrad |
| Swath Width | 2,045 m |
| Swath Overlap | 55% |
| Intensity | 16-bit |
| Accuracy | RMSE _z (Non-Vegetated) \leq 9 cm |
| | NVA (95% Confidence Level) \leq 20 cm |



Riegl VQ-1560i

All areas were surveyed with an opposing flight line side-lap of $\geq 55\%$ ($\geq 100\%$ overlap) in order to reduce laser shadowing and increase surface laser painting. To accurately solve for laser point position (geographic coordinates x, y and z), the positional coordinates of the airborne sensor and the attitude of the aircraft were recorded continuously throughout the LiDAR data collection mission. Position of the aircraft was measured twice per second (2 Hz) by an onboard differential GPS unit, and aircraft attitude was measured 200 times per second (200 Hz) as pitch, roll and yaw (heading) from an onboard inertial measurement unit (IMU). To allow for post-processing correction and calibration, aircraft and sensor position and attitude data are indexed by GPS time.

Ground Survey

Ground control surveys were conducted to support the airborne acquisition. Ground control data were used to geospatially correct the aircraft positional coordinate data and to perform quality assurance checks on final LiDAR data.

Base Stations

Base stations were utilized for collection of ground survey points using real time kinematic (RTK) and post processed kinematic (PPK) survey techniques.

QSI utilized two existing permanent active CORS on the SMARTNET network for the Ruhenstroth LiDAR project (Table 4, Figure 2). QSI's professional land surveyor, Steven J. Hyde (NVPLS#22474) certified the ground survey work.

Table 4: Base Station positions for the Ruhenstroth acquisition. Coordinates are on the NAD83 (2011) datum, epoch 2010.00

| Base Station ID | Latitude | Longitude | Ellipsoid (meters) |
|-----------------|-------------------|---------------------|--------------------|
| P143 | 38° 45' 36.58612" | -119° 45' 53.35789" | 1734.147 |
| NVCC | 39° 10' 50.94039" | -119° 45' 55.01479" | 1419.696 |

QSI utilized static Global Navigation Satellite System (GNSS) data collected at 1 Hz recording frequency for each base station. During post-processing, the static GNSS data were triangulated with nearby Continuously Operating Reference Stations (CORS) using the Online Positioning User Service (OPUS¹) for precise positioning. Multiple independent sessions over the same monument were processed to confirm antenna height measurements and to refine position accuracy.

¹ OPUS is a free service provided by the National Geodetic Survey to process corrected monument positions. <http://www.ngs.noaa.gov/OPUS>.

Ground Survey Points (GSPs)

Ground survey points were collected using real time kinematic (RTK) and post-processed kinematic (PPK) survey techniques. For RTK surveys, a roving receiver receives corrections from a nearby base station or Real-Time Network (RTN) via radio or cellular network, enabling rapid collection of points with relative errors less than 1.5 cm horizontal and 2.0 cm vertical. PPK surveys compute these corrections during post-processing to achieve comparable accuracy. RTK and PPK surveys record data while stationary for at least five seconds, calculating the position using at least three one-second epochs. All GSP measurements were made during periods with a Position Dilution of Precision (PDOP) of ≤ 3.0 with at least six satellites in view of the stationary and roving receivers. See Table 5 for Trimble unit specifications.

GSPs were collected in areas where good satellite visibility was achieved on paved roads and other hard surfaces such as gravel or packed dirt roads. GSP measurements were not taken on highly reflective surfaces such as center line stripes or lane markings on roads due to the increased noise seen in the laser returns over these surfaces. GSPs were collected within as many flightlines as possible; however, the distribution of GSPs depended on ground access constraints and monument locations and may not be equitably distributed throughout the study area (Figure 2).

Table 5: QSI ground survey equipment identification

| Receiver Model | Antenna | OPUS Antenna ID | Use |
|----------------|--------------------|-----------------|-------|
| Trimble R8 | Integrated Antenna | TRM_R8_GNSS | Rover |

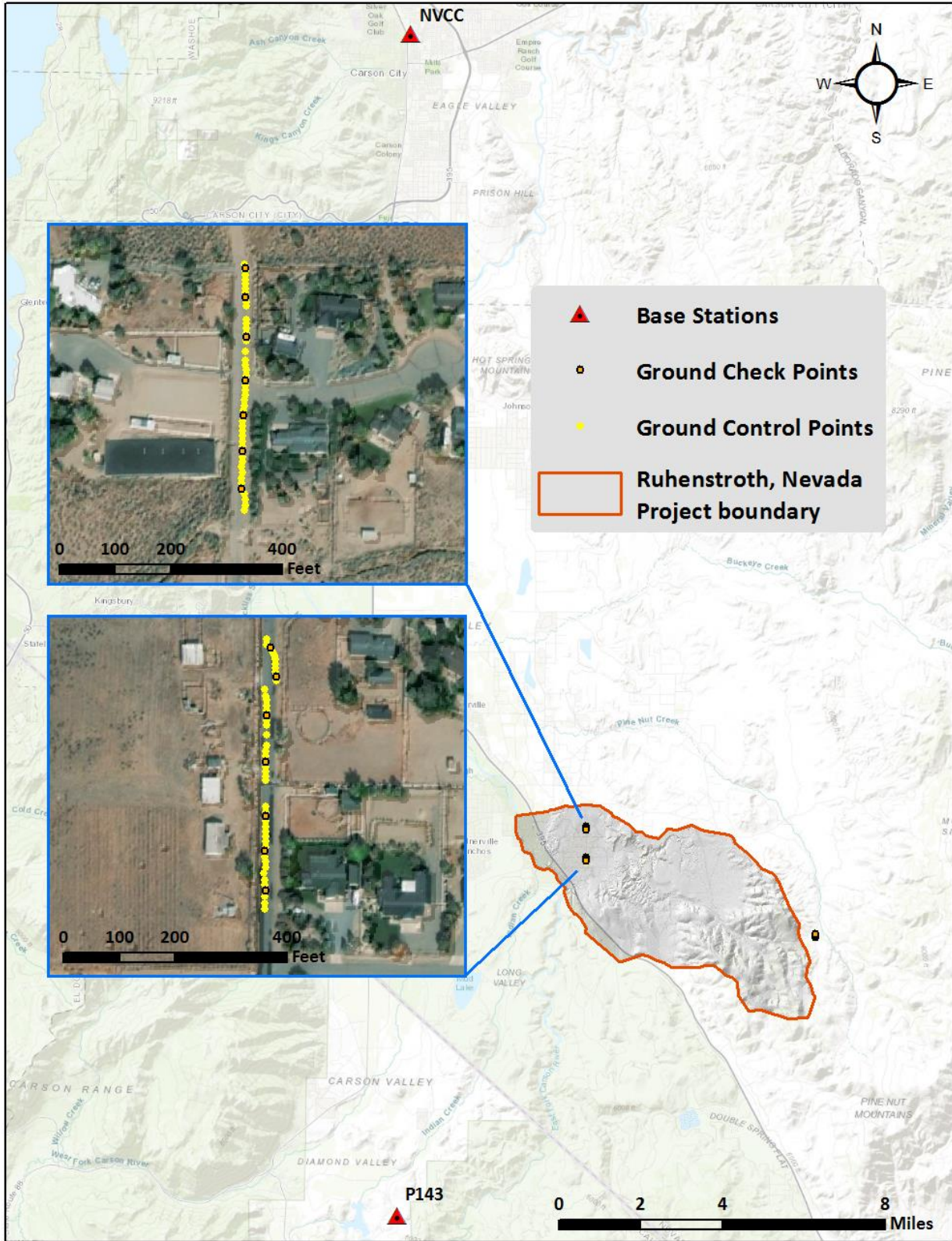


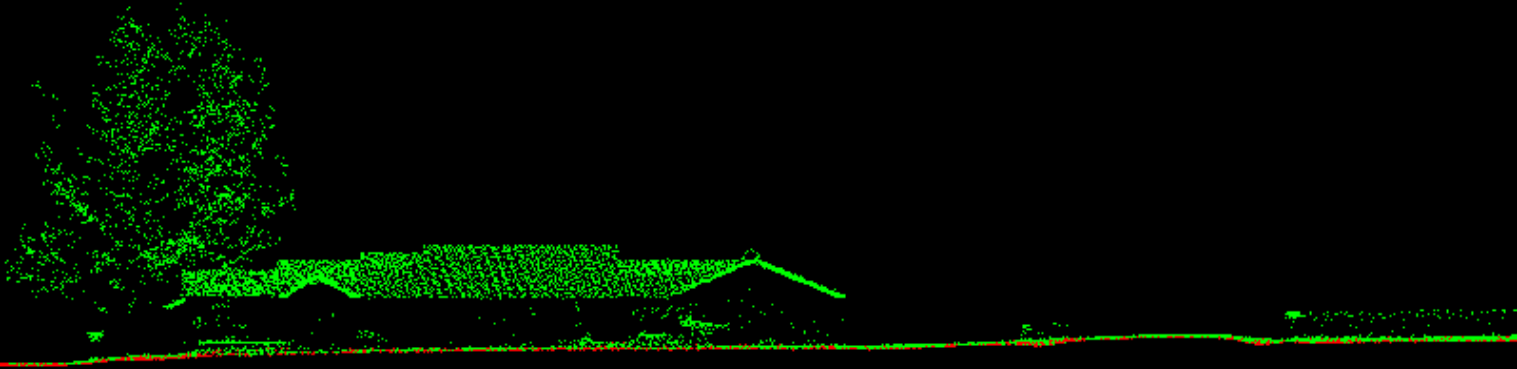


Figure 2: Ground survey location map

This LiDAR cross section shows a view of a house and trees in the Ruhestroth project boundary, colored by point classification.

Default 
Ground 



LiDAR Data

Upon completion of data acquisition, QSI processing staff initiated a suite of automated and manual techniques to process the data into the requested deliverables. Processing tasks included GPS control computations, smoothed best estimate trajectory (SBET) calculations, kinematic corrections, calculation of laser point position, sensor and data calibration for optimal relative and absolute accuracy, and LiDAR point classification (Table 6). Processing methodologies were tailored for the landscape. Brief descriptions of these tasks are shown in Table 7.

Table 6: ASPRS LAS classification standards applied to the Ruhestroth dataset

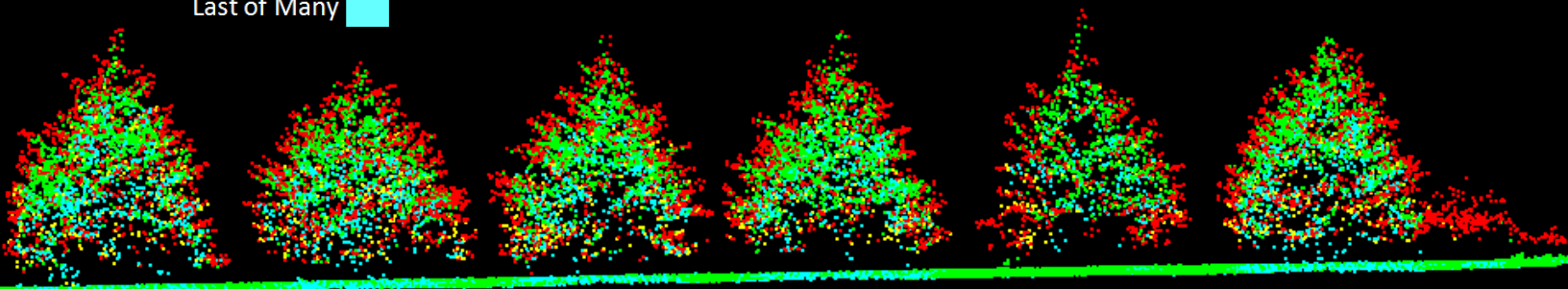
| Classification Number | Classification Name | Classification Description |
|-----------------------|----------------------|--|
| 1 | Default/Unclassified | Laser returns that are not included in the ground class, composed of vegetation and anthropogenic features |
| 2 | Ground | Laser returns that are determined to be ground using automated and manual cleaning algorithms |
| 7 | Noise | Laser returns that are often associated with birds, scattering from reflective surfaces, or artificial points below the ground surface |
| 129 | Edge Clip | Laser returns at the outer edges of flightlines that are geometrically unreliable |

Table 7: LiDAR processing workflow

| LiDAR Processing Step | Software Used |
|---|---|
| Resolve kinematic corrections for aircraft position data using kinematic aircraft GPS and static ground GPS data. Develop a smoothed best estimate of trajectory (SBET) file that blends post-processed aircraft position with sensor head position and attitude recorded throughout the survey. | POSPac MMS v.8.3 |
| Calculate laser point position by associating SBET position to each laser point return time, scan angle, intensity, etc. Create raw laser point cloud data for the entire survey in *.las (ASPRS v. 1.4) format. Convert data to orthometric elevations by applying a geoid correction. | RiProcess v.1.8.5 |
| Import raw laser points into manageable blocks to perform manual relative accuracy calibration and filter erroneous points. Classify ground points for individual flight lines. | TerraScan v.19 |
| Using ground classified points per each flight line, test the relative accuracy. Perform automated line-to-line calibrations for system attitude parameters (pitch, roll, heading), mirror flex (scale) and GPS/IMU drift. Calculate calibrations on ground classified points from paired flight lines and apply results to all points in a flight line. Use every flight line for relative accuracy calibration. | TerraMatch v.19 |
| Classify resulting data to ground and other client designated ASPRS classifications (Table 6). Assess statistical absolute accuracy via direct comparisons of ground classified points to ground control survey data. | TerraScan v.19 TerraModeler v.19 |
| Generate bare earth models as triangulated surfaces. Export all surface models as ESRI GRIDs at a 3.0 foot pixel resolution. | LAS Product Creator 3.0 (QSI proprietary) |



This LiDAR cross section shows a view of vegetation and bare ground in the Ruhenstroth project area, colored by point laser echo.



LiDAR Density

The acquisition parameters were designed to acquire an average first-return density of 8 points/m² (0.74 points/ft²). First return density describes the density of pulses emitted from the laser that return at least one echo to the system. Multiple returns from a single pulse were not considered in first return density analysis. Some types of surfaces (e.g., breaks in terrain, water and steep slopes) may have returned fewer pulses than originally emitted by the laser. First returns typically reflect off the highest feature on the landscape within the footprint of the pulse. In forested or urban areas the highest feature could be a tree, building or power line, while in areas of unobstructed ground, the first return will be the only echo and represents the bare earth surface.

The density of ground-classified LiDAR returns was also analyzed for this project. Terrain character, land cover, and ground surface reflectivity all influenced the density of ground surface returns. In vegetated areas, fewer pulses may penetrate the canopy, resulting in lower ground density.

The average first-return density of LiDAR data for the Ruhenstroth project was 1.99 points/ft² (21.38 points/m²) while the average ground classified density was 0.57 points/ft² (6.14 points/m²) (Table 8). The statistical and spatial distributions of first return densities and classified ground return densities per 100 m x 100 m cell are portrayed in Figure 3 to Figure 5.

Table 8: Average LiDAR point densities

| Classification | Point Density |
|-------------------|-----------------------------|
| First-Return | 1.99 points/ft ² |
| | 21.38 points/m ² |
| Ground Classified | 0.57 points/ft ² |
| | 6.14 points/m ² |

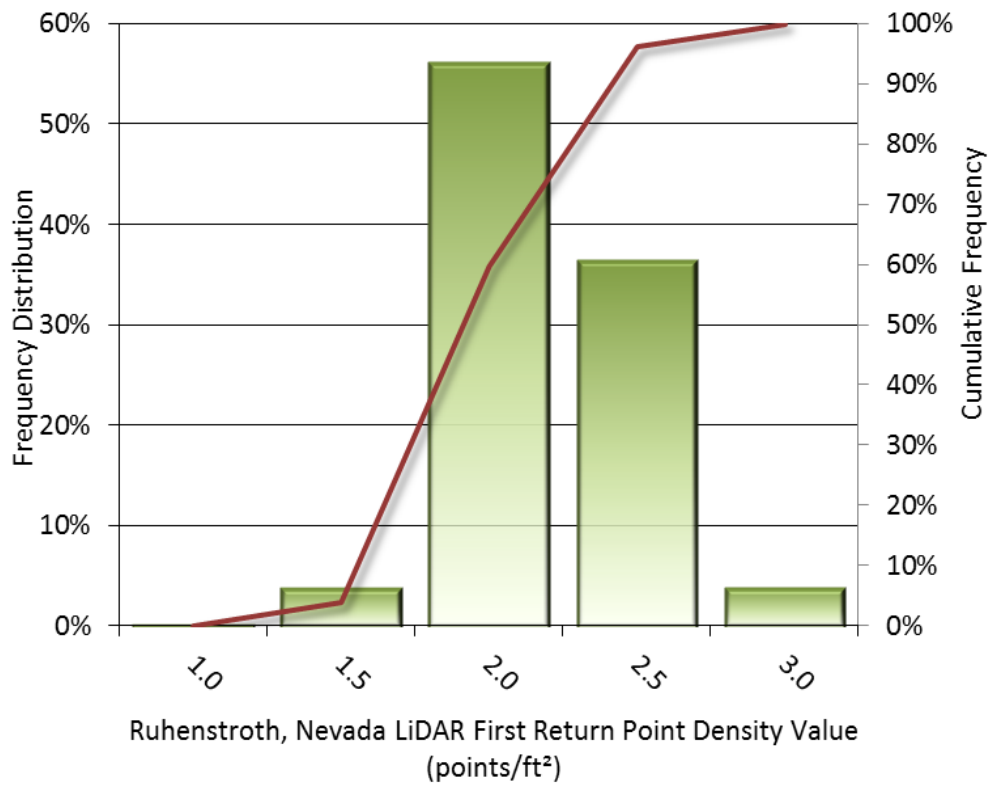


Figure 3: Frequency distribution of first return point density values per 100 x 100 m cell

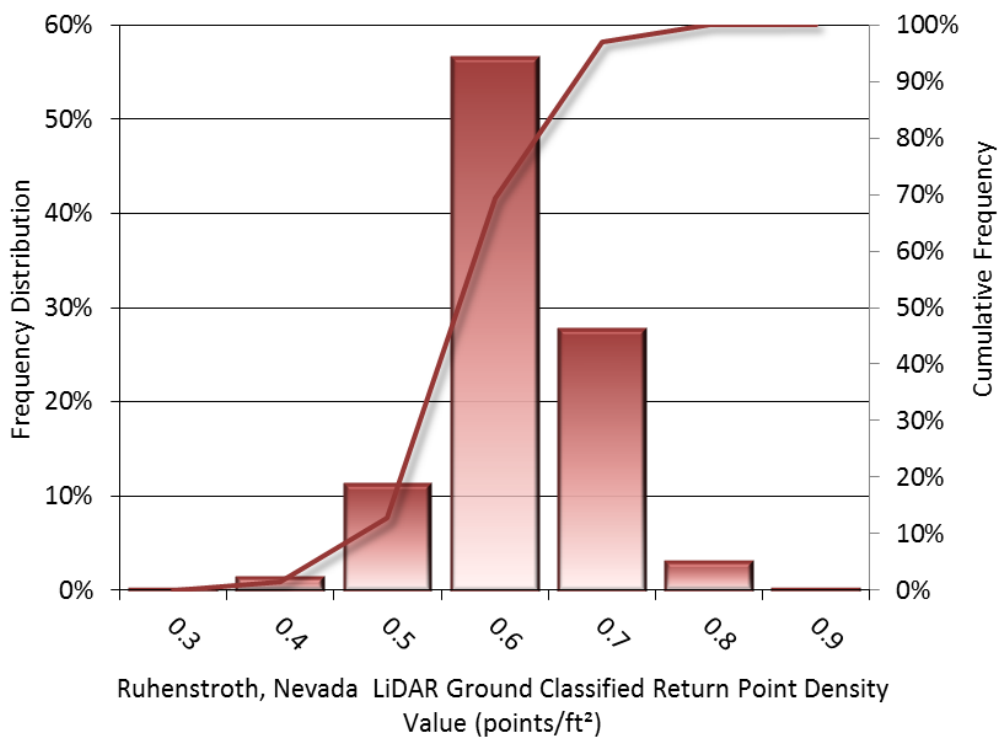


Figure 4: Frequency distribution of ground-classified return point density values per 100 x 100 m cell

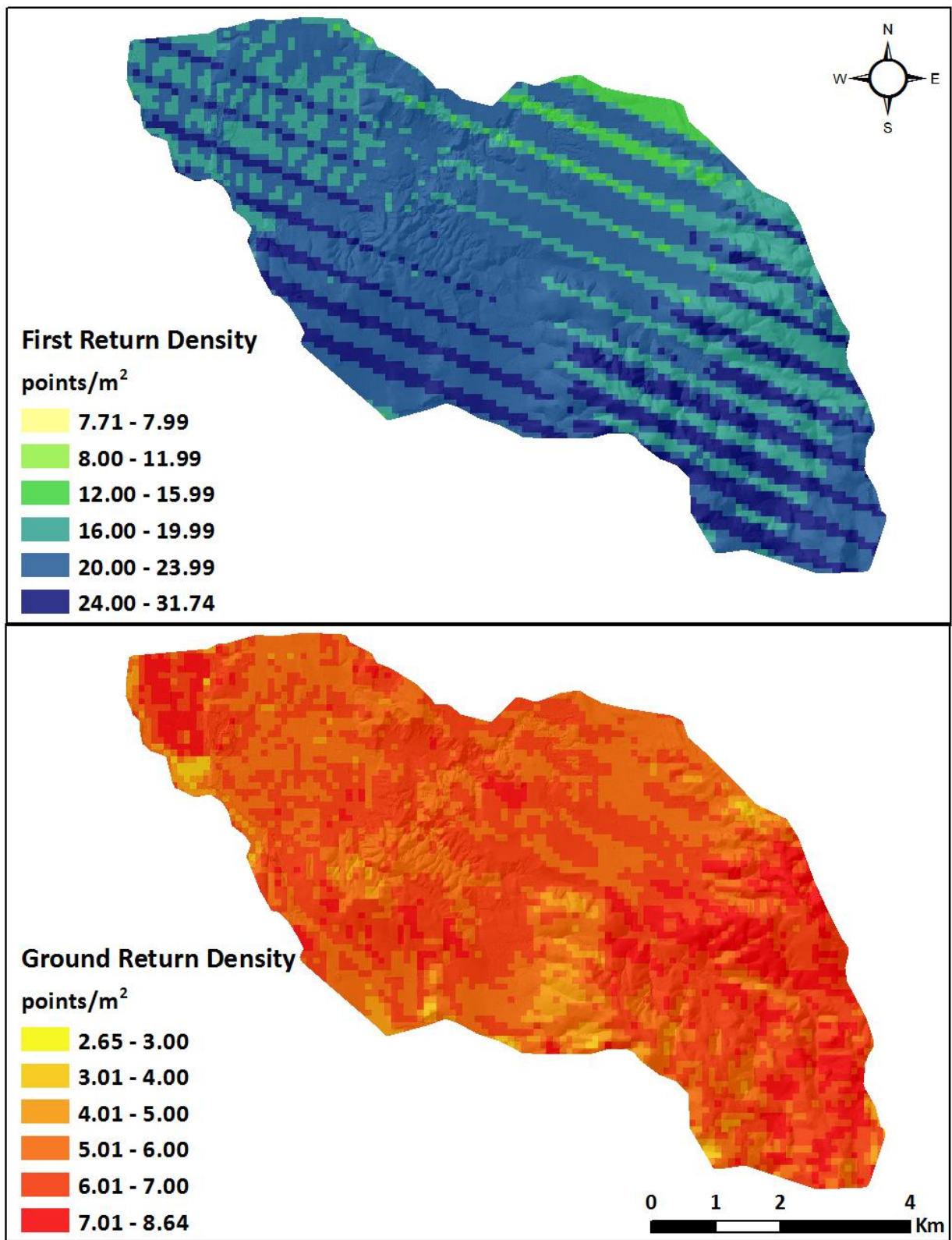


Figure 5: First return and ground-classified point density map for the Ruhenstroth site (100 m x 100 m cells)

LiDAR Accuracy Assessments

The accuracy of the LiDAR data collection can be described in terms of absolute accuracy (the consistency of the data with external data sources) and relative accuracy (the consistency of the dataset with itself). See Appendix A for further information on sources of error and operational measures used to improve relative accuracy.

LiDAR Non-Vegetated Vertical Accuracy

Absolute accuracy was assessed using Non-Vegetated Vertical Accuracy (NVA) reporting designed to meet guidelines presented in the FGDC National Standard for Spatial Data Accuracy². NVA compares known ground check point data that were withheld from the calibration and post-processing of the LiDAR point cloud to the triangulated surface generated by the unclassified LiDAR point cloud as well as the derived gridded bare earth DEM. NVA is a measure of the accuracy of LiDAR point data in open areas where the LiDAR system has a high probability of measuring the ground surface and is evaluated at the 95% confidence interval ($1.96 * RMSE$), as shown in Table 9.

The mean and standard deviation (sigma σ) of divergence of the ground surface model from quality assurance point coordinates are also considered during accuracy assessment. These statistics assume the error for x, y and z is normally distributed, and therefore the skew and kurtosis of distributions are also considered when evaluating error statistics. For the Ruhestroth survey, 21 ground check points were withheld from the calibration and post processing of the LiDAR point cloud, with resulting non-vegetated vertical accuracy of 0.227 feet (0.069 meters) as compared to unclassified LAS, and 0.233 feet (0.071 meters) as compared to the bare earth DEM, with 95% confidence (Figure 6, Figure 7).

QSI also assessed absolute accuracy using 124 ground control points. Although these points were used in the calibration and post-processing of the LiDAR point cloud, they still provide a good indication of the overall accuracy of the LiDAR dataset, and therefore have been provided in Table 9 and Figure 8.

Table 9: Absolute accuracy results

| Absolute Vertical Accuracy | | | |
|---------------------------------------|--------------------------------------|------------------------------------|-----------------------|
| | NVA, as compared to unclassified LAS | NVA, as compared to bare earth DEM | Ground Control Points |
| Sample | 21 points | 21 points | 124 points |
| 95% Confidence (1.96*RMSE) | 0.227 ft 0.069 m | 0.233 ft 0.071 m | 0.197 ft 0.060 m |
| Average | 0.055 ft 0.017 m | 0.022 ft 0.007 m | 0.001 ft 0.000 m |

² Federal Geographic Data Committee, ASPRS POSITIONAL ACCURACY STANDARDS FOR DIGITAL GEOSPATIAL DATA EDITION 1, Version 1.0, NOVEMBER 2014. <http://www.asprs.org/PAD-Division/ASPRS-POSITIONAL-ACCURACY-STANDARDS-FOR-DIGITAL-GEOSPATIAL-DATA.html>.

| Absolute Vertical Accuracy | | | |
|----------------------------------|--------------------------------------|------------------------------------|-----------------------|
| | NVA, as compared to unclassified LAS | NVA, as compared to bare earth DEM | Ground Control Points |
| Median | 0.092 ft 0.028 m | -0.001 ft 0.000 m | 0.041 ft 0.013 m |
| RMSE | 0.116 ft 0.035 m | 0.119 ft 0.036 m | 0.101 ft 0.031 m |
| Standard Deviation (1 σ) | 0.104 ft 0.032 m | 0.120 ft 0.037 m | 0.101 ft 0.031 m |

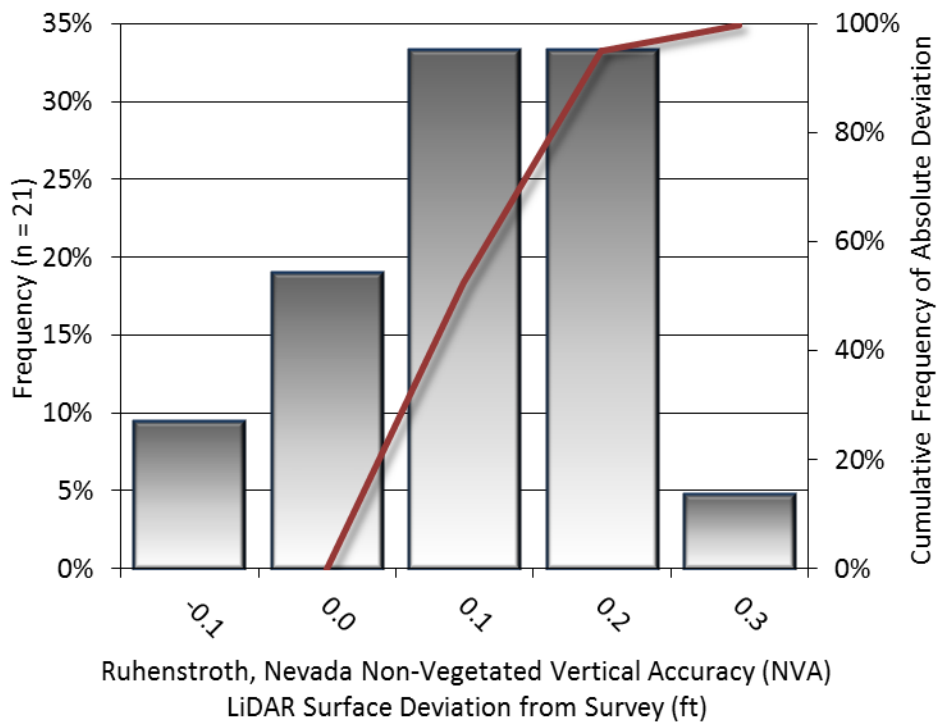


Figure 6: Frequency histogram for LiDAR unclassified LAS deviation from ground check point values (NVA)

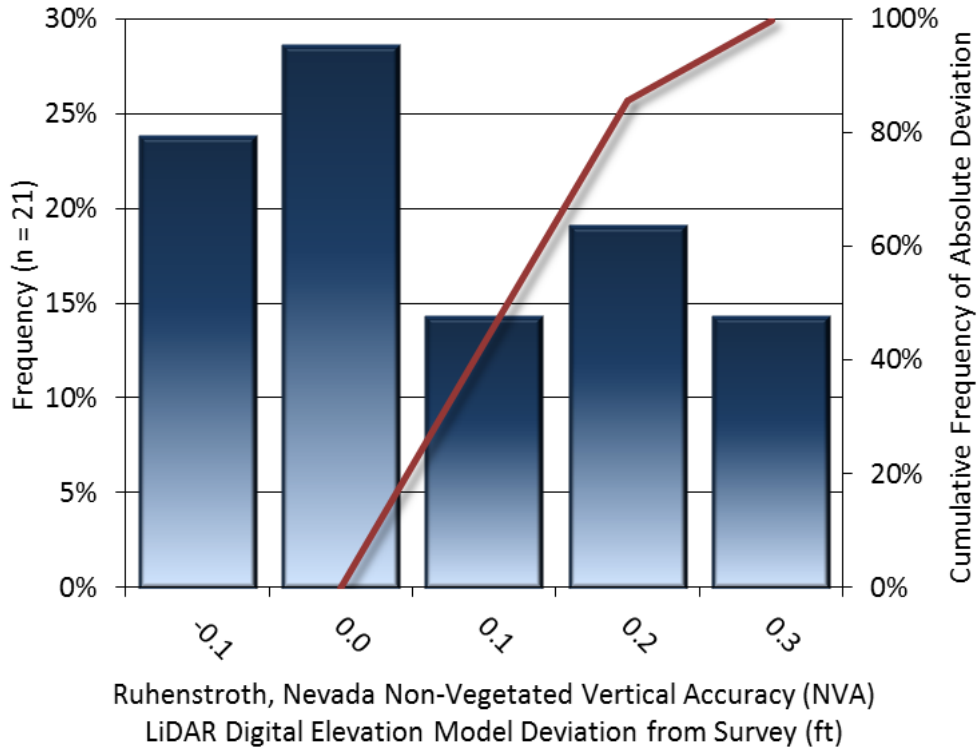


Figure 7: Frequency histogram for LiDAR bare earth DEM surface deviation from ground check point values (NVA)

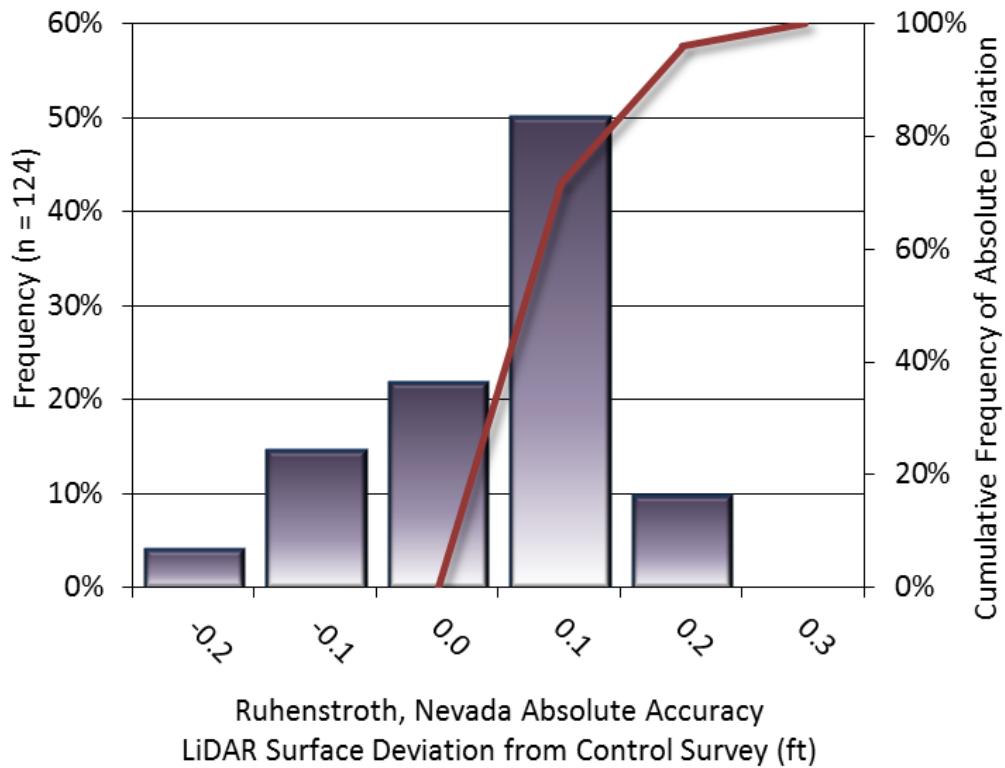


Figure 8: Frequency histogram for LiDAR surface deviation from ground control point values

LiDAR Relative Vertical Accuracy

Relative vertical accuracy refers to the internal consistency of the data set as a whole: the ability to place an object in the same location given multiple flight lines, GPS conditions, and aircraft attitudes. When the LiDAR system is well calibrated, the swath-to-swath vertical divergence is low (<0.10 meters). The relative vertical accuracy was computed by comparing the ground surface model of each individual flight line with its neighbors in overlapping regions. The average (mean) line to line relative vertical accuracy for the Ruhenstroth LiDAR project was 0.082 feet (0.025 meters) (Table 10, Figure 9).

Table 10: Relative accuracy results

| Relative Accuracy | |
|----------------------------------|-------------------------|
| Sample | 12 flight line surfaces |
| Average | 0.082 ft 0.025 m |
| Median | 0.077 ft 0.023 m |
| RMSE | 0.083 ft 0.025 m |
| Standard Deviation (1 σ) | 0.012 ft 0.004 m |
| 1.96 σ | 0.023 ft 0.007 m |

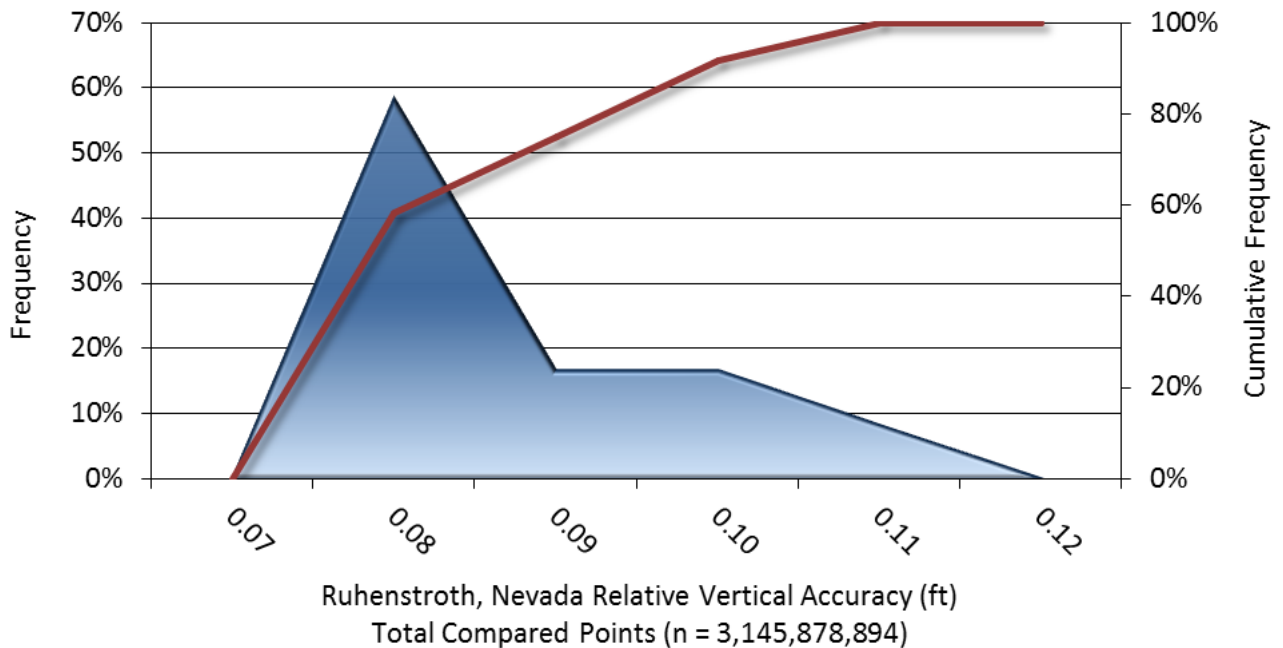


Figure 9: Frequency plot for relative vertical accuracy between flight lines

LiDAR Horizontal Accuracy

LiDAR horizontal accuracy is a function of Global Navigation Satellite System (GNSS) derived positional error, flying altitude, and INS-derived attitude error. The obtained RMSE_r value is multiplied by a conversion factor of 1.7308 to yield the horizontal component (ACC_r) of the National Standards for Spatial Data Accuracy (NSSDA) reporting standard where a theoretical point will fall within the obtained radius 95 percent of the time. Using a flying altitude of 1,825 meters, an IMU error of 0.015 decimal degrees, and a GNSS positional error of 0.002 meters, the horizontal accuracy (ACC_r) for the LiDAR collection is 0.65 feet (0.20 meters) at the 95% confidence level (Table 13). Data from the Ruhenstroth dataset have been tested to meet horizontal requirements at the 95% confidence level, using NSSDA reporting methods.

Table 11: Horizontal Accuracy

| Horizontal Accuracy | |
|---------------------|---------|
| RMSE _r | 0.95 ft |
| | 0.29 m |
| ACC _r | 1.65 ft |
| | 0.50 m |

CERTIFICATIONS

Quantum Spatial, Inc. provided LiDAR services for the Ruhenstroth project as described in this report.

I, Jackie Monge, have reviewed the attached report for completeness and hereby state that it is a complete and accurate report of this project.


Jackie Monge (Dec 18, 2019)

Dec 18, 2019

Jackie Monge
Project Manager
Quantum Spatial, Inc.

I, Steven J. Hyde, PLS, being duly registered as a Professional Land Surveyor in and by the state of Nevada, hereby certify that the methodologies, static GNSS occupations used during airborne flights, and ground survey point collection were performed using commonly accepted Standard Practices. Field work conducted for this report was conducted on October 25, 2019.

Accuracy statistics shown in the Accuracy Section of this Report have been reviewed by me and found to meet the "National Standard for Spatial Data Accuracy".




Steven J Hyde, PLS
Quantum Spatial, Inc.
Corvallis, OR 97330

1-sigma (σ) Absolute Deviation: Value for which the data are within one standard deviation (approximately 68th percentile) of a normally distributed data set.

1.96 * RMSE Absolute Deviation: Value for which the data are within two standard deviations (approximately 95th percentile) of a normally distributed data set, based on the FGDC standards for Non-vegetated Vertical Accuracy (NVA) reporting.

Accuracy: The statistical comparison between known (surveyed) points and laser points. Typically measured as the standard deviation (σ) and root mean square error (RMSE).

Absolute Accuracy: The vertical accuracy of LiDAR data is described as the mean and standard deviation (σ) of divergence of LiDAR point coordinates from ground survey point coordinates. To provide a sense of the model predictive power of the dataset, the root mean square error (RMSE) for vertical accuracy is also provided. These statistics assume the error distributions for x, y and z are normally distributed, and thus we also consider the skew and kurtosis of distributions when evaluating error statistics.

Relative Accuracy: Relative accuracy refers to the internal consistency of the data set; i.e., the ability to place a laser point in the same location over multiple flight lines, GPS conditions and aircraft attitudes. Affected by system attitude offsets, scale and GPS/IMU drift, internal consistency is measured as the divergence between points from different flight lines within an overlapping area. Divergence is most apparent when flight lines are opposing. When the LiDAR system is well calibrated, the line-to-line divergence is low (<10 cm).

Root Mean Square Error (RMSE): A statistic used to approximate the difference between real-world points and the LiDAR points. It is calculated by squaring all the values, then taking the average of the squares and taking the square root of the average.

Data Density: A common measure of LiDAR resolution, measured as points per square meter.

Digital Elevation Model (DEM): File or database made from surveyed points, containing elevation points over a contiguous area. Digital terrain models (DTM) and digital surface models (DSM) are types of DEMs. DTMs consist solely of the bare earth surface (ground points), while DSMs include information about all surfaces, including vegetation and man-made structures.

Intensity Values: The peak power ratio of the laser return to the emitted laser, calculated as a function of surface reflectivity.

Nadir: A single point or locus of points on the surface of the earth directly below a sensor as it progresses along its flight line.

Overlap: The area shared between flight lines, typically measured in percent. 100% overlap is essential to ensure complete coverage and reduce laser shadows.

Pulse Rate (PR): The rate at which laser pulses are emitted from the sensor; typically measured in thousands of pulses per second (kHz).

Pulse Returns: For every laser pulse emitted, the number of wave forms (i.e., echoes) reflected back to the sensor. Portions of the wave form that return first are the highest element in multi-tiered surfaces such as vegetation. Portions of the wave form that return last are the lowest element in multi-tiered surfaces.

Real-Time Kinematic (RTK) Survey: A type of surveying conducted with a GPS base station deployed over a known monument with a radio connection to a GPS rover. Both the base station and rover receive differential GPS data and the baseline correction is solved between the two. This type of ground survey is accurate to 1.5 cm or less.

Post-Processed Kinematic (PPK) Survey: GPS surveying is conducted with a GPS rover collecting concurrently with a GPS base station set up over a known monument. Differential corrections and precisions for the GNSS baselines are computed and applied after the fact during processing. This type of ground survey is accurate to 1.5 cm or less.

Scan Angle: The angle from nadir to the edge of the scan, measured in degrees. Laser point accuracy typically decreases as scan angles increase.

Native LiDAR Density: The number of pulses emitted by the LiDAR system, commonly expressed as pulses per square meter.

APPENDIX A - ACCURACY CONTROLS

Relative Accuracy Calibration Methodology:

Manual System Calibration: Calibration procedures for each mission require solving geometric relationships that relate measured swath-to-swath deviations to misalignments of system attitude parameters. Corrected scale, pitch, roll and heading offsets were calculated and applied to resolve misalignments. The raw divergence between lines was computed after the manual calibration was completed and reported for each survey area.

Automated Attitude Calibration: All data were tested and calibrated using TerraMatch automated sampling routines. Ground points were classified for each individual flight line and used for line-to-line testing. System misalignment offsets (pitch, roll and heading) and scale were solved for each individual mission and applied to respective mission datasets. The data from each mission were then blended when imported together to form the entire area of interest.

Automated Z Calibration: Ground points per line were used to calculate the vertical divergence between lines caused by vertical GPS drift. Automated Z calibration was the final step employed for relative accuracy calibration.

LiDAR accuracy error sources and solutions:

| Type of Error | Source | Post Processing Solution |
|---------------------------|------------------------------|---|
| GPS (Static/Kinematic) | Long Base Lines | None |
| | Poor Satellite Constellation | None |
| | Poor Antenna Visibility | Reduce Visibility Mask |
| Relative Accuracy | Poor System Calibration | Recalibrate IMU and sensor offsets/settings |
| | Inaccurate System | None |
| Laser Noise | Poor Laser Timing | None |
| | Poor Laser Reception | None |
| | Poor Laser Power | None |
| | Irregular Laser Shape | None |

Operational measures taken to improve relative accuracy:

Low Flight Altitude: Terrain following was employed to maintain a constant above ground level (AGL). Laser horizontal errors are a function of flight altitude above ground (about 1/3000th AGL flight altitude).

Focus Laser Power at narrow beam footprint: A laser return must be received by the system above a power threshold to accurately record a measurement. The strength of the laser return (i.e., intensity) is a function of laser emission power, laser footprint, flight altitude and the reflectivity of the target. While surface reflectivity cannot be controlled, laser power can be increased and low flight altitudes can be maintained.

Reduced Scan Angle: Edge-of-scan data can become inaccurate. The scan angle was reduced to a maximum of $\pm 29.25^\circ$ from nadir, creating a narrow swath width and greatly reducing laser shadows from trees and buildings.

Quality GPS: Flights took place during optimal GPS conditions (e.g., 6 or more satellites and PDOP [Position Dilution of Precision] less than 3.0). Before each flight, the PDOP was determined for the survey day. During all flight times, a dual frequency DGPS base station recording at 1 second epochs was utilized and a maximum baseline length between the aircraft and the control points was less than 13 nm at all times.

Ground Survey: Ground survey point accuracy (<1.5 cm RMSE) occurs during optimal PDOP ranges and targets a minimal baseline distance of 4 miles between GPS rover and base. Robust statistics are, in part, a function of sample size (n) and distribution. Ground survey points are distributed to the extent possible throughout multiple flight lines and across the survey area.

50% Side-Lap (100% Overlap): Overlapping areas are optimized for relative accuracy testing. Laser shadowing is minimized to help increase target acquisition from multiple scan angles. Ideally, with a 50% side-lap, the nadir portion of one flight line coincides with the swath edge portion of overlapping flight lines. A minimum of 50% side-lap with terrain-followed acquisition prevents data gaps.

Opposing Flight Lines: All overlapping flight lines have opposing directions. Pitch, roll and heading errors are amplified by a factor of two relative to the adjacent flight line(s), making misalignments easier to detect and resolve.

APPENDIX B

**Digital Data Submittal
(separate submittal)**